University of Kentucky
UKnowledge

University of Kentucky Master's Theses | Graduate School

2004

FRICTION STIR PROCESSING OF ALUMINUM ALLOYS

RAJESWARI R. ITHARAJU
University of Kentucky, itharaju@engr.uky.edu

Right click to open a feedback form in a new tab to let us know how this document benefits you.

Recommended Citation

ITHARAJU, RAJESWARI R., "FRICTION STIR PROCESSING OF ALUMINUM ALLOYS" (2004). *University of Kentucky Master's Theses*. 322.
https://uknowledge.uky.edu/gradschool_theses/322

This Thesis is brought to you for free and open access by the Graduate School at UKnowledge. It has been accepted for inclusion in University of Kentucky Master's Theses by an authorized administrator of UKnowledge. For more information, please contact UKnowledge@lsv.uky.edu.

ABSTRACT OF THESIS

FRICTION STIR PROCESSING OF ALUMINUM ALLOYS

Friction stir processing (FSP) is one of the new and promising thermomechanical processing techniques that alters the microstructural and mechanical properties of the material in single pass to achieve maximum performance with low production cost in less time using a simple and inexpensive tool. Preliminary studies of different FS processed alloys report the processed zone to contain fine grained, homogeneous and equiaxed microstructure. Several studies have been conducted to optimize the process and relate various process parameters like rotational and translational speeds to resulting microstructure. But there is only a little data reported on the effect of the process parameters on the forces generated during processing, and the resulting microstructure of aluminum alloys especially AA5052 which is a potential superplastic alloy.

In the present work, sheets of aluminum alloys were friction stir processed under various combinations of rotational and translational speeds. The processing forces were measured during the process and the resulting microstructure was analyzed using TEM. The results indicate that the processing forces and the microstructure evolved during FSP are sensitive to the rotational and translational speed. It is observed that the forces generated increase with the increasing rotational speed. The grain refinement was observed to vary directly with rotational speed and inversely with the translational speed. Also these forces generated were proportional to the grain refinement i.e., greater refinement of grains occurred at lower forces. Thus the choice of process parameters especially the rotational speed has a significant effect on the control and optimization of the process.

Key words: FSP, forces, microstructure, aluminum alloys, finite element analysis

RAJESWARI R. ITHARAJU

Date: 05/28/2004

Friction Stir Processing of Aluminum Alloys

By

Rajeswari R. Itharaju

Dr. Marwan Khraisheh

Director of Thesis

Dr. George Huang

Director of Graduate Studies

RULES FOR THE USE OF THESES

Unpublished theses submitted for the Master's degree and deposited in the University of Kentucky Library are a rule open for inspection, but are to be used only with due regard to the rights of the authors. Bibliographical references may be noted, but quotations or summaries of parts may be published only with the permission of the author, and with the usual scholarly acknowledgements.

Extensive copying or publication of the theses in whole or in part also requires the consent of the Dean of the Graduate School of the University of Kentucky.

THESIS

Rajeswari R. Itharaju

The Graduate School

University of Kentucky

2004

FRICTION STIR PROCESSING OF ALUMINUM ALLOYS

THESIS

A thesis submitted in partial fulfillment of the requirements for the degree of Master of Science in Mechanical Engineering in the College of Engineering at the University of Kentucky

By

Rajeswari R. Itharaju

Lexington, Kentucky

Director: Dr. M.K. Khraisheh
Assistant Professor of Mechanical Engineering
Lexington, Kentucky

2004

Dedicated to My Parents

Acknowledgements

I would like to sincerely acknowledge the mentorship and support that my advisor, Dr. Marwan Khraisheh, has extended throughout the course of my MS. It wouldn't have been possible to succeed without his enthusiasm for research, and the excellent guidance. I would like to thank him for his financial support. It is with his support and guidance that I could overcome the difficulties during the course of my research successfully.

I would like to extend my thankfulness to Dr. Rouch, for agreeing to be on my committee. I express my sincere gratefulness for the support and guidance that Dr. Male has extended throughout my M.S. and also for his kindness in agreeing to be on my committee. I would like to acknowledge Dr. Jawahir for all his support and guidance. I would like to express my sincere gratitude to Mr. Anderson for his technical support and guidance through out the course of the experiments. I would like to acknowledge the support and guidance of Dr. Dozier, Mr. Rice in Electron Microscopy Center at University of Kentucky, Dr. Long and the team at SECAT.Inc. I would like to thank my D.G.S. Dr. Huang, for giving me an opportunity to pursue my MS at University of Kentucky. I would also like to thank all the faculty members and staff of ME and MFS dept. for their continued cooperation. I also have to acknowledge all the members of my research team and all my friends, for their support and encouragement.

I would like to thank my parents, brother, sister and other family members for providing the motivation and support for pursuing my master's. It would have been impossible without the blessings, encouragement and support of my parents to achieve this degree.

Table of Contents

List of Tables

List of Figures

Chapter 1 Introduction

1.1 Significance of Friction Stir Processing [25]

Selection of material with specific properties is the key parameter in many industrial applications, especially in the aircraft and automotive industries. However, processing of such alloys with specific properties, like high strength, suffers from certain limitations in terms of cost and time of production, apart from the reduction in ductility. High strength accompanied by high ductility is possible with materials having fine and homogenous grain structures. Hence there arises a necessity to develop a processing technique that would produce a material with small grain size that satisfies the requirements of strength and ductility as well as the cost and time of production. There are new processing techniques like Friction Stir Processing (FSP), Equal Channel Angular Extrusion (ECAE), being developed for this purpose in addition to the improvements in conventional processing techniques like the Rockwell process, powder metallurgy technique.

FSP expands the innovation of friction stir welding (FSW) developed by The Welding Institute (TWI) of United Kingdom in 1991 to develop local and surface properties at selected locations. FSP is a new and unique thermomechanical processing technique that alters the microstructural and mechanical properties of the material in a single pass to achieve maximum performance with low production cost in less time. In the present work, FSP is investigated as a potential processing technique for aluminum alloys because of various advantages it offers over other processes as mentioned above.

One of the potential applications of FSP is in superplastic forming (SPF), which is a net shape forming technique. Superplasticity is a phenomenon exhibited by fine-grained material during which these materials exhibit an elongation of more than 200% under controlled conditions. Microstructural superplasticity is shown by materials with fine grain size, usually less than 10μm, when they are deformed within the strain rate range $10^{-5}s^{-1}$ to $10^{-2}s^{-1}$ at temperatures greater than $0.5T_m$, where T_m is the melting point in ^0K. It is an established fact that as the grain size decreases the strain rate sensitivity index (m) increases and optimum strain rate at which the forming can be performed also increases as indicated in Figure 1-1. In addition, elaborate thermo-mechanical

processing is needed to obtain a microstructure conducive to superplastic deformation. Hence it can be said that the widespread use of SPF of aluminum alloys is hampered by the slow optimum strain rate required for superplasticity, particularly in commercial aluminum alloys as well as fine grain size requirement that can be attributed to the lack of simple, fast and cost effective material processing techniques. Hence there have been efforts made not only to improve the existing conventional material processing techniques but also to develop some new techniques.

Improved thermo-mechanical processing involves solution treatment, over-aging, multiple warm rolling passes (200–220°C) with intermittent re-heating and a final recrystallization treatment. Thus the thermo-mechanical processing is still complex and also the optimum superplastic strain rate is lower than that desired for widespread use of SPF especially in automotive industries, which resulted in the development of newer processing techniques, which utilize the severe plastic deformation (SePD) processing approach such as equal channel angular extrusion (ECAE), torsional strain severe plastic deformation (TS)-SePD and FSP that make SPF even more popular and efficient by shifting the optimum superplastic strain rate to at least 10^{-2} s^{-1} in commercial aluminum alloys produced by casting route.

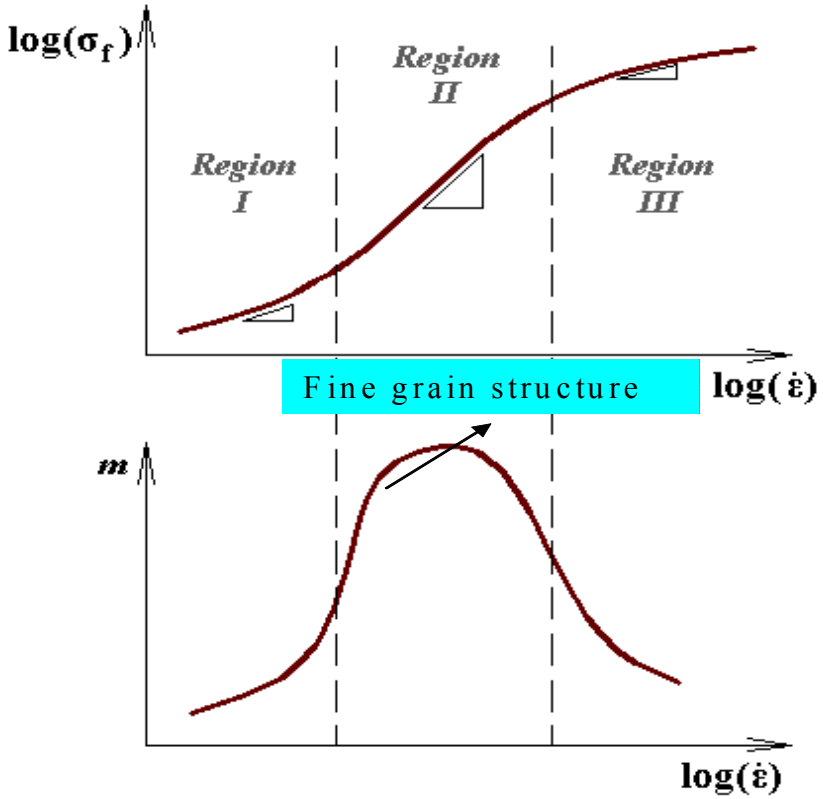

Figure 1-1 Characteristic curve of superplastic material showing the effect of using fine grain structure

ECAE is one of the newer materials processing techniques used to obtain high strain rate superplasticity at significantly lower temperature. A typical grain refinement schedule by ECAE consists of 8–10 passes at intermediate temperatures. (TS)-SePD is another new technique that produces even higher shift in optimum superplastic strain rate and decrease to lower temperature that also produces a nano-crystalline microstructure, but is limited by the size of the processed sheet. FSP is a unique process, which produces fine, equiaxed, and homogeneous grain structure (<10μm) in a single pass that enhances high strain rate superplasticity at lower temperatures even in aluminum alloy sheets of thickness as high as 75mm.

FSP offers many advantages over the conventional and also the newer techniques of material processing which include being a single step process, use of simple and inexpensive tool, no expensive time consuming finishing process requirement, less processing time, use of existing and readily available machine tool technology, suitability to automation, adaptability to robot use, being energy efficient and environmental friendly. Though the limitations of FSP are being reduced by intensive research and development, it still has few limitations that include rigid clamping of the work pieces, backing plate requirement, and the keyhole at the end of each pass. These above mentioned features of FSP make it a potential processing technique not only of aluminum alloys for various industrial applications especially for the SPF but also in the fields of surface engineering, like metal-matrix composite production.

1.2 Principle of FSP

The schematic of FSP is shown in Figure 1-2. To process a sheet by friction stir, a specially designed cylindrical tool is used which while rotating is plunged into the selected area. The tool has a small diameter pin with a concentric larger diameter shoulder. When the tool is plunged into the sheet, the rotating pin contacts the surface and friction between the sheet surface and the shoulder rapidly heats and softens a small column of metal, enabling the transverse movement of the tool through the material. The tool shoulder and length of the probe control the depth of penetration.

During FSP, the area to be processed and the tool are moved relative to each other such that the tool traverses, with overlapping passes, until the entire selected area is processed to a

desired (fine) grain size. The processed zone cools as the tool passes, forming a defect free, and dynamically recrystallized equiaxed fine-grained microstructure.

1.3 Current research in the field of FSP

As FSP is a relatively new process, researchers are not only investigating the possible aluminum alloys that can be processed but are also looking into effects of process parameters on various mechanical and microstructural properties. This process can be easily adopted as a processing technique to obtain finer grains.

Extensive studies are carried out in FSP in order to make it cost effective in the aerospace and automotive industries. Many researchers have taken up the microstructural investigation of various friction stir welded and processed aluminum alloys [7-19]. They basically investigated the grain refinement in the processed and heat affected zones and it has been observed that the FSP of commercial 1100, 2024, 5083, 6061, 7075 and 7475 Al alloys result in significant enhancement of superplastic properties. Different material properties like tensile strength, micro-texture, fatigue and hardness are also being examined for different alloys of aluminum [20-34].

There have also been efforts made to investigate the effect of various process parameters like rotational speed on the properties and microstructure evolved during FSP. The heat generated, residual stress during the process are being investigated experimentally as well as by modeling the process both numerically as well as using by finite element analysis.

1.4 Motivation

As the concept of FSP is relatively new, there are many areas, which need thorough investigation to optimize and make it commercially viable. In order to obtain the desired finer grain size, certain process parameters, like rotational and translation speeds, tool geometry etc., are to be controlled. Several investigations are being carried out in order to study the effects of these process parameters on the grain structure.

The main motivation behind this project is that FSP being similar to a machining process, the study of forces generated during the process with respect to the process parameters like rotational and translational speeds might result in optimizing the process and also relating these forces generated with the microstructure evolved would make the process widely applicable.

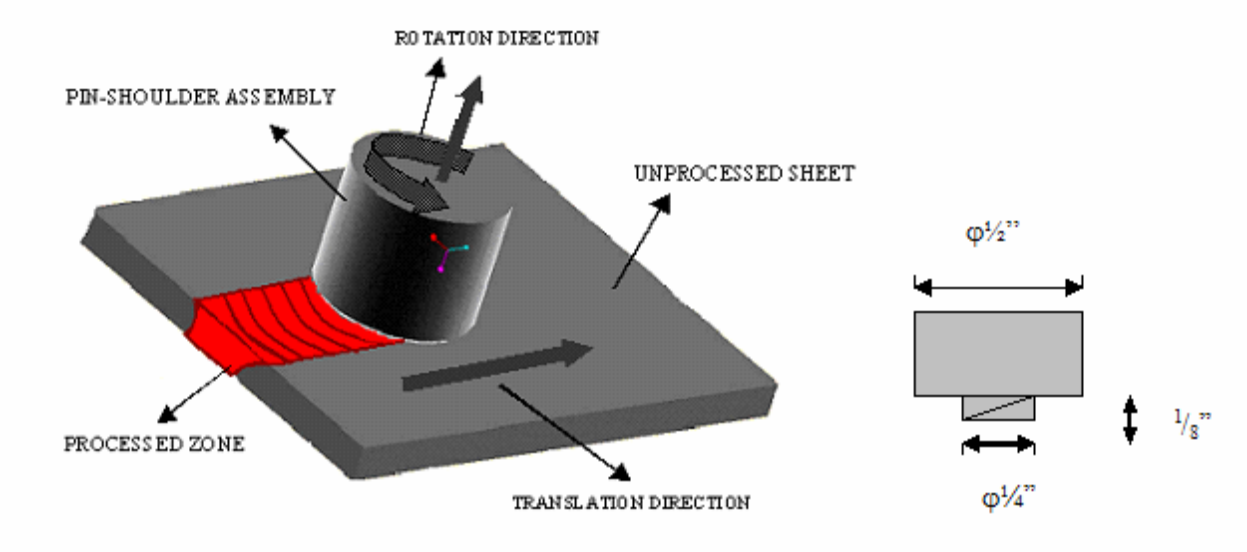

Figure 1-2 Schematic of friction stir process

The present work aims at studying the FSP of AA 5052. The motivation behind choosing AA 5052 is that it is a newer alloy, which has potential in automotive and aerospace applications. Recently it has been demonstrated that commercially available coarse-grained AA5052 exhibits superplastic-like behavior with a maximum elongation of 194% at relatively high initial strain rate of $2.08X10^{-1}s^{-1}$ [57-58]. Hence it is likely that this alloy might exhibit higher elongations if it were fine grained i.e., refining the grain structure of the coarse grained AA5052 by FSP would result in enhanced superplastic behavior of the alloy.

1.5 Objectives

Having understood the significance of FSP, the main objective of this thesis is to investigate the effect of process parameters like rotational and translational speeds on the forces generated

during FSP of aluminum alloys and relate these forces with the microstructure evolved in order to optimize the process. The specific objectives of the work presented are:

a) Design and conduct FS processing experiments on aluminum alloy for different combinations of rotational and translation speeds.

b) Measuring the generated processing forces during FSP of aluminum alloys

c) Examine the microstructural of the processed sheets using transmission electron microscope (TEM).

d) Attempt to establish a correlation between these measured forces and the resulting microstructure.

1.6 Thesis Layout

The present thesis is organized into six chapters. The first chapter gives a brief introduction to the present work i.e., the significance, motivation and objectives of the work. The second chapter would deal with a detailed literature review on the concept of FSP. Third chapter explains the experimental methodology used for achieving the set objectives. In the fourth chapter results obtained are presented. The fifth chapter briefly describes the finite element modeling and analysis of FSP. Finally in chapter 6 we conclude the work presented in previous chapters and suggest some future work that can be done further to make the study complete.

Chapter 2 Literature Review

Friction stir technology is a revolution in the field of welding. This innovative technique produce very fine grains in weld zones. If this could be used as a processing technique, it would replace the existing traditional, complex and expensive processing techniques especially for aluminum alloys. FSP can enhance superplasticity in aluminum alloy. FSW can be considered as a hot-working process in which a large amount of deformation is imparted to the work piece through the rotating pin and the shoulder. Such deformation gives rise to a weld nugget (whose extent is comparable to the diameter of the pin), a thermo-mechanically-affected region (TMAZ) and a heat-affected zone (HAZ). Frequently, the weld nugget appears to comprise of equiaxed, fine, dynamically recrystallized grains whose size is substantially less than that in the parent material. This feature of friction stirred zone resulted in the development of new economical, energy efficient, thermomechanical material processing technique called FSP. It was performed on aluminum alloys for example 7075 Al and 6061 Al especially to render them superplastic and also was used as a technique to produce aluminum surface metal matrix composite.

FSP being an emerging technique, the amount of literature available is less compared to FSW. Particularly, the effect of process parameters on microstructure and relation between the forces developed and resultant microstructure are not much investigated.

There has been extensive study on the microstructure of friction stir welded aluminum alloys. These studies mainly concentrated on the grain size obtained in the weld zone. There are studies on the temperature distribution over the entire weld zone and its effect on the microstructure. Some studies were specifically concentrating on the precipitation phenomenon and type of precipitants thus obtained in the welded region. Hardness profiles for different weld regions were experimentally studied. Investigations were made on the effect of rotational speed on microstructure. Tool wear and different optimum tool designs are also being investigated. Mechanical properties like tensile strength of a friction stir welded joint have been studied.

This section presents overview of research that has been and is being done in the field of FS technology. This chapter on literature review thus gives an insight into the potential, the

amount of work done in the field of friction stir technology and also the potential of commercially available AA5052 for FSP which is a new alloy for automotive industry.

2.1 General idea of the friction stir technology

This section gives an insight into the innovative technology called friction stir technology.

The action of rubbing two objects together causing friction to provide heat is one dating back many centuries as stated by Thomas et.al [1]. The principles of this method now form the basis of many traditional and novel friction welding, surfacing and processing techniques. The friction process is an efficient and controllable method of plasticizing a specific area on a material, and thus removing contaminants in preparation for welding, surfacing/cladding or extrusion. The process is environmentally friendly as it does not require consumables (filler wire, flux or gas) and produces no fumes. In friction welding, heat is produced by rubbing components together under load. Once the required temperature and material deformation is reached, the action is terminated and the load is maintained or increased to create a solid phase bond. Friction is ideal for welding dissimilar metals with very different melting temperatures and physical properties. Some of the friction stir technologies are shown in the Fig.2-1.

Work carried out at TWI by Thomas et.al [2,3] has demonstrated that several alternative techniques exist or are being developed to meet the requirement for consistent and reliable joining of mass production aluminum alloy vehicle bodies. Three of these techniques (mechanical fasteners, lasers and friction stir welding) are likely to make an impact in industrial processing over the next 5 years. FSW could be applied in the manufacture of straight-line welds in sheet and extrusions as a low cost alternative to arc welding (e.g. in the fabrication of truck floors or walls). The development of robotized friction stir welding heads could extend the range of applications into three dimensional components.

Mishra et.al [4] extended the FSW innovation to process Al 7075 and Al 5083 in order to render them superplastic. They observed that the grains obtained were recrystallized, equiaxed and homogeneous with average grain sizes <5μm. They had high angles of misorientation

ranging from 20^0 to 60^0. They had also performed high temperature tensile testing in order to understand the superplastic behavior of FSP aluminum sheets.

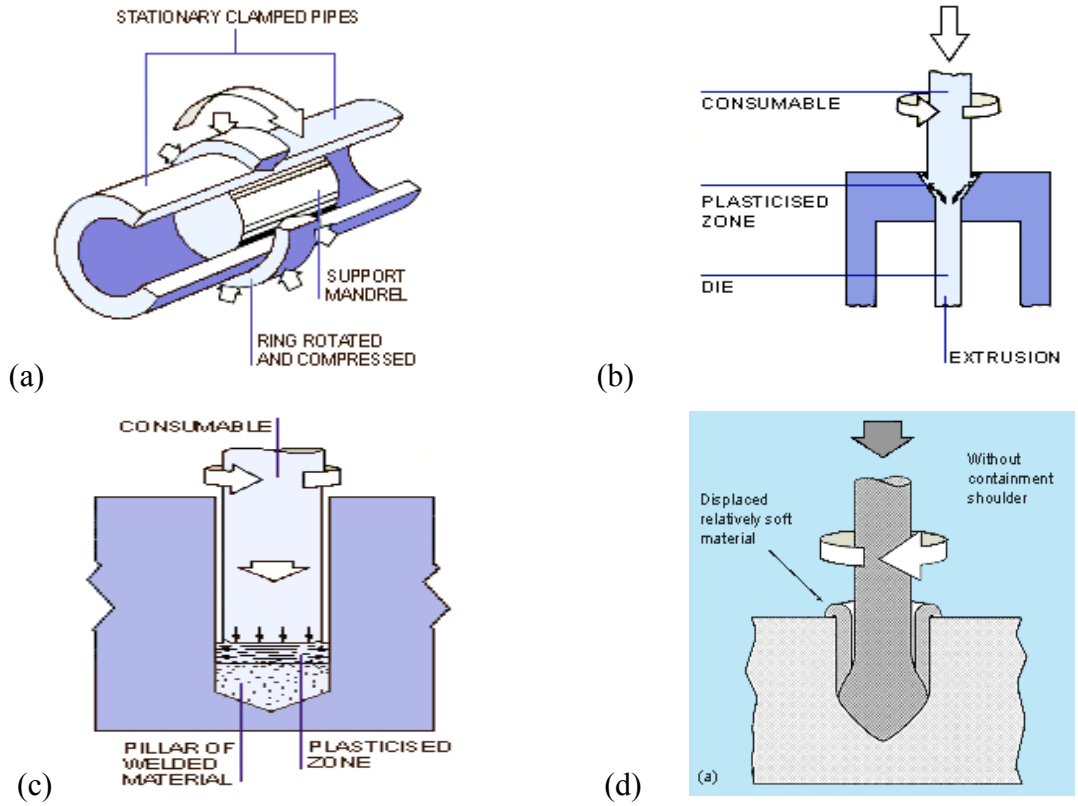

Figure 2-1 Schematic of a) radial friction welding, b) friction extrusion, c) friction hydro pillar processing d) friction plunge welding without containment shoulder [1]

Metal matrix composites reinforced with ceramics exhibit high strength, high elastic modulus and improved resistance to wear, creep and fatigue compared to unreinforced metals. Mishra et al. [5] experimented and proved that surface composites could be fabricated by friction stir processing. Al-SiC surface composites with different volume fractions of particles were successfully fabricated. The thickness of the surface composite layer ranged from 50 to 200µm. The SiC particles were uniformly distributed in the aluminum matrix. The surface composites have excellent bonding with the aluminum alloy substrate. The micro hardness of the surface composite reinforced with 27 volume % SiC of 0.7 µm average particle size was ~173 HV, almost double of the 5083Al alloy substrate (85 HV). The solid-state processing and very fine microstructure that results are also desirable for high performance surface composites.

Thomas et al. [6] presented a review of friction technologies for stainless steel, aluminum, and stainless steel to aluminum, which are receiving widespread interest. Friction hydro pillar processing, friction stir welding (FSW), friction plunge welding are some of these unique techniques. They observed that this technology made possible the welding of unweldable aluminum alloys and stainless steel feasible. Using this technology sheets up to 75mm thickness can also be easily welded.

2.2 Microstructural studies on friction stirred alloys

A basic understanding of the evolution of microstructure in the dynamically recrystallized region of FS material and relation of this with the deformation process variables of strain, strain rate, temperature and process parameters is very essential. This section would give an insight into such studies.

Peel et.al. [7] reported the results of microstructural, mechanical property and residual stress investigations of four AA5083 FS welds produced under varying conditions. It was found that the weld properties were dominated by the thermal input (thermal excursion) rather than the mechanical deformation by the tool, resulting in a >30 mm wide zone of equiaxed grains around the weld line. Increasing the traverse speed and hence reducing the heat input narrowed the weld zone. It is observed that the recrystallization resulting in the weld zone had considerably lower hardness and yield strength than the parent AA5083. During tensile testing, almost all the plastic flow occurred within the recrystallized weld zone and the synchrotron residual stress analysis indicated that the weld zone is in tension in both the longitudinal and transverse directions. The peak longitudinal stresses increased as the traverse speed increases. This increase is probably due to steeper thermal gradients during welding and the reduced time for stress relaxation to occur. The tensile stresses appear to be limited to the softened weld zone resulting in a narrowing of the tensile region (and the peak stresses) as the traverse speed increased. Measurements of the unstrained lattice parameter (d_0) indicated variations with distance from the weld line that would result in significant errors in the inferred residual stresses if a single value for d_0 were used for diffraction based experiment.

The evolution of the fine-grained structure in friction-stir processed aluminum has been studied by Rhodes et.al. [8] using a rotating-tool plunge and extract technique. In these experiments, the rotating tool introduced severe deformation in the starting grain structure, including severe deformation of the pre-existing sub-grains. Extreme surface cooling was used to freeze in the starting structure. Heat generated by the rotating tool was indicated as a function of the rotation speed and the external cooling rate. At slower cooling rates and/or faster tool rotation speeds, recrystallization of the deformed aluminum was observed to occur. The initial sizes of the newly recrystallized grains were in the order of 25–100 nm, considerably smaller than the pre-existing sub-grains in the starting condition. Subsequent experiments revealed that the newly recrystallized grains grow to a size (2–5μm) equivalent to that found in friction-stir processed aluminum, after heating 1–4 min at 350–450 °C. It is postulated that the 2–5 μm grains found in friction-stir welded and friction-stir processed aluminum alloys arose as the result of nucleation and growth within a heavily deformed structure and not from the rotation of pre-existing sub-grains.

Sato et.al [9] applied FSW to an accumulative roll-bonded (ARBed) Al alloy 1100. FSW resulted in reproduction of fine grains in the stir zone and small growth of the ultrafine grains of the ARBed material just outside the stir zone. FSW was reported to suppress large reductions of hardness in the ARBed material, although the stir zone and the TMAZ experienced small reductions of hardness due to dynamic recrystallization and recovery. Consequently, FSW effectively prevented the softening in the ARBed alloy which had an equivalent strain of 4.8.

The microstructure evolution of a joint of Al–Si–Mg alloys A6056-T4 and A6056-T6 was characterized using transmission electron microscopy (TEM) by Cabibbo et.al. [10]. Metallurgical investigations, hardness and mechanical tests were also performed to correlate the TEM investigations to the mechanical properties of the produced FSW butt joint. After FSW thermal treatment was carried out at 530 °C followed by ageing at 160 °C (T6). The base material (T4) and the heat-treated one (T6) were put in comparison showing a remarkable ductility reduction of the joint after T6 treatment i.e., it was 80-90% of that of the parent material.

The microstructure of a FSW Al–6.0Cu–0.75Mg–0.65Ag (wt.%) alloy in the peak-aged T6 temper was characterized by TEM by Lityńska et.al. [11]. Strengthening precipitates found in the base alloys dissolved in the weld nugget, while it was observed that in the heat-affected zone

they were coarsened considerably, causing softening inside the weld region. Precipitates of the Ω (Al_2Cu) phase, was considered as the main strengthening phase in base material, grew up to 200–300 nm in the heat-affected zone, but their density decreased. It was observed that they co-existed with Φ'(Al_2Cu), S'(Al_2CuMg), Φ(Al_2Cu) and σ ($Al_5Cu_6Mg_2$) phases. The density of the Φ' and S' phases as well as their sizes increased in comparison to the base material. The high-resolution observation allowed them to compare the morphology of the Ω phase plates in the heat-affected zone and in the base material.

The grain structure, dislocation density and second phase particles in various regions including the dynamically recrystallized zone (DXZ), thermo-mechanically affected zone (TMAZ), and heat affected zone (HAZ) of a FSW aluminum alloy 7050-T651 were investigated and compared with the unaffected base metal by Su et.al. [12]. The various regions were studied in detail to better understand the microstructural evolution during FSW. They concluded that the microstructural development in each region was a strong function of the local thermo-mechanical cycle experienced during welding. Using the combination of structural characteristics observed in each weld region, a new dynamic recrystallization model was proposed. The precipitation phenomena in different weld regions were also discussed.

The laser beam and friction stir processes were applied to the ECA pressed Al alloy 1050 with the thickness of 1 mm by Sato et.al. [13]. The ECA pressed alloy after two passes through the die consisted of cell structure with cell size of about 0.58 μm, and the hardness value was approximately 46 Hv. The LBW produced as-cast coarse microstructure and coarse equiaxed grain structure at the fusion zone and the HAZ respectively, which led to the hardness reduction to <30 Hv in the LB weld. Where as the fine microstructures obtained in the FS weld by introducing the lower heat generation and the plastic strain simultaneously during the FSW. The grain and cell sizes of the weld zone and the transition region were lower than 1 μm. The microstructures led to the high hardness in the FS weld. Their study revealed that the FSW was one of the most effective welding processes for retention of the high strength and toughness of the fine-grained Al alloys.

Optical and TEM microstructures of friction stir welds of an Al-Li alloy were examined by Jata et.al. [14] to establish the mechanism of the evolution of microstructure in the dynamically recrystallized (DRX) region of FSW welds. The average grain diameter in the DRX region was 9 μm. Using orientation imaging microscopy, many of the grain boundary

misorientations created in the DRX region were observed to be between 15 to 35°. It was concluded that recrystallized grains in the DRX region form by a continuous dynamic recrystallization mechanism. Using reasonable estimates of the strain rate and temperature in the FSW nugget, the dependence of the DRX grain size was found to have the same dependence on the Zener-Hollomon parameter as material deformed via conventional hot working process.

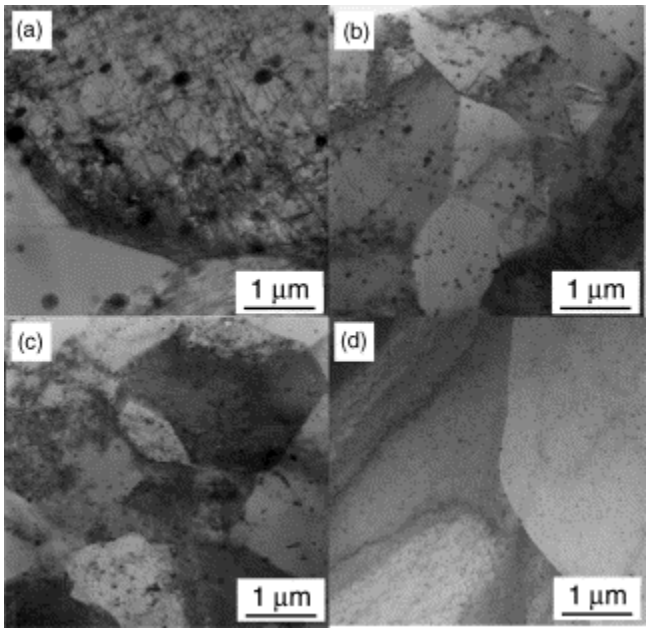

Figure 2-2 Microstructure of T4-FSW material. (a) Elongated grain zone of the heat-affected region; (b) dynamically recrystallized grains. T4 and T6 microstructure after FSW; dynamically recrystallized zone of T4 (c) and T6 (d). TEM [10]

Bensavides et al. [15] studied and compared the grain sizes and microstructures of Al 2024 friction stir weld at room temperature (~30°C) and at low temperature (-30°C). There was an increase in the weld zone equiaxed grain size from the bottom to the top at room temperature, while in the low temperature weld there is a smaller difference from bottom to top. Furthermore, the grain size is considerably smaller in the low-temperature weld, and this observation is consistent with simple grain growth relations of the form $D^2 - Do^2 = A \exp(-Q/RT)(t^n)$. It was observed that as the process reference temperature (T) decreased, the value of $D^2 - Do^2$ decreased, and if Do was assumed to represent a constant or threshold grain size produced by dynamic recrystallization to allow for superplastic deformation by grain boundary sliding, then

the decrease was simply reflected in a decrease in D. The average grain sizes were measured to be 3 μm and 0.65 μm.

Rhodes et al. [16] studied the effects of FSW on the microstructure of Al7075. The critical issues dealt with included microstructure control and localized mechanical property variations. Their experiments revealed that microhardness variations are small from the base metal. There were three groups of strengthening precipitants studied in this work: 1) one group at 50-75nm, 2) second group at 10-20nm and 3) third group found at the grain boundaries at 30-40nm. Dislocation density was modest comprising of loose tangles. The average size of the recrystallized, fine equiaxed grains in the FS welded zone was found to be the order of 2-4 μm.

Liu et al. [17] have used light metallography (LM) and transmission electron microscopy (TEM) to characterize the microstructure in FS weld zone and compared them with that of the original 6061-T6 Al. They measured the microhardness profiles extending from the work piece and through the weld zone. Their work concluded that residual hardness varies from 55 and 65VHN in weld zone in contrast to 85 and 100VHN in the work piece near top and bottom respectively. The weld zone grain size was 10μm as compared to 100μm in the work piece.

FSW of AA6061 and AA7075 alloys have been carried out at different welding parameters by Krishnan [18]. The appearance of onion rings have been attributed to a geometrical effect in that a section through a stack of semicylinders would appear like onion rings with ring spacing being wider at the centre and narrower towards the edge. It was concluded that the formation of the onion rings was due to the process of friction heating due to the rotation of the tool and the forward movement extrudes the metal around to the retreating side of the tool and the spacing of the rings was equal to the forward movement of the tool in one rotation.

Sutton et.al. [19] performed a series of micro-mechanical experiments to quantify how the FSW process affects the material response within the periodic bands that have been shown to be a common feature of FSW joints. Micro-mechanical studies employed sectioning of small samples and micro-tensile testing using digital image correlation to quantify the local stress–strain variations in the banded region. Results indicated that the two types of bands in 2024-T351 and 2524-T351 aluminum FSW joints (a) have different hardening rates with the particle-rich bands having the higher strain hardening exponent, (b) exhibit a periodic variation in micro-

hardness across the bands and (c) the individual bands in each material have the same initial yield stress.

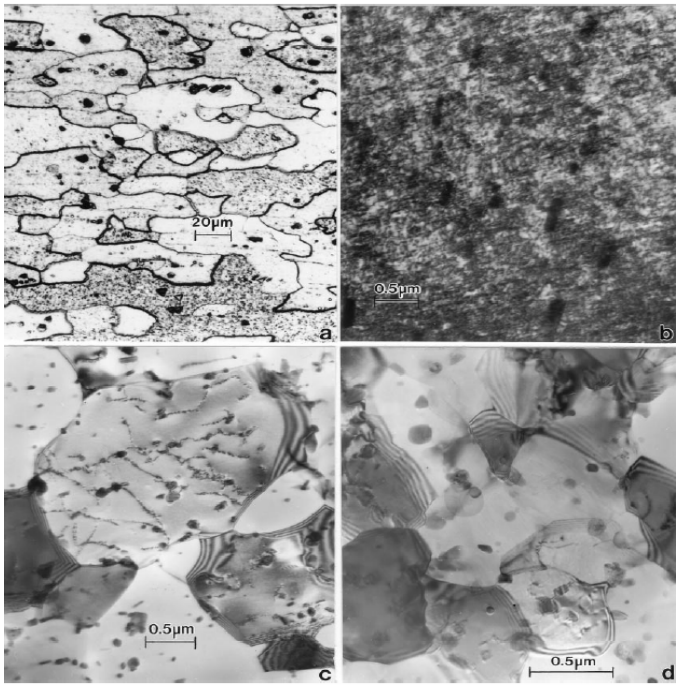

Figure 2-3 Comparison of room temperature and low-temperature FSW microstructures in 2024 Al with the base metal microstructures. (a) Light metallography view of base metal. (b) TEM view of base metal. (c) TEM view of room-temperature weld zone center. (d) TEM view of low-temperature weld zone center. Note dense dislocation density in (b) in contrast to (c) and (d) [15]

2.3 Process parameters and properties during FSP

In order to optimize any process it is very essential to understand the effect of process parameters on the properties of the processed material. Hence this section gives an overview of such investigation in the field of friction stir welding process.

The effect of tool geometry and process parameters are very important factors to be considered for controlling friction stir welding process. Reynolds et.al. [20] made an attempt to study the effects of tool geometry and process parameters like rotational and translational speeds on the properties of welds by investigating x-axis force and power. The highest energy per unit

weld length was observed in Al 6061 welds. It was also observed that the required x-axis force increased and the weld energy decreased with increasing welding speeds for all the Al alloys except for Al 6061alloy because of the relatively high thermal conductivity.

Kwon et.al [21] studied the FS processed Al 1050 alloy. The hardness and tensile strength of the FS processed 1050 aluminum alloy were observed to increase significantly with decreased tool rotation speed. It was noted that, at 560 rpm, these characteristics seemed to increase as a result of grain refinement by up to 37% and 46% respectively compared to the starting material.

In order to demonstrate the FSW of the 2017-T351 aluminum alloy and determine optimum welding parameters, the relations between welding parameters and tensile properties of the joints have been studied by Liu et.al. [22]. The experimental results showed that the tensile properties and fracture locations of the joints are significantly affected by the welding process parameters. When the optimum revolutionary pitch is 0.07 mm/rev corresponding to the rotation speed of 1500 rpm and the welding speed of 100 mm/min, the maximum ultimate strength of the joints is equivalent to 82% that of the base material. Though the voids-free joints were fractured near or at the interface between the weld nugget and the thermo-mechanically affected zone (TMAZ) on the advancing side, the fracture occurs at the weld center when the void defects exist in the joints.

Lee et.al. [23] studied the joint characteristics of FSW A356 alloys, especially concerning the improvement of mechanical properties at the weld zone for various welding speeds. Sound joints were acquired below 187 mm min^{-1} welding speed when the tool rotating speed was fixed at 1600 rpm. The dendrite structures, which were characteristic in the BM, disappeared and showed the dispersed eutectic Si particles in the stirred zone (SZ). The eutectic Si particles were found to be distributed more homogeneously in the SZ at lower welding speeds. The hardness of the weld zone showed more homogeneous distribution in comparison with that of BM due to finer and homogeneously distributed Si particles. It was observed that the transverse ultimate and yield strength had similar values with the BM. All the specimens were fractured at the unaffected BM. The longitudinal ultimate tensile strength has over 178 MPa, which is 20% improvement of that of the BM, and the yield strength also shows higher value. The mechanical properties of the SZ were improved by the dispersed Si particles and the homogeneous microstructure compared with that of BM.

Lumsden et.al. [24] observed that the rapid thermal cycle generated during FSW produces a gradient of microstructures and precipitate distributions in the HAZ and TMAZ of the FS welded aluminum7050 and 7075 alloys. In their study the investigated the effect of pre and post weld heat treatments on the corrosion properties of the FS welds nuggets. They concluded that that FSW produced sensitized microstructure that rendered the materials susceptible to intergranular corrosion. While they also concluded that the thermal treatments can restore most of the SCC resistance to these alloys, this might degrade the strength and ductility of the materials.

Charit et.al. [25] presented preliminary superplasticity studies on various aluminum alloys. They presented new approaches to control the abnormal grain growth observed in few FSP aluminum alloy via improved process optimization and/or alloy designs and realize the full potential of FSP for high strain rate superplasticity. They presented the variation of grain size with tool rotation speed in a friction stir processed 2024 Al at a constant transverse speed of 25.4 mm/min. They have also presented the effect of process parameters on the average grain size obtained in various FSP aluminum alloy. At low traverse speed and for all rotational speeds >300 rpm no abnormal grain size was observed.

Friction stir processing of nanophase aluminum alloys led to high strength ~ 650 MPa with good ductility above 10% [Figure 2-4]. Improvements in ductility were due to a significantly improved homogenization of the microstructure during FSP. The FSP technique is very effective in producing ductile, very high specific strength aluminum alloys, such as the Al-Ti-Cu and Al-Ti-Ni as investigated by Beron et al. [26]. The authors investigated two processes: hot isostatic pressing (HIP) and friction stir process (FSP) and compared the microstructures and corresponding properties resulted from the respective processes on 7075 Al alloy. HIP results in a very high strength alloy with low ductility and inhomogeneous structure. But FSP results in comparatively low strength below 740Mpa but very high ductility at temperatures above 300°C at ~500°C. However the FS processing parameters can be optimized to lower both the operating temperature and time at the temperature in order to improve the strength further. Thus this paper concludes that FSP produces high strength Al alloys with significant ductility.

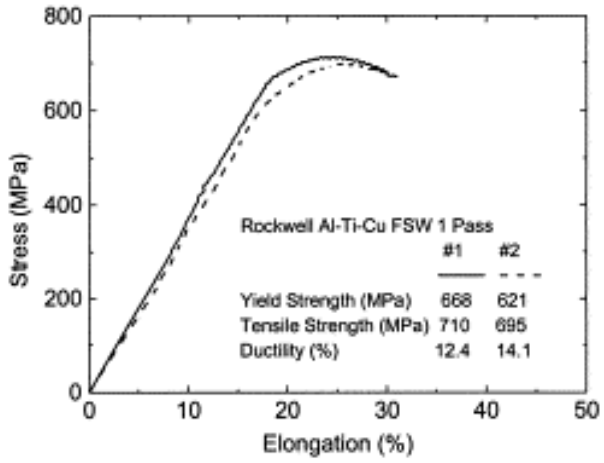

Figure 2-4 Tensile tests of the FS processed material show an excellent strength and more than 10% ductility [26]

Sato et al. [27] investigated the effect of rotational speed on the microstructure and hardness during friction stir welding of Al 6063-T5. They concluded that the maximum temperature of the welding thermal cycle increased with increase in rotational speed. And also it is observed that the recrystallized grain size increased exponentially with the increasing maximum temperature. Thus they clearly indicated that there is an increase in grain size as the rotational speed increased.

Sato et al. investigated the precipitation sequence in friction stir weld of 6063 Al alloy during aging [28] and concluded that post weld annealing at 440K for 12hrs gives greater hardness in overall weld than in the as- received base material and also shifted the minimum hardness from as-welded minimum hardness region to the precipitated-coarsened region. They have also studied the micro-texture of the friction stir welded 6063-T5 Al alloy using orientation imaging microscopy [29].

Sato et al. [30] examined the dominant microstructural factors governing the global tensile properties of a FS welded joint of 6063 Al alloy by estimating the distribution of local tensile properties corresponding to local microstructure and hardness. They concluded that the minimum hardness determined global yield and ultimate tensile strengths of the weld joint. They stated that in a homogeneously hard joint, such as a solution heat treated and aged weld, a fracture was observed to be located in a region with a minimum average Taylor factor (M) which

is equivalent to σ/τ_c where σ is the applied uniaxial stress and τ_c the shear stress working on active plane systems.

Lockwood et al. [31] studied the global and local mechanical response of FS welded AA2024 both experimentally and numerically. Transverse loaded tensile specimens via the digital image correlation technique obtained full field strain measurements. Assuming an iso-stress configuration, local constitutive data were determined for the various weld regions and were used as input for a 2D finite element model. The numerical results compared well with the experimental results in predicting the global mechanical response especially the strain levels. It was also observed that the global strain level was approximately 4% for both the model and experiment.

Mahoney et al. [32] conducted longitudinal and transverse (to the friction stir welded) tensile testing on AA 7075 alloy, which demonstrated that the weakest region associated with FSW was the low temperature location within the heat-affected zone about 7 to 8 mm from the edge of the weld nugget. The yield strength at this location was 45pct less than that of the base metal while; the ultimate tensile strength was 25pct less. Thus concluded that in weldable Al alloys typically, the weld zone would exhibits a 30 to 60 pct reduction in yield and ultimate strengths, hence the losses due to friction stir process were at the lower end of the range for Al alloys.

Mitchell et al. [33] performed FSW of ¼" thick AA6061 sheets for eight combinations of rotational and translational speeds. In their work they presented the forces generated especially the transverse and translation forces and also the temperatures. The temperature is measured using thermocouples. They observed that the transverse force was greater than translation force for all the combinations of speeds and feeds. Their work clearly showed that there exists a unique combination of shear and normal forces that produces a friction stir weld and have stated that the understanding of the contribution of two forces and the relationship to each other was important in modeling the FSW process.

Jata et al. [34] FS welded Al 7050-T7451 alloy to investigate the effects on the microstructure and mechanical properties. Results were discussed for the as-welded condition (as-FSW) and for a postweld heat-treated condition consisting of 121°C for 24 hours (as-FSW + T6) did

not result in an improvement either in the strength or the ductility of the welded material. It was evident from TEM analysis that the FS welding process transformed the initial 1mm sized pancake-shaped grains in the parent material to fine 1to5μm dynamically recrystallized grains. Tensile specimens tested transverse to the weld showed that there was a 25 to 30 pct reduction in the strength level, a 60 pct reduction in the elongation in the as-FSW condition, and that the fracture path was observed in the HAZ. Comparison of fatigue-crack growth rates (FCGRs) between the parent T7451 material and the as-FSW + T6 condition, at a stress ratio of $R = 0.33$, showed that the FCG resistance of the weld-nugget region decreased, while that of the HAZ increased.

2.4 Studies on tool and tool wear during FSW

The tool design plays a very crucial role in friction stir technology. Hence it becomes an important area of study to make the process more efficient. There have been few contributions in this area which can be jotted as follows.

The design of the tool is the key to the successful application of the process to a greater range of materials and over a wider range of thickness. A number of different high performance tool designs have been investigated. The investigations by Thomas et al. [35] describe the recent developments using these enhanced tools from the perspective of existing and potential applications. Aluminum alloy plates of thickness 1mm to 50mm have been successfully friction stir welded in one pass and a 75mm thick FSW weld in 6082 T6 aluminum alloy plate. Encouraging results and good performance have been achieved by using the MX Triflute™ type tools to make single pass welds in a number of materials, from 6mm to 50mm in thickness. Typically, the Whorl™ reduced the displaced volume by about 60%, while the MX Triflute™ reduced the displaced volume by about 70%.

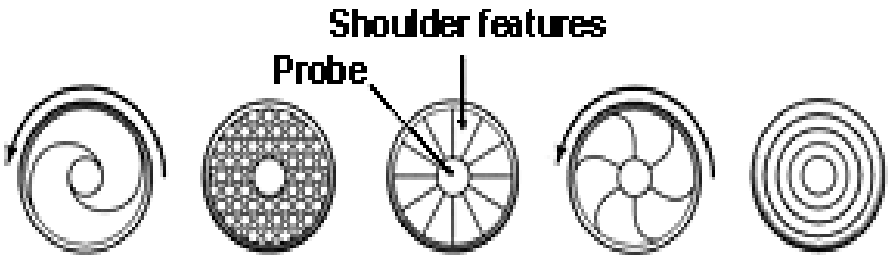

Figure 2-5 Shoulder profiles of FSW tools [35]

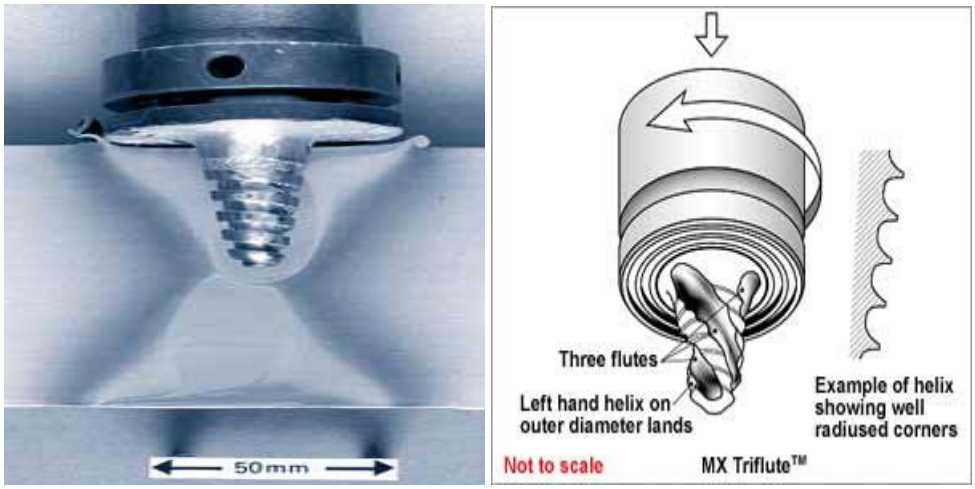

Figure 2-6 a) Prototype Whorl™ tool superimposed on a transverse section of a weld b) MX Triflute™ (Copyright © 2001, TWI Ltd) [35]

Tool wear in a right-hand-threaded, carbon steel nib reached a maximum at 1000 rpm counter-clockwise rotation speed in the FSW of an aluminum 6061+20 vol. % Al_2O_3 MMC where the corresponding, effective wear rate was approximately 0.64%/cm as studied by Prado et al. [36]. Above 1000 rpm the wear rate declined. It was approximately 0.42% /cm at 1500 rpm and 0.56%/cm at 2000 rpm. There was no measurable wear and essentially zero wear rate for the same nib rotating at 1000rpm for the FSW of a commercially Al6061 alloy.

2.5 Modeling and simulation of FSW

FSW/FSP is a complex phenomenon. The process results in localized modification of the material properties. Hence understanding of the thermo-mechanics involved by understanding the relation between the process parameters and the material properties during the process is of great significance in optimizing the process to make it more efficient and commercially viable. Many researchers are working in this area. In order to understand, model and simulate the process experimental methods, analytical or numerical and finite element methods are being employed.

Li et.al. [37] stated FSW as a solid-state, extreme plastic deformation process, which, culminates in dynamic recrystallization to provide a mechanism for superplastic flow, which accommodates the stirring of one metal work piece into another. They found that in the welding of 6061Al to itself, maximum, measured centerline temperatures have been observed not to exceed about $0.8T_M$. In the case of fluid flow, and especially complex turbulence, it is often very difficult to examine and characterize the flow due to the inability to visualize it. They hence studied the complex flow patterns developed in the FSW of 2024Al to 6061Al. These flows were visualized by the differential etching of the two Al alloys, which revealed that the dynamic recrystallization created complex vertex, whorl and swirl features characteristic of chaotic-dynamic mixing.

Dong et al. [38] reported a series of general findings based on a set of simplified numerical models. Those were designed to elucidate various aspects of the complex thermomechanical phenomena associated with FSW. They investigated the following phenomena in separate numerical models: i) coupled friction heat generation ii) plastic flow slip zone development and iii) three dimensional heat and material flow. The friction induced heat generation model was used to quantify the contributions of coupled thermomechanical frictional heating including nonlinear interfacial phenomena between the tooling and the material being welded.

Colligan [39] documented the movement of the material during FSW of AA7075 as a means of developing a conceptual model of the deformation process. From the results he concluded that the material movement is either by simple extrusion or chaotic mixing, depending on where the weld zone material originates. He had used two new techniques to document the movement of the material during FSW, namely steel shot tracer technique and stop action test. Based on his study of welds in 6061 and 7075 it is evident that much of the material movement takes place by simple extrusion.

Huertier et.al. [40] proposed a new mechanical analysis for modeling the material flow pattern during FSW of AA2024 and thus obtained the pertaining strain and temperature maps. The flow generated during the process was derived from the classical fluid mechanics velocity fields. In this study the affected zone was divided into two parts, in which incompressible and

kinematically admissible velocity fields are applied, which was according to microscopic observations of AA2024 weld joint and mechanical analysis of the process. By numerical integration of these model equations, relevant strain, strain rates and temperatures of various zones were obtained. The results of this simulation agreed well with the experimental results. Even though the model had advantages like reduced CPU time it suffered from a major limitation of insertion of the vortex in a rectangle, which led to a discontinuity of the velocity field at the border of the second zone.

Frigaard et al. [41] presented a 2D numerical heat flow model for FSW of aluminum alloys based on finite difference method. This program written in MATLAB 5.1 calculates thermal effects in butt welds for fixed starting conditions. The results showed that the temperature in the front of the tool is most critical, hence the parent material needs to be pre-heated to a certain temperature in order for it to sustain the severe plastic deformation cause by friction stirring. They had identified that at a pseudo steady state different welding variables could be combined in a single process parameter which would control the thermal program during FSW and had defined it as $q_o/\upsilon d$, where q_o the net power, υ welding speed and d the plate thickness.

Frigaard et al. [42] also developed a numerical 3D heat flow model for FSW based on the finite difference method. This algorithm implemented in MATLAB 5.2, with a separate modulus for calculation of the microstructure evolved and the resulting hardness distribution. The results are validated by comparison with in-situ thermocouple measurements and experimental hardness profiles measured at particular intervals. The model yielded a temperature-time pattern that was consistent with the experimental results. The computed temperatures are 20^0 C to 30^0 C higher than the measured ones. Their simulation also attributed the strength loss in age hardenable alloys during FSW to the thermal effects during the process.

Chao et al. [43] presented a three-dimensional finite element model of FSW process. Their model includes a decoupled heat transfer and subsequent thermomechanical analysis. The temperature fields during the welding, residual stress distribution and distortion of the work piece after the FSW process were studied. Two unique features in FSW, namely 1) effect of the fixture used to clamp the work piece to the support backing plate and 2) the reduction of yield

strength near the weld nugget area of the heat-treatable aluminum in the FSW process, incorporated into the modeling.

Ulysse [44] modeled the stir welding process using 3D visco-plastic modeling. This study of his mainly focused on effects of tool speeds on plate temperature and also the forces acting on tool for various rotational and welding speeds and concluded that the pin forces increase with increasing weld speeds and decreasing rotational speeds. He used FIDAP - advanced CFD software to achieve the task. The basic properties of the materials for the present project are taken from this work. This forms the basis for all the work done in the present project.

Deng et.al. [45] developed solid mechanics based finite element models and conceptual designs to study and simulate FSW. They presented a 2D model which simulated the material flow pattern, spatial velocity field and position of the particles after welding. These results compared well with the experimental observation. They suggested that material particles in front of the tool pin tend to pass and get behind the rotating pin from the retreating side of the pin. They also studied the difference between the velocity fields based on two different tool material interface models.

Song et. al. [46] developed a 3D heat transfer model for FSW. They introduced a moving coordinate to reduce the difficulty of modeling a moving tool. Heat input from the tool shoulder and the pin were considered in the model. The finite difference method was applied for solving the control equations and the results obtained were in good agreement with the experimental results. The important conclusion of their work is that preheating the work-piece was proven to be beneficial to FSW. This model reduced the difficulty of determining the temperature distribution over the moving tool pin. This model can be applied to both tool and the work piece.

Lockwood et.al. [47] developed 2D plane stress and plane strain, finite element models of welded specimens of AA2024, using the local constitutive properties as input data and local and global responses in tension were simulated. Their simulation resulted in nearly plane stress condition in the specimen as demonstrated by the correspondence with the experimental results and 2D model predictions. These developed findings were extended to 3D finite element model.

Chen et.al. [48] proposed a three-dimensional model based on finite element analysis to study the thermal history and thermo-mechanical process in the butt-welding of aluminum alloy 6061-T6. The model incorporated the mechanical reaction of the tool and thermo-mechanical process of the welded material. The heat source incorporated in the model involves the friction between the material and the probe and the shoulder. In order to provide a quantitative framework for understanding the dynamics of the FSW thermo-mechanical process, the thermal history and the evolution of longitudinal, lateral, and through-thickness stress in the friction stirred weld are simulated numerically. The X-ray diffraction (XRD) technique is used to measure the residual stress of the welded plate, and the measured results are used to validate the efficiency of the proposed model.

2.6 Superplasticity in Friction stirred materials

It has been an established fact that the primary requirement for material to exhibit superplasticity is to have a fine grain structure and friction stirred zone was observed to have a very fine grain [49]. This motivated researchers to investigate the superplastic behavior of friction stirred materials. In this section an attempt is made to provide an overview of current research in this area.

Mishra et.al. [50] investigated the FSP of a commercial 7075 Al alloy that resulted in significant enhancement of superplastic properties. The optimum superplastic strain rate was observed to be 10^{-2} s^{-1} at 490 °C in the FSP 7075 Al alloy, and the maximum elongation was observed to be about 1000%. Also, the average grain size was determined by mean linear intercept technique (grain size = 1.78 × mean linear intercept), and was approximately 3.3±0.4μm.

Ma et.al. [51] FS processed commercial 7075Al rolled plates with different processing parameters, resulting in two fine-grained 7075Al alloys with a grain size of 3.8 and 7.5 μm. They observed that heat treating the FS processed sheets at 490 °C for an hour showed that the fine grain microstructures were stable at high temperatures. Superplastic investigations in the temperature range of 420–530 °C and strain rate range of 1×10^{-3}–1×10^{-1} s^{-1} were carried out and they demonstrated that a decrease in grain size resulted in significantly enhanced superplasticity

and a shift to higher optimum strain rate and lower optimum deformation temperature. They also observed that for the 3.8 μm 7075Al alloy, superplastic elongations of >1250% were obtained at 480 °C in the strain rate range of 3×10^{-3}–3×10^{-2} s^{-1}, whereas the 7.5 μm 7075Al alloy exhibited a maximum ductility of 1042% at 500 °C and 3×10^{-3} s^{-1}. They concluded that grain boundary sliding mechanism was responsible for the superplastic behavior of the FS processed alloy and this was also proved using SEM technique.

Ma et.al [52] also FS processed Al–4Mg–1Zr extruded bar which, resulted in generation of a fine microstructure of 1.5 μm grain size. Superplastic deformation behavior of FSP Al–4Mg–1Zr alloy was investigated in strain rate range of 1×10^{-3} to 1 s^{-1} and temperature range of 350–550 °C and compared with that of as-rolled one. It was observed that the FSP alloy exhibited significantly enhanced superplasticity at a high strain rate of 1×10^{-1} s^{-1}, and a maximum elongation of 1280% was obtained at 525 °C and 1×10^{-1} s^{-1}. They had also concluded that the FSP Al–4Mg–1Zr alloy exhibited excellent thermal stability at high temperature, and a large elongation of 1210% was observed at 550 °C and 1×10^{-1} s^{-1}. It was also observed that FSP resulted in a significant decrease in the flow stress in Al–4Mg–1Zr alloy. At a strain rate of 10^{-2} s^{-1}, the flow stress (~7 MPa) of FSP Al–4Mg–1Zr at 450 °C was comparable to that of as-rolled alloy at 550 °C.

Charit et.al. [53] investigated the effect of FSW, both in single and multi-passes on a superplastic 7475 Al alloy with emphasis on the thermal and mechanical responses of FSW joints at superplastic temperatures. According to them the critical issue confronting the practical realization of FSW/SPF technology for aluminum alloys was the thermal stability of the fine-grain microstructure in friction stir welded regions (both single and multiple-pass) at SPF temperatures. Abnormal grain growth throughout the weld nugget at SPF temperatures resulted in reduction of room temperature mechanical properties. But they observed that the microstructure in the weld HAZ is stable and retains superplastic properties. The high strength weld nugget, because of the higher flow stress at 783 K compared to the parent metal (16–18 MPa versus 2–9 MPa), seemed unlikely to deform during SPF.

In another study Charit et.al [54] demonstrated that superplasticity at higher strain rates can be achieved in a commercial 2024 Al alloy via friction stir processing. Ductility values for the FSP alloy were observed to be substantially higher than that of the parent alloy (non-superplastic) at comparable temperature and strain rate ranges. It was observed that superplasticity was achieved at higher strain rates of 10^{-2}–10^{-1} s^{-1} in this alloy, which was hitherto not possible with conventional thermo-mechanical processing. The maximum elongation of ~525% was obtained at 430 °C and a strain rate of 10^{-2} s^{-1} in this FSP alloy. The strain rate sensitivity (m) value was found to be ~0.5, indicating the operation of grain boundary sliding related deformation mechanism. At or above 470 °C, they observed a sharp deterioration of ductility because of abnormal grain growth in the friction stir processed region.

Mahoney et.al. [55] presented friction stir processing as a thermo-mechanical process to create a fine grain microstructure in thick section (>5mm) of Al 7050-T651 which resulted in high strain rate (>10^{-3}) superplasticity. Further FSP produced a relatively uniform fine grain through out the thickness of the sheet. This allowed fine grain microstructures to be created in a thick section >5mm i.e., a thickness considerably greater than that attained by conventional thermo-mechanical processing. It was shown that high levels of elongation, even at highest strain rates, remains uniform, i.e. no diffusion necking.

Salem et.al. [56] investigated the ability of friction stir welded Weldalite 2095 to maintain superplastic properties in the weld region. They observed that higher welding rates result in higher % elongation to fracture. A welding rate of 2.1 mm/s at 1000 RPM caused sub-grain coarsening that resulted in reduced superplastic capability. High welding rates increased the density of dislocations and develop microstructures consisting of tangled dislocation structures and sub-grains with small misorientations. Sheets welded at 3.2 and 4.2 mm/s displayed uniform superplastic deformation up to strains of ≈1.3. At the cessation of uniform deformation, necking took place within the region adjacent to the friction stir weld nugget, followed by fracture.

2.7 Potential of AA5052 for FSP

AA 5052 is relatively new alloy which has potential in automotive and aerospace industry because of this low density, high strength, corrosion resistance etc. It has gained importance with the observation that it has superplastic-like behavior even when it is coarse grained. Hence this alloy has greater potential in the forming industry (SFP), especially when the grain size is reduced by special process like FSP.

Chow et.al [57] studied the cavitation behavior of commercially available AA5052 alloy under hot uniaxial and biaxial tension for the first time. They stated that the 194% elongation of commercially available coarse-grained AA 5052 shows its superplastic-like behavior and also its potential in SPF industry. The tensile specimens were strained to different strain levels at various initial strain rates and temperatures. A lower cavitation growth was observed for AA5052 alloy in comparison to that of superplastic alloy AA5083. It was also observed cavitation rate increased with increasing strain rate and the low hot formability of AA5052 alloy would not correlate with its cavitation behavior, but also its relatively low strain-rate sensitivity.

Chow et.al [58] also investigated the effect of stress state on cavitation and deformation behavior of superplastic or superplastic-like material. A coarse-grained Al5052 alloy was deformed at its optimal temperature of 873K under different biaxial stress states. A superplastic gas forming tester with die aspect ratios of 1, 0.75, 0.5 and 0.375 was used. It was observed that the amount of cavities increased with increasing strain level.

Summary

From the above literature study it is evident that there is a potential for FSP in various fields. As this process is new there are many areas that need to be explored. There have been no data presented relating the forces generated during FSP with the microstructure evolved. Hence this makes the present chosen topic for the research significant. And also the literature clearly shows the potential of AA5052 as a superplastic alloy.

Chapter 3 Experimental Procedure

In this project we intend to experimentally investigate the effects of various process parameters on the forces generated during FSP of aluminum alloys microstructure and relate these forces to the microstructure evolved. This task is accomplished in four steps.

1. Commercial aluminum alloy of $^{1}/_{8}$" thickness cut into sheets of dimensions, 4"x 6" for various combinations of rotational and translational speeds as shown in Table 3-2
2. Measure the forces generated during the process using 3 component KESTLER's dynamometer
3. Observe the microstructure using Joel 2000FX TEM for each of the combinations of rotational and translational speeds

The present chapter would give an overview of the experimental setup, experimental procedure, force analysis procedure, microstructural analysis procedure for both optical and transmission electron microscopes.

3.1 Experimental set up

One of the advantages of FSP as mentioned earlier is that it can utilize the existing machine tool technology and requires a simple tool. The experimental setup required to FS process aluminum alloys is discussed in this section. The basic equipment used is as follows (Figure 3-1 and Figure 3-2):

- HAAS VF-0F vertical milling machine.
- Most important element in FSP is the tool. The tool assembly designed consists of a pin and a shoulder. It is made of ¼ -20, 01 tool steel nib Rockwell hardness of 62C with right hand threads, nominal shoulder diameter of ½", and pin diameter of ¼" slightly force shortened and rounded. The height of the pin is equal to the thickness of the sheet to be processed.

- A 3-component piezoelectric KISTLER dynamometer to measure the forces in three axes namely, X, Y, Z. This dynamometer is placed on the bed of the machine
- Backing plate made of steel is placed on the dynamometer to support the FS processed sheet during the process

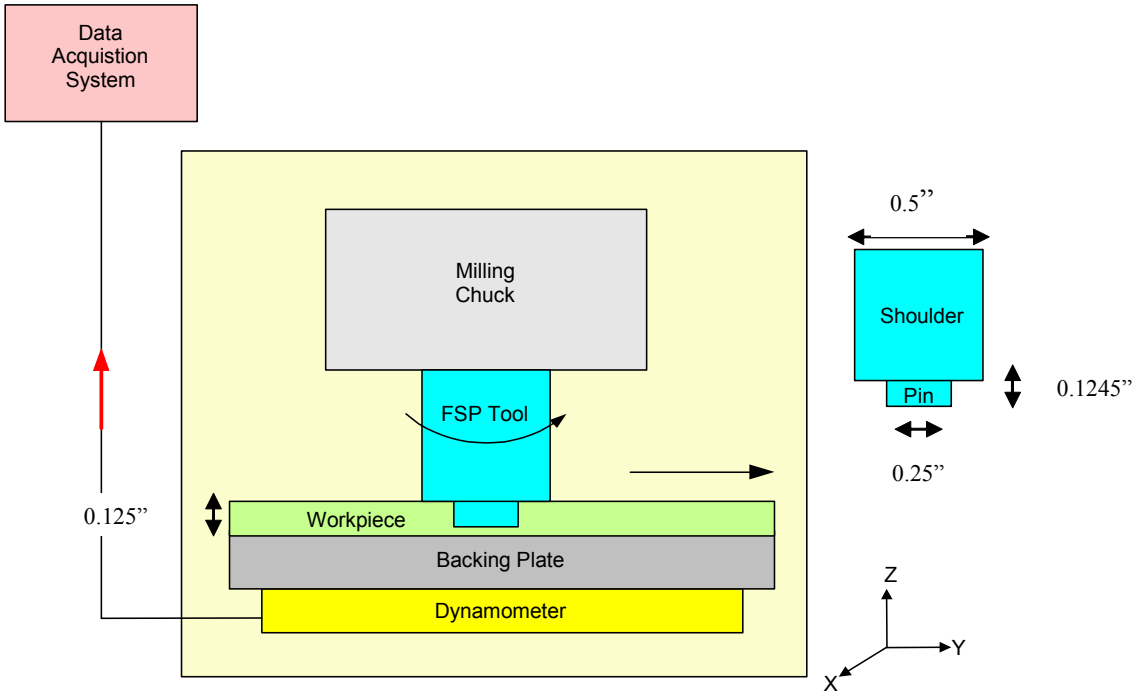

Figure 3-1 Schematic FSP experimental set up

3.2 Experimental procedure

As received AA5052 sheets are used for FSP Table 3-1. The process of FSP begins with the work piece being firmly clamped to a worktable via backing plate which is placed on the dynamometer. A small hole is drilled at the beginning of the sheet to initiate the penetration of the tool. The rotating pin is forced into the work piece and moved along the desired direction with a specific combination of rotational and translation speeds Table 3-2. Frictional heating is produced from the relative motion of the rotating shoulder with respect to the sheet being processed, while the rotating pin deforms rather generates a ‘stirring’ action which locally heats up and creates severe plastic deformation in the material. FSP can be considered as a hot

working process in which a large amount of deformation is imparted to the work piece than the rotating pin and the shoulder. Figure 3-2 shows the FSP tool and experimental set up.

FS processed zone is characterized by dynamic recrystallization which arises through either localized or large scale instabilities forming narrow or extended adiabatic shear bands. There is an apparent extrusion like behavior of material around the pin tool, the process is more characteristic of solid state flow facilitated by the adiabatic shear creating recrystallization regimes to accommodate the large deformations at high deformation rates. The result of this process is a homogeneous, equiaxed, dynamically recrystallized, fine grained material. In order to process the complete sheet, overlapping passes are used. The process is initiated by drilling a hole in the work piece, as it allows the pin to easily penetrate into the work piece as there is not enough heat generate at the beginning of the process to make the material soft.

The forces generated during the entire process are recorded using the data acquisition system. The processed sheets are then prepared for microstructural and mechanical testing.

Table 3-1 Composition of AA5052 by % weight

Alloy	Al	Cr	Cu	Fe	Mg	Mn	Si	Zn
% Wt	97.5	0.15-0.35	Max 0.1	Max 0.4	2.2-2.8	Max 0.1	Max 0.25	Max 0.1

Table 3-2 Experimental matrix of FSP of Al 5052

Rotational speed (rpm)	Translational speed (ipm)			
	1.5	2.0	2.5	3.0
400	√	√	√	√
600	√	√	√	√
800	√	√	√	√
1000	√	√	√	√

3.3 Force analysis procedure

As the process of FSP is similar to a machining process one of the best methods to control and optimize the process is through studying the forces generated during the process and controlling these forces by controlling the process parameters.

Thus the forces generated especially the processing forces (Fx, Fy, Fz) are recorded during FSP of Al 5052 under various combinations of rotational and translation speeds using a 3-component piezoelectric KISTLER dynamometer which is connected to a DAQ system as shown in Figure 3-1. The force data obtained is transferred into an Excel spread sheet and are sample using the root mean square (RMS) and averaging techniques (example 1) [59].

Example 1:

$Fz = (\sqrt{}(\sum fzi^2))/ N$ …… where fz force at a particular instance

N number of data points

i = 1, 2 ...N

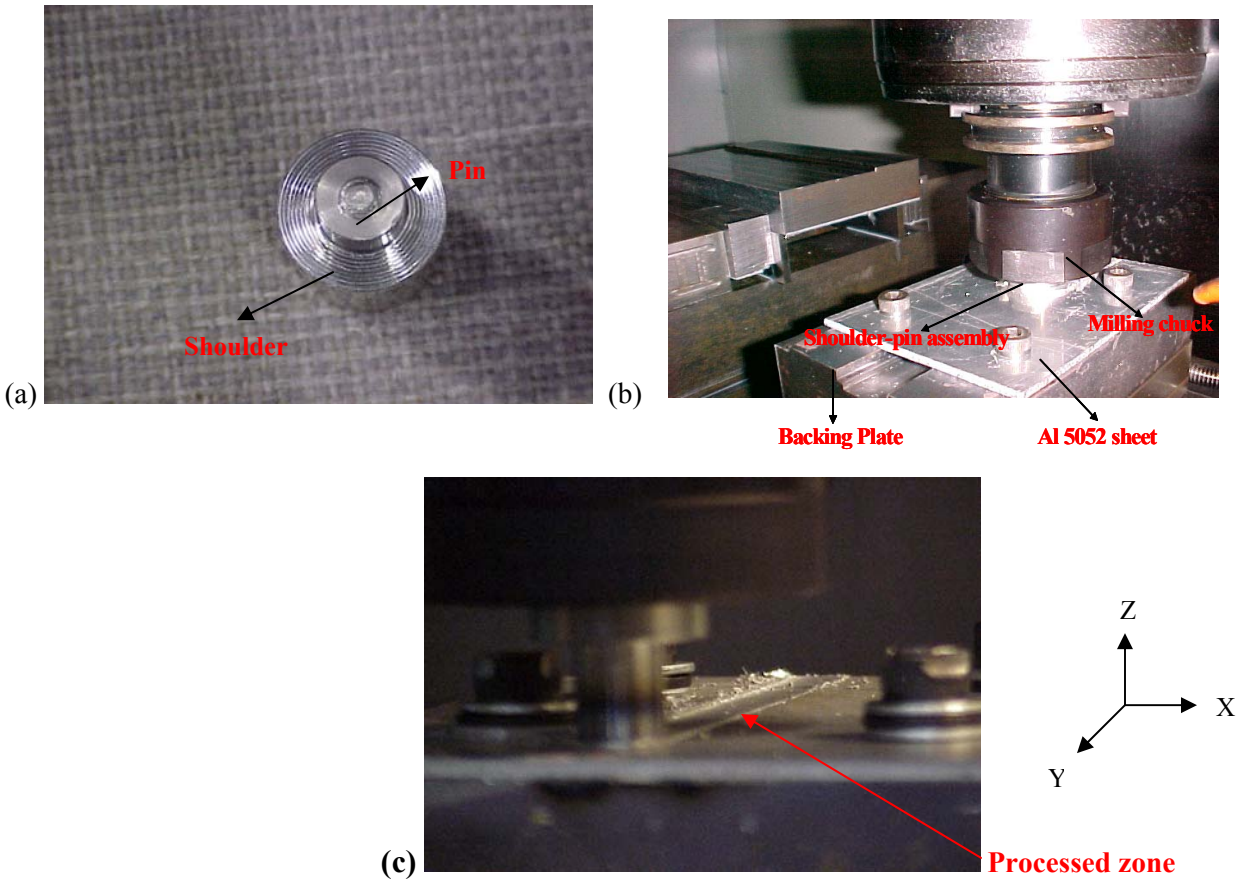

Figure 3-2 a) FSP tool made of tool steel, b) experimental setup for FSP of Aluminum alloys c) FS processed zone

These sampled force data are plotted with respect to the time of FSP. The average force data is also plotted with respect to the rotational and translational speeds. These plots give clear

idea of the trends of the force with respect to speeds which can be used to control the process parameters and thus optimize the process.

3.4 Microstructural analysis procedure

As received AA5052 samples are cold mounted, polished to 1μm flat and are finally anodized and observed under the polarized light optical microscope. After FSP, the surface of the sheet is cleaned and samples are cut for microstructural study from three different locations of the processed sheet as shown in Figure 3-3. The samples are cut across the cross section of the processed zone. They are cold molded and mechanically and electro polished to study under a polarized light optical microscope which would enable us to qualitatively comment on the grain refinement by friction stir processing. Further to quantify this refinement, the samples are prepared for TEM analysis.

In order to investigate the grain refinement and measure the grain size 3mm discs are cut from the FS processed zone of AA5052 and thin foils were prepared by TenuPol-5 double jet electro-polisher, using a solution of 25% HNO3 in methanol. These samples are then observed under transmission electron microscope for which Jeol-2000FX TEM was used. The microstructure pictures are captured on a film which is then developed for further analysis. The film is then calibrated according to the standard grid at each magnification and then the average grain size is determined using line intercept method. This method in brief can be explained as drawing a line of known length across the image such that it contains maximum number of grain. And the length when divided by the number of grains it contains gives the average grain size.

Example 2:

d = l/n---------where d avg. grain size in microns

l- length of the line, n -No. of grains crossed by the line

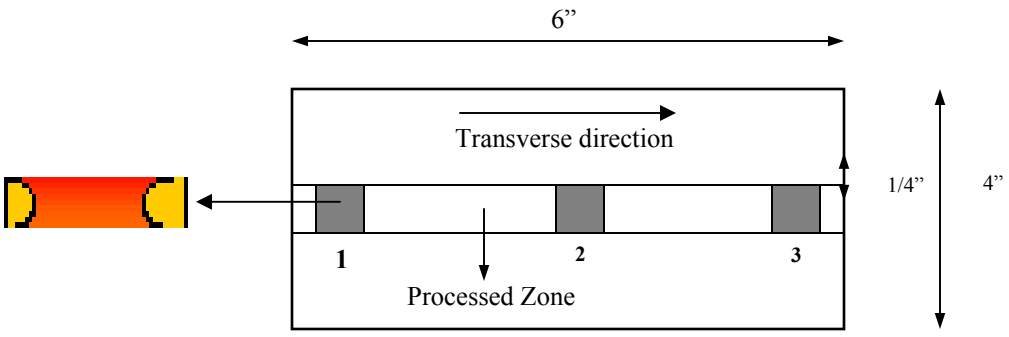

Figure 3-3 Location of samples cut for microstructural study

Chapter 4 Result and Discussion

Initial FSP experiments were performed on AA 6061-T6 and AA 2024-O alloy sheets in order to understand the process, choose the right dimensions and design of the tool and other process parameters. From these initial FSP experiments standardized procedures for processing and analysis i.e. both microstructure and force analyses were established. Further experiments were conducted on AA5052 as it was recently established that this alloy exhibits a superplastic like behavior (190% elongation) at room temperature even with a coarse grained structure (~50μm). Hence with a finer grain this alloy might exhibit an enhanced superplastic behavior

In the present section, the FSP tool design development and different modes of failure observed are also discussed along with the results for single pass friction stir processed AA5052 and some results of the initial experiments conducted on AA6061-T6. Adapting the procedure as explained in Chapter 3, sheets of aluminum alloys are friction stir processed. These results are presented mainly as two different sections which include 1) force analysis (for AA5052 and AA 6061) 2) microstructural analysis (for AA5052) during FSP. Finally a correlation is established between the forces generated and microstructure evolved.

4.1 FSP tool design

The crucial part in this project was to design an experimental setup which would fit in the available machine tool. Understanding the tool design plays a very important role in friction stir processing. The initial FSP tool designed was a simple cylindrical tool with 1" shoulder diameter, diameter and height of the pin equal to the thickness of the sheets processed i.e., ¼". The forces generated using this tool especially during the penetration of the tool into the wok-piece, which were very high and beyond the capability of the dynamometer to measure. Then we threaded the pin in order to reduce the initial high forces during penetration. This resulted in the reduction of forces but the forces seemed still higher to be measured. This led to the reduction in thickness of the work-piece. The sheets selected for processing where now 1/8" and accordingly the height of the pin was reduced to match the thickness of the sheet i.e., the height of the pin was reduced to 1/8". And also a small hole was drilled to initiate the penetration of the tool and

thus decrease the forces generated. It was the observed that the heat generated was very high and in order to reduce this frictional heat the shoulder diameter was reduced to ½". Hence, we finally came up with a design that resulted in good processed zone at reduced forces. The tools design development discussed above is shown in Figure 4-1.

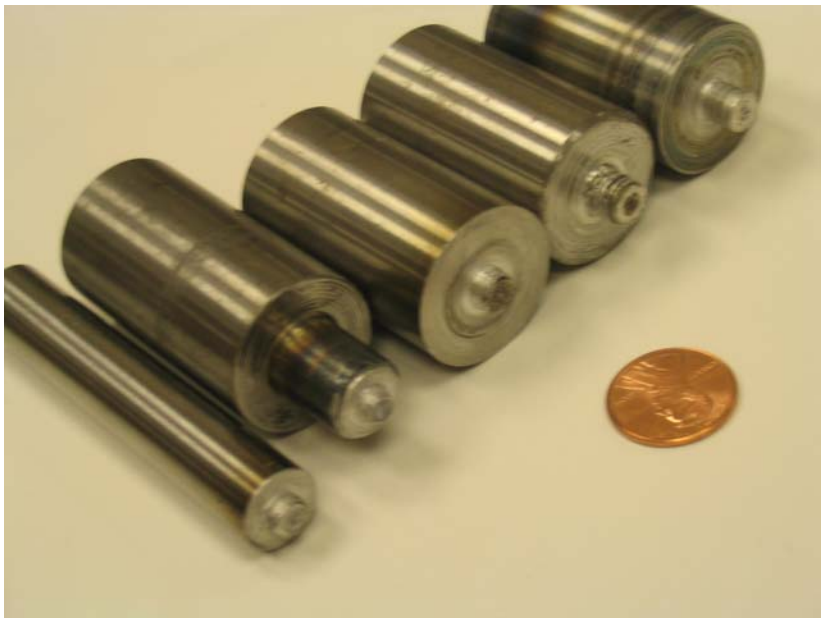

Figure 4-1 FSP tool designs latest to the oldest (left to right)

4.2 Modes of failure in FSP

FSP depends greatly on the amount of frictional heat generated during the process. The factors influencing the frictional heat generated during FSP include the processing conditions, tool design, use of backing plate and depth of penetration of the tool. Some of the modes of failure observed during FSP are shown in Figure 4-2. Tool design and alignment during processing are very important in order to obtain a good processed region. The ratio of shoulder and pin diameters is and important aspect of consideration. As this ratio increases the amount of frictional heat generated also increases and as a results of too much of heat generated at the shoulder-sheet interface the sheet material starts melting. Also it has been observed that the backing plate though increases the forces generated, supports the material to flow and beneath the pin and reduces the defects at the rare side of the processed sheet. This defect is also reduced by the using a smaller clearance between the tool tip and the lower surface of the sheet. Choice

of process parameters like rotational and translational speeds also plays a crucial role. At lower rotational speeds the frictional heat generated is insufficient and produces a defective processed zone which can be attributed to the process similar to that associated with the built-up edge formation in metal cutting process.

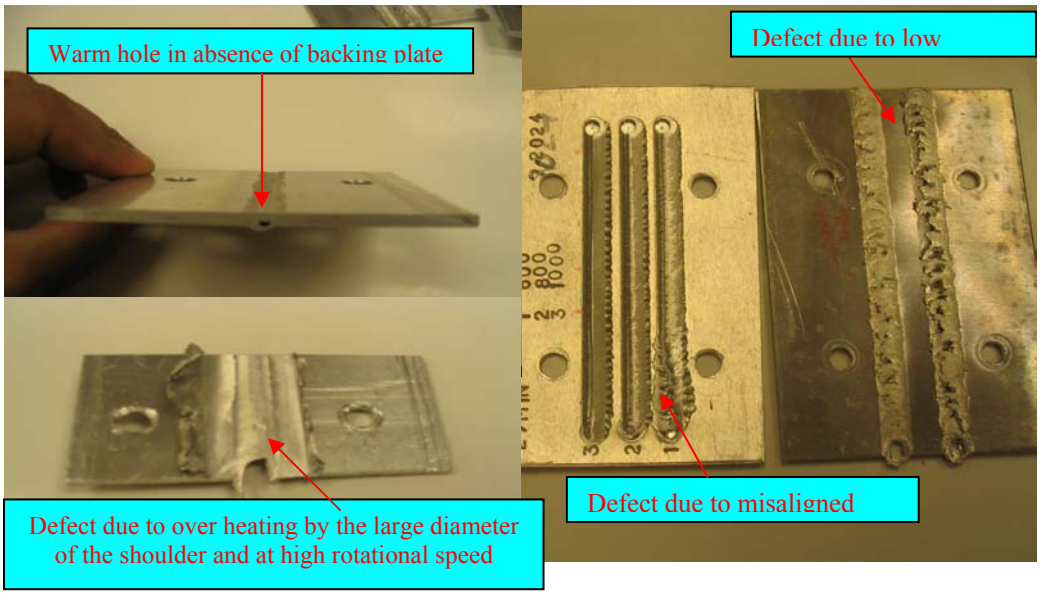

Figure 4-2 Failure modes observed during FSP of aluminum sheets

4.3 Force analysis

Aluminum alloy sheets are friction stir processed at various speeds and feeds and the processing forces (Fx, Fy, Fz) are measured using a 3-component piezoelectric KISTLER dynamometer for each combination of rotational and translational speeds. The measured forces are sampled using the root mean square technique as discussed in the previous chapter. Figure 4-3 clearly shows that the sampling technique used is in good accordance with the raw data acquired. These sampled cutting forces, plotted with respect to time are presented in Appendix A.

The processing forces during FSP were observed to be very high during penetration of the tool but later as there was sufficient amount of frictional heat generated, the forces tend to decrease and then remain almost constant throughout the process. Figure 4-4 and Figure 4-6 show the variation of the processing forces (Fx, Fy and Fz) with respect to rotational and

translational speeds respectively. From these figures it can be observed that there is a significant variation in the plunge force Fz with the variations in the other process parameters Hence the behavior of plunging force (Fz) is studied with the variation of the process parameters such as rotational and translational speeds. Figure 4-5 shows the variation of Fz with the rotational speed for different constant translational speeds for AA5052. It is observed that at low rotational speed of 400 rpm the forces generated are very high and the process zone is also not defect free. As the speed is increased to 600 rpm the force generated is very low at all the translational speeds. A better and almost defect free process zone was obtained as the rotational speed was increased from 600-1000 rpm, for all translational speeds. However, it was observed that the forces generated during the process significantly increased as the rotational speed was increased from 600-1000rpm.

Figure 4-7 shows the variation of Fz with translation speed at constant rotational speeds during FSP of AA5052. At 1.5in/min the forces generated are high in comparison to the other conditions. As the speed increases to 2.5in/min the forces generated decreases. As the speed further increases from 2.5-3in/min the forces generated increase significantly at 800 and 1000rpm. However, at 600 rpm the forces generated decreases as the speed increases from 1.5 to 2in/min and there after the forces generated increase with the increasing speeds.

But, it is also observed that the force generated at 400 rpm increased as the translational speed was increased from 1.5-2.0in/min and further increase in speed to 2.5 in/min decreased the force. Further increase in speed to 3in/min resulted in increase of the force. It is also observed at low translation speed the surface of the processed sheet is not defect free. Good surface finish is observed at higher translational and rotational speeds. Thus, from the two graphs presented it is concluded that the ideal combination in terms of plunge forces used is 600 rpm and 2in/min. It can also be concluded that very low speeds - both translational and rotational speeds result in very uneven forces and a bad process as there is not enough frictional heat generated for the softening the material and allowing the flow of the material.

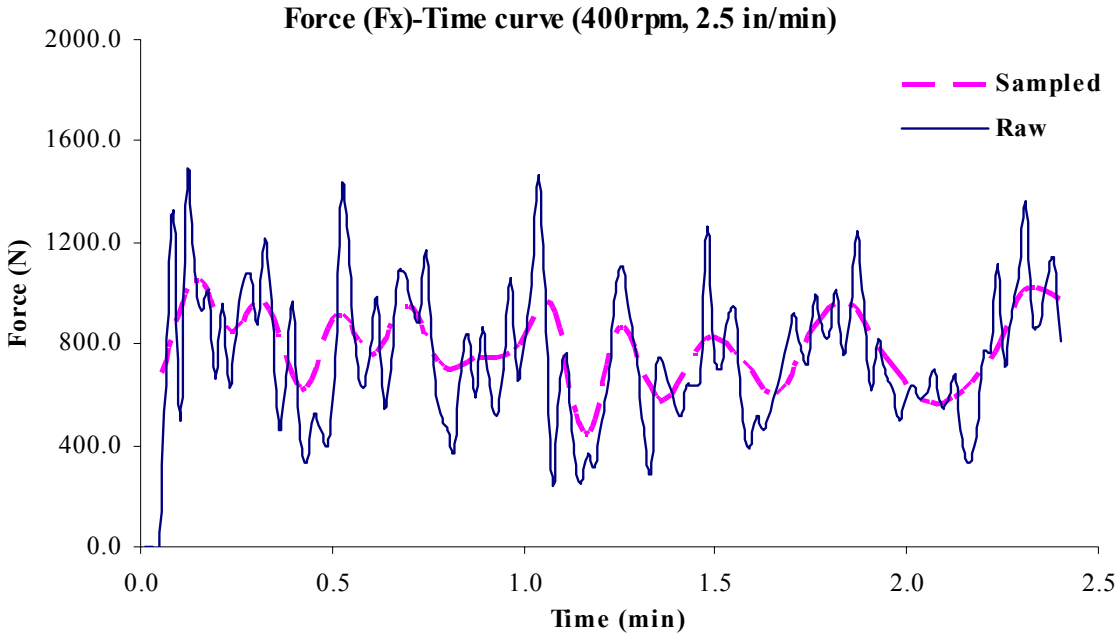

Figure 4-3 Plot showing raw and sampled forces data Fx with respect to time for FSP AA5052@400rpm,2.5in/min

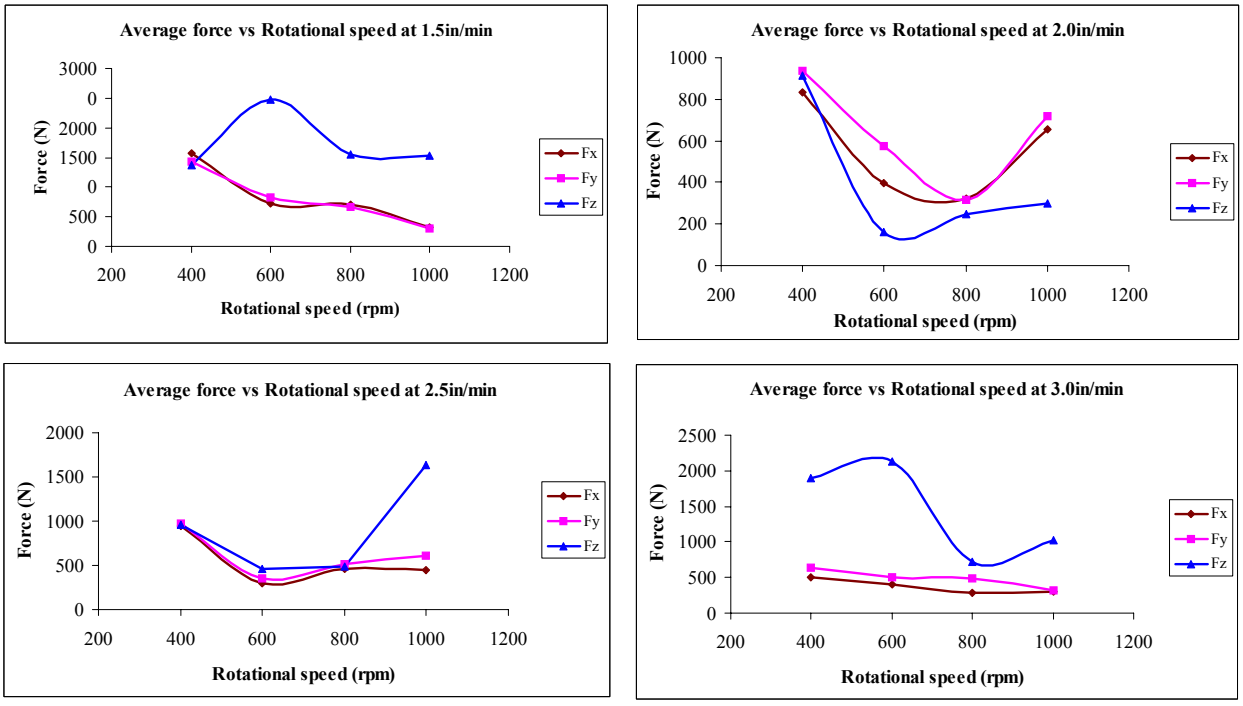

Figure 4-4 Plots of average forces (Fx, Fy and Fz) vs rotational speed @ various translational speeds

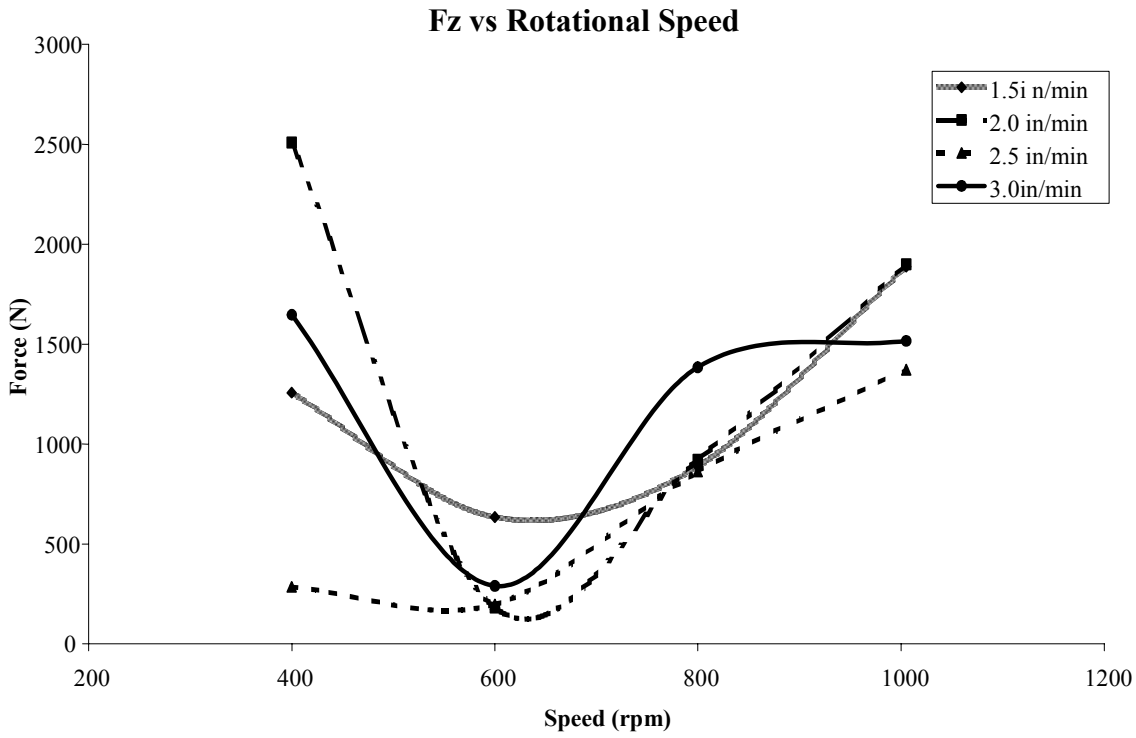

Figure 4-5 Plot of Force Fz vs. Rotational speeds at different translational speeds for AA5052

AA 6061-T6 sheets were friction stir processed and the cutting forces (Fx, Fy and Fz) are measured. The plots of these processing forces with the time of processing are presented in Figure 4-8 and Figure 4-9. The results indicate that processing forces are becoming unstable and varying with time as the rotational speed is increased. It can be thus concluded that the forces generated are highly dependent on the material of the sheet processed.

Figure 4-10 shows the Fz vs time plot for multiple pass FSP process. The forces seemed to increase until the third pass but as the sheet was heated up because of the frictional heat generated the processing forces decreased. From this we can conclude that the preheating of the sheet would reduce the processing forces.

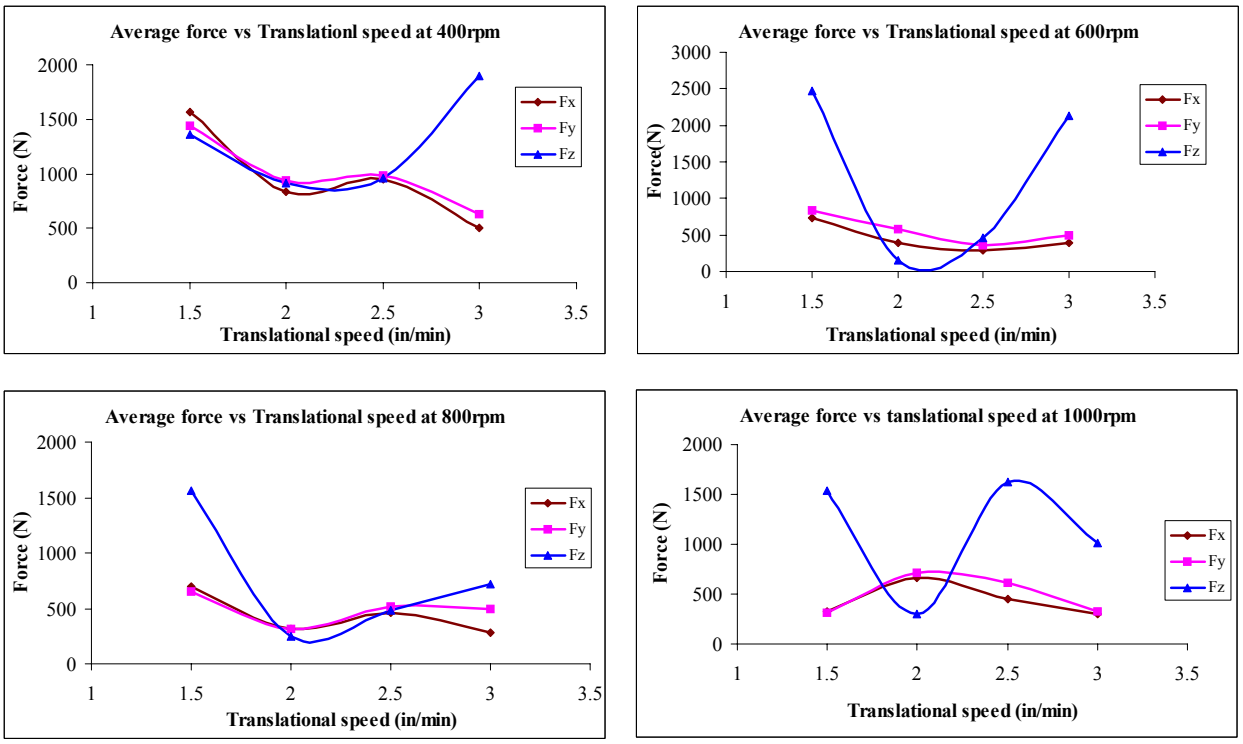

Figure 4-6 Plots of average forces (Fx, Fy and Fz) vs translational speed @ various rotational speeds

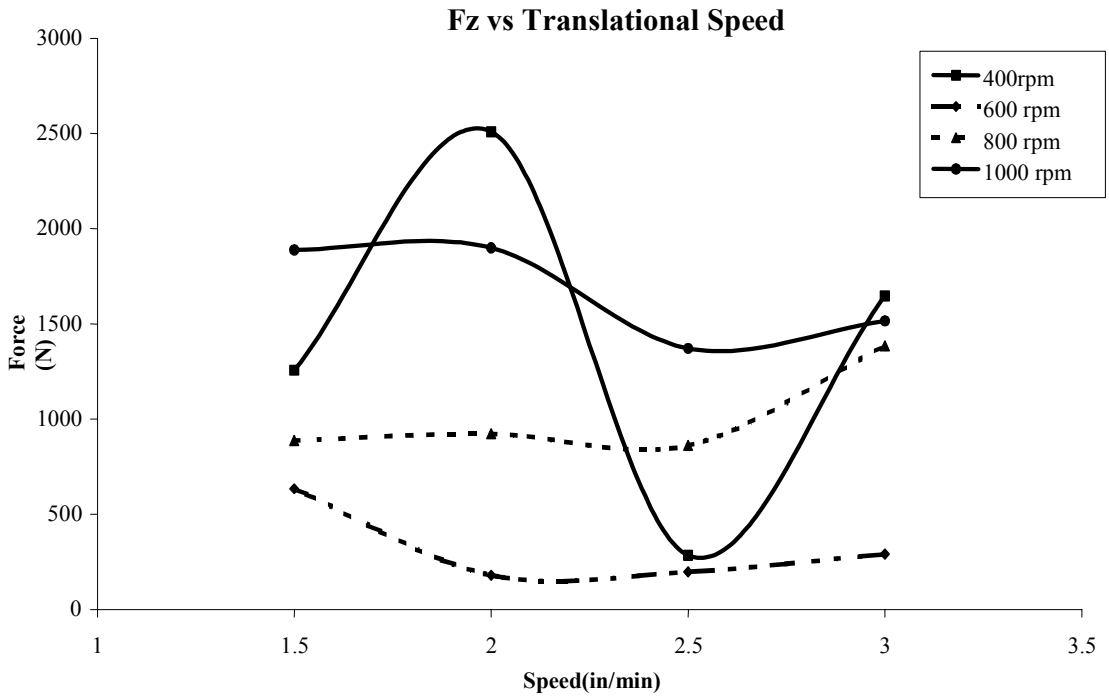

Figure 4-7 Plot of Force Fz vs. Translational speeds at different rotational speeds

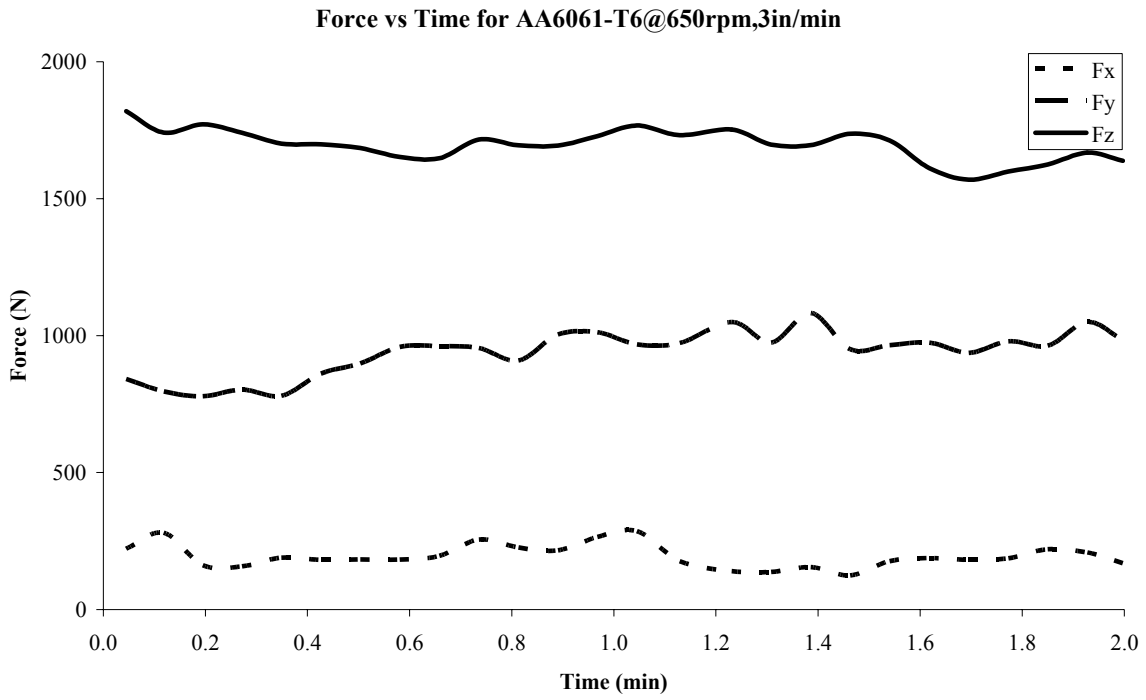

Figure 4-8 Processing force plot with respect to time for AA6061-T6 alloy FS processed at 650rpm and 3in/min

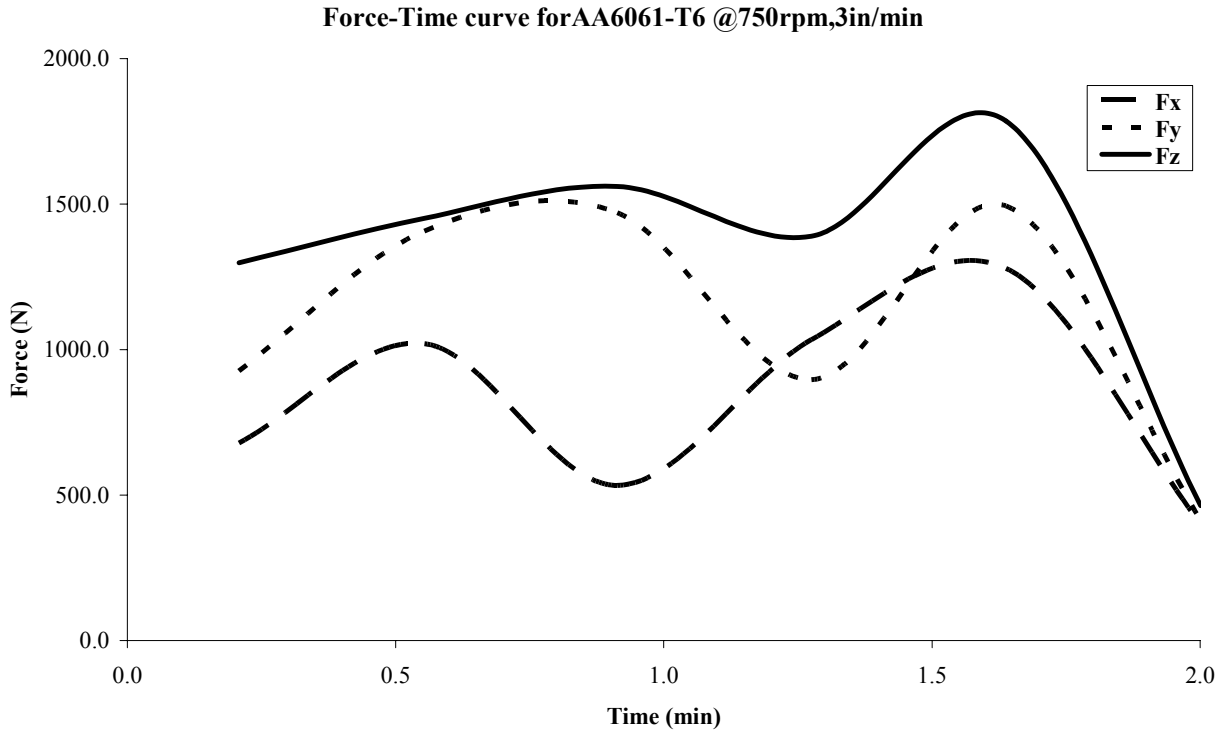

Figure 4-9 Processing force plot with respect to time for AA6061-T6 alloy FS processed at 750rpm and 3in/min

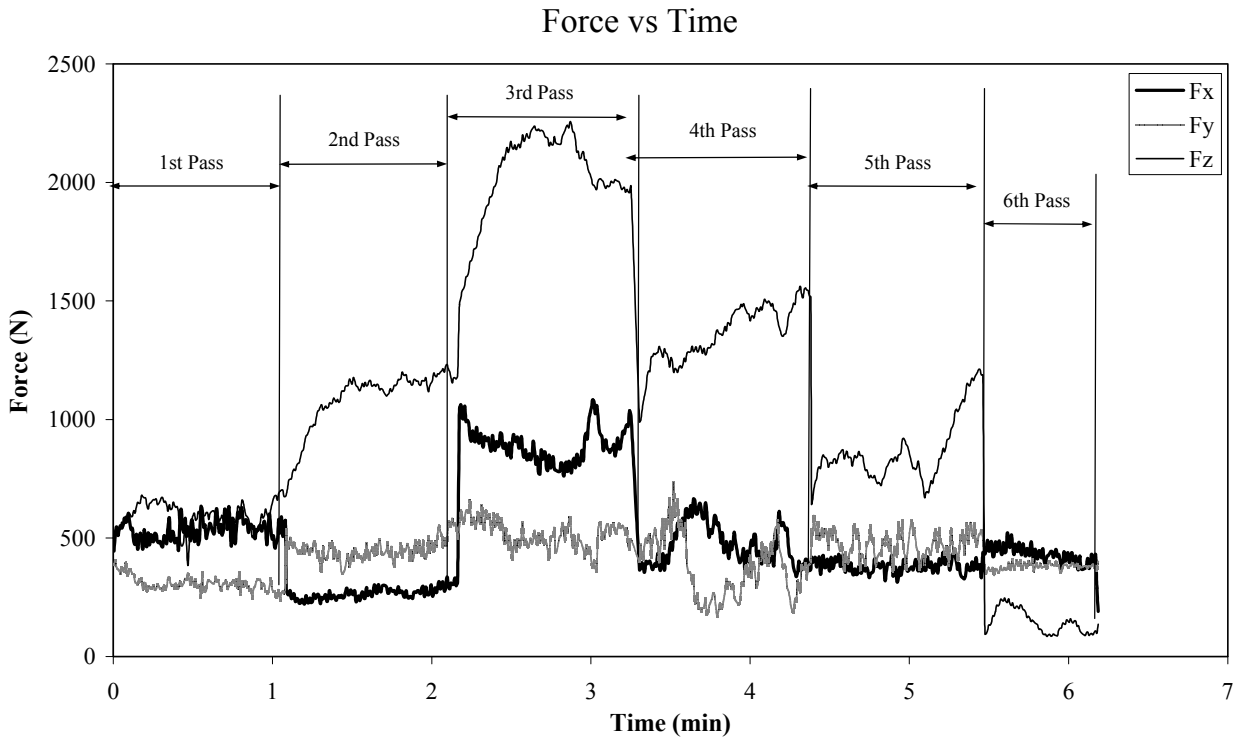

Figure 4-10 Plot of average forces vs time during multiple passes FSP of AA5052 @ 800rpm, 2.5in/min

4.4 Microstructural analysis

The microstructure of the AA5052 unprocessed was observed under polarized light of an optical microscope and FS processed zone under Jeol-2000FX TEM. AA5052 sheets FS processed at various combinations of rotational and translational speeds are cut along the cross section and are prepared for metallographic study (to observe under both the optical microscope and also under transmission electron microscope for qualitative and quantitative analysis respectively). The optical microscope pictures of the FS processed AA 5052 are presented in Error! Reference source not found.. The grain refinement as a result of FSP can be qualitatively analyzed using these optical microscope pictures. In order to quantify this refinement the processed zone is observed under TEM.

Figure 4-13 shows the optical microscope pictures of the unprocessed (Figure 4-13a) and TEM pictures of the processed zone (Figure 4-13 b, c and d) with increasing translational speeds at a constant rotational speed of 600rpm. These results indicate that the grain size of as received

AA 5052 is about 37.5μm and the processed zone shows a significant grain refinement after FS processing. It is observed from this figures that at 600 rpm as the translational speed varied from 1.5-3.0 in/min the grain size decreases from 2.25- 1.3μm. This variation is plotted in Figure 4-15a.

Similarly the Figure 4-14 shows the TEM pictures of the FS processed zone at 2.5ipm and varied rotational speed (400 rpm-1000rpm). It is observed that the grain size increased as the rotational speed was increased even though there was a significant grain refinement at each speed which resulted in equiaxed and homogeneous grains. The variation of grain size with respect to the rotational speed is plotted in Figure 4-15b.

FSP of large grained and inhomogeneous AA5052 resulted in fine grained homogeneous and equiaxed grains. This is clearly depicted in Figure 4-11. It is observed that the grain refinement decreases at any particular translational speed with increasing rotational speed, which is accordance to the observations made by Sato et.al. [9]. According to this observation of Sato et.al, the grain size increase was exponential with the maximum temperature which was proportional to the increase in the rotational speed. Thus it is very evident that as either rotational speed increases the frictional heat produced increases and thus is the maximum temperature in the processed zone leading to the increase in the grain size.

There is another interesting characteristic called the onion rings formation, was also observed in the processed zone as shown in Figure 4-12. Onion rings are formed because of the frictional heat generated due to tool rotation and extrusion of the material on the retracting end due to forward movement. It is termed as a geometric effect characterized by semicylindrical rings. There are wide bands at the center and they become narrow as moved towards the end, spacing between rings equal to the forward movement of the tool. These rings were also observed by Khrishnan [8] according to the literature.

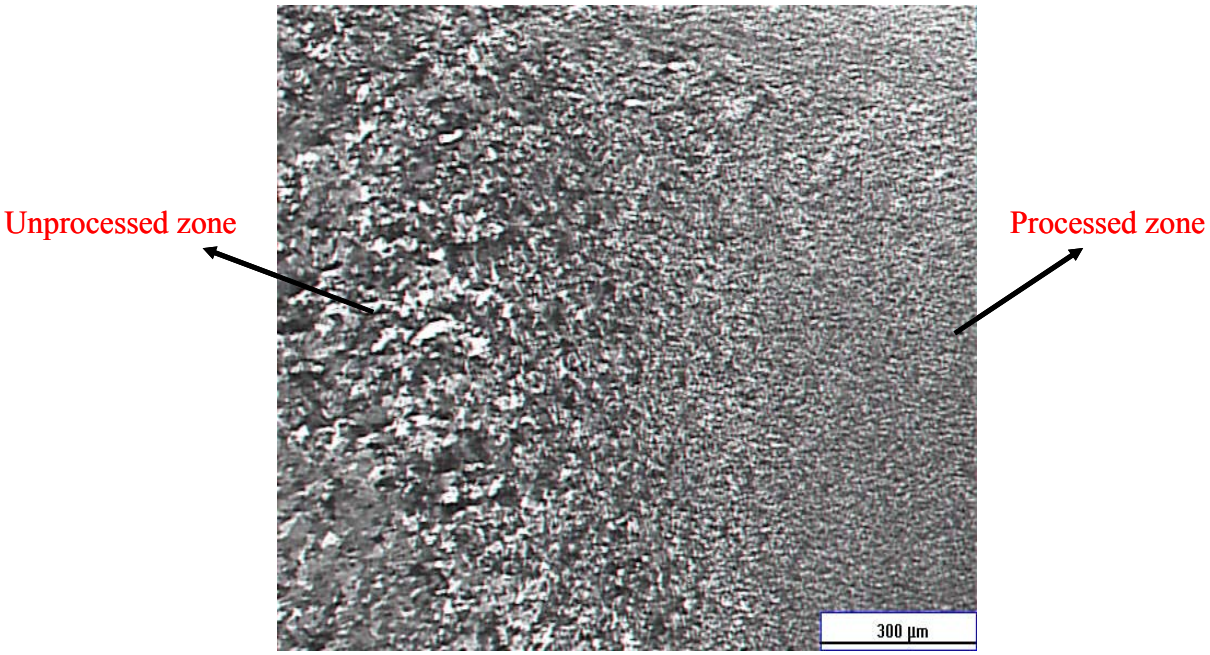

Figure 4-11 Transition zone from unprocessed to FS processed AA5052

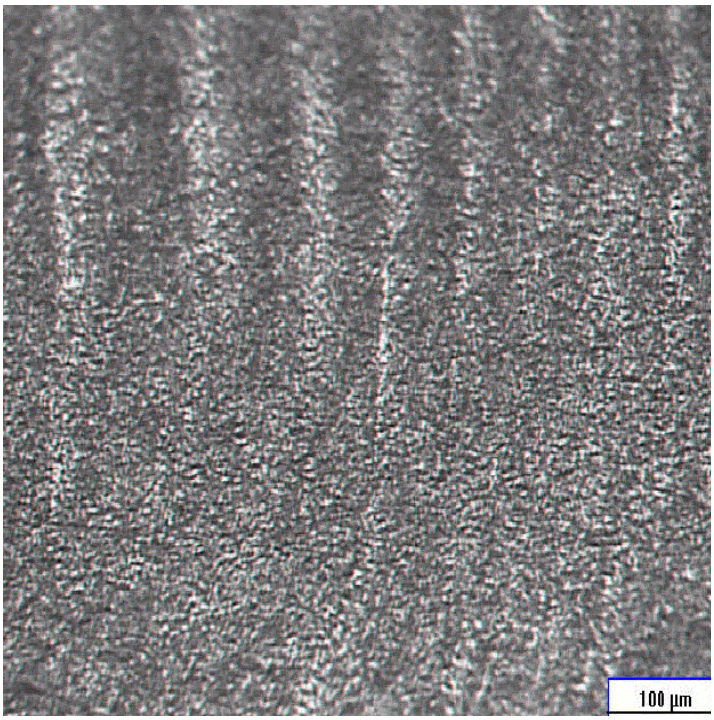

Figure 4-12 Optical microscope picture showing the onion rings in FS processed zone

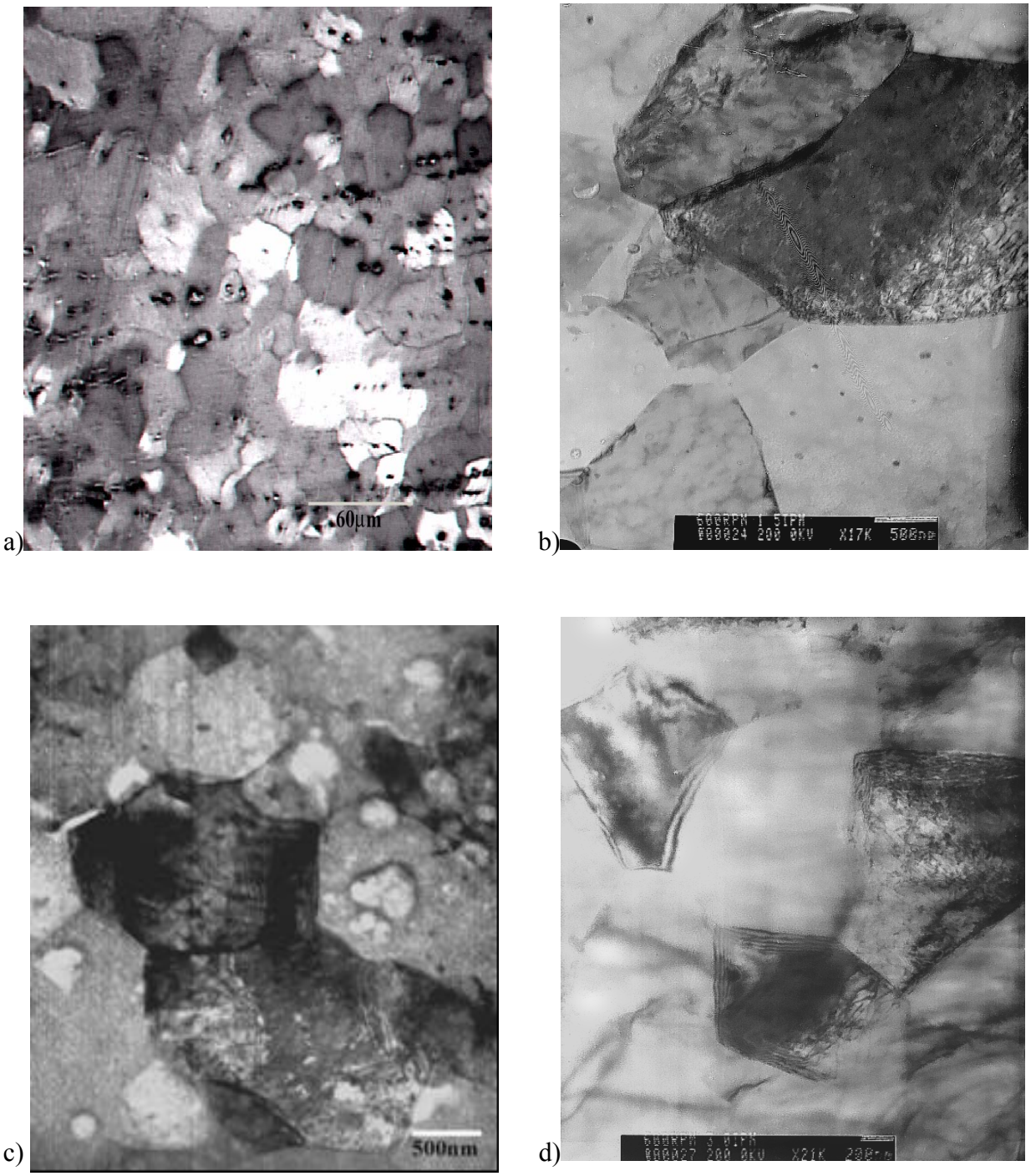

Figure 4-13 a) Optical microscope picture of as received AA 5052 and TEM pictures of FS processed AA 5052 at 600rpm and b) 1.5, c) 2.5 and d) 3.0 in/min

a)

b)

c)

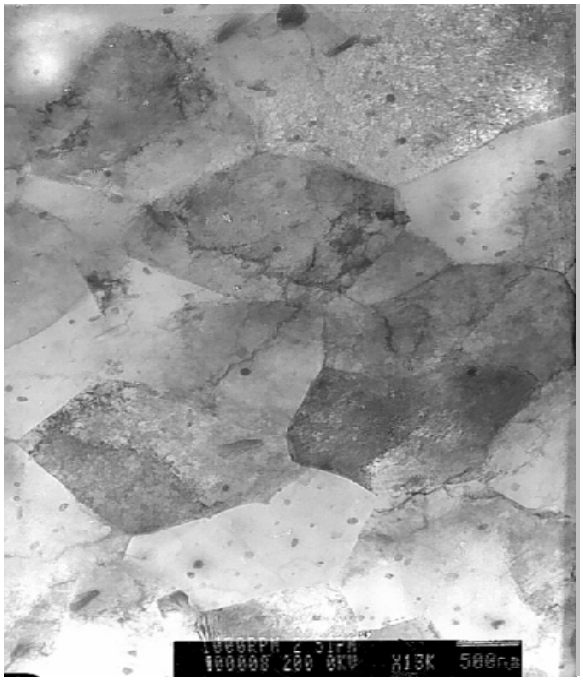

d)

Figure 4-14 FS processed AA 5052 at 2.5in/min a) 400 rpm, b) 600 rpm, c) 800 rpm and d) 1000rpm

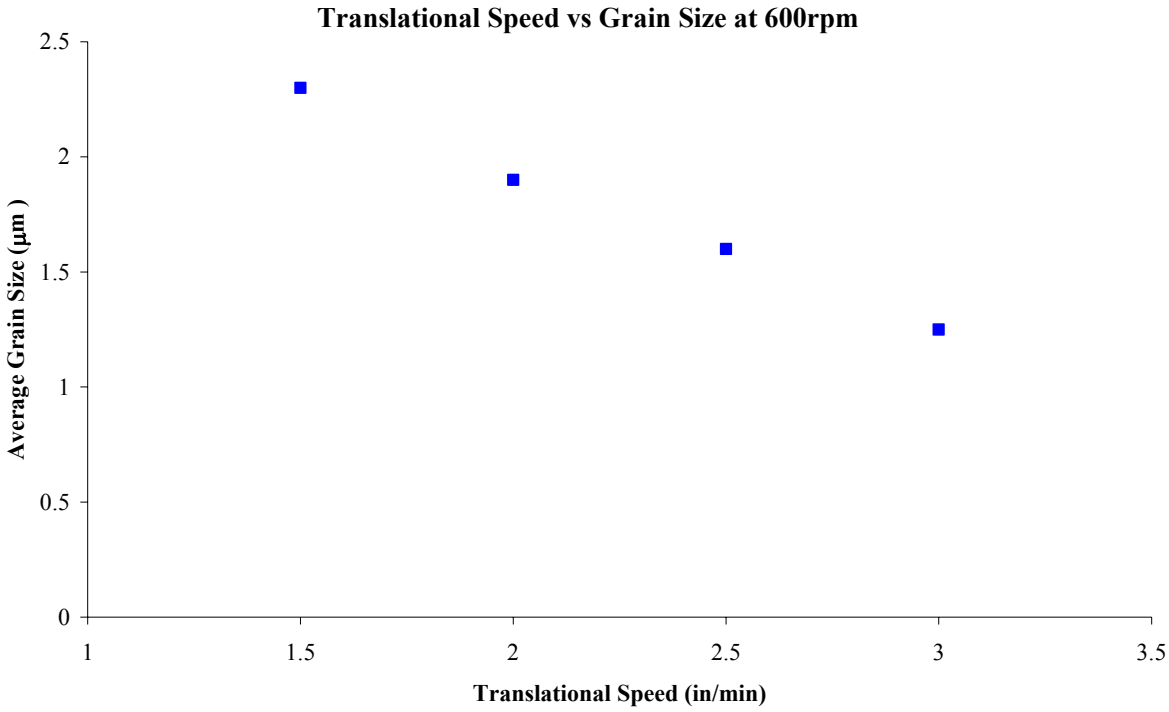

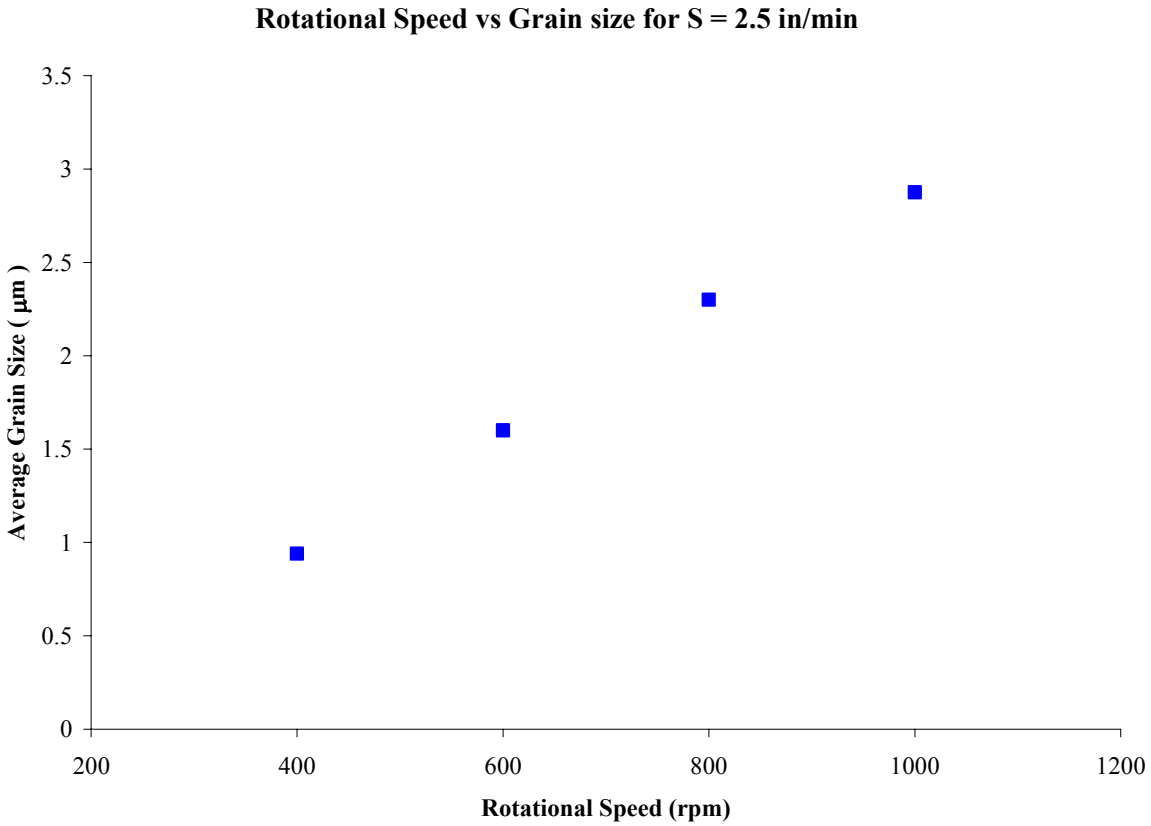

Figure 4-15 Plot of Average grain size with a) translational speed and b) rotational speed

4.5 Correlation between the forces and the microstructure

From the above two sections we can observe that there exists a relationship between the grain size, plunging force Fz and rotational speed i.e. it is observed that as the rotational speed increases the forces increase and also the resulting grain refinement decreases. The increase in force with respect to the rotational speed seems to be exponential where as the grain size seems to be linear. And also the grain refinement is more at higher translational speeds though there is no significant influence of the translational speed on the plunging force. This might be because of lack of sufficient time available for the temperature increase and thus the grain growth of the refined grains at higher translational speeds.

Chapter 5 Finite element simulation of FSP of aluminum alloys

A number of studies have been carried out on the metallurgical characteristics of friction stir processing in aluminum alloys. Some simplified analytical models have also been used to analyze the heat flow and distribution during friction stirring which could be related with microstructure evolved in order to optimize and make the process commercially viable. Finite element method is one of the methods which have proven to be the best for predicting and understanding a process especially when it is complex and new.

The microstructure of friction stir processed region of aluminum shows three different zones: thermo-mechanical affected zone (TMAZ), heat affected zone (HAZ) and the parent metal. The temperature field and mechanical deformation during the FSP appears to dictate the formation of various microstructure zones. In addition to microstructural investigations, several simplified analytical models have been used to analyze the heat flow process associated with FSP/FSW. These heat flow analysis procedures were based on Rosenthal point heat source solutions, which were calculated assuming constant surface area and pressure between the tool and work piece.

In this work an attempt is made to understand the phenomena associated with FSP and compare it with the experimental data. The presented results are preliminary and have to be improvised further. The present study mainly focuses on analyzing the temperature distribution over the tool during FSP using the commercial code – Fluent, as the tool design and material play a very important role in FSP.

5.1 Methodology [60]

The finite element simulation of any process in general consists of different stages. These are clearly depicted in Figure 5-1.

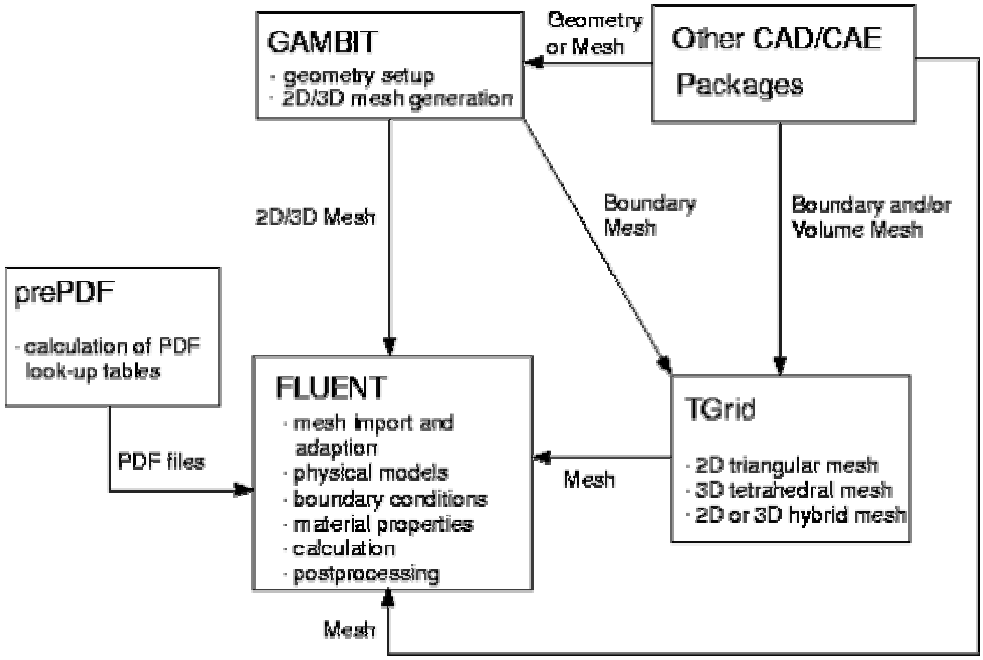

Figure 5-1 Basic Program Structure

Following are the steps involved in finite element analysis of FSP

1. Create the model geometry and grid
2. Start the appropriate solver for 2D or 3D modeling
3. Import the grid
4. Check the grid
5. Select the solver formulation
6. Choose the basic equations to be solved: laminar or turbulent (or inviscid), chemical species or reaction, heat transfer models, etc.
7. Identify additional models needed: fans, heat exchangers, porous media, etc
8. Specify material properties
9. Specify the boundary conditions
10. Adjust the solution control parameters
11. Initialize the flow field
12. Calculate a solution
13. Examine the results
14. Save the results

15. If necessary, refine the grid or consider revisions to the numerical or physical model

5.2 Modeler Details

GAMBIT is a software package designed to build and mesh models for computational fluid dynamics (CFD) and other scientific applications. GAMBIT receives user input by means of its graphical user interface (GUI). The GAMBIT GUI makes the basic steps of building, meshing, and assigning zone types to a model simple and intuitive, yet it is versatile enough to accommodate a wide range of modeling applications.

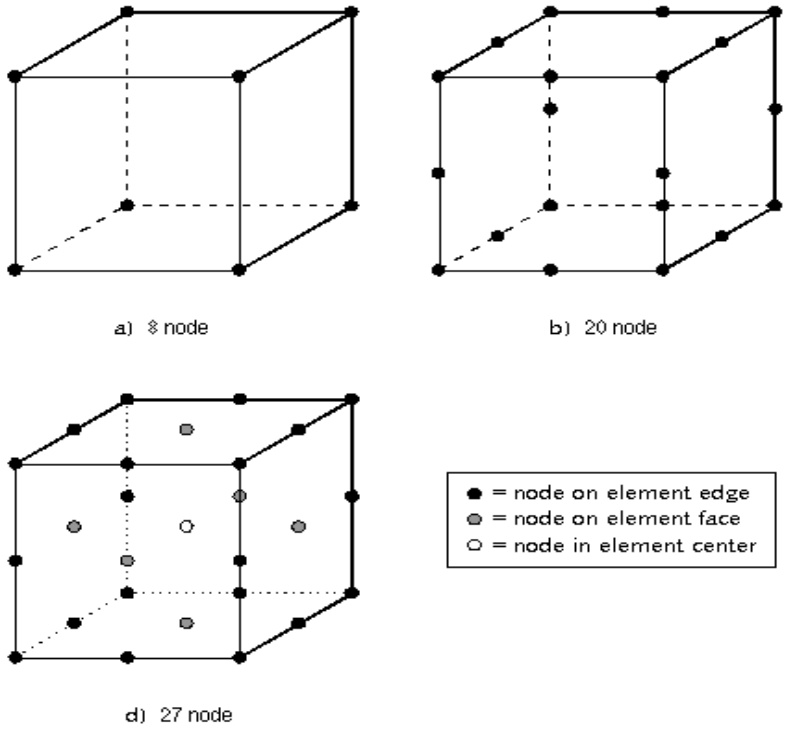

Figure 5-2 Hexahedron volume element node patterns

Each mesh element includes at least eight nodes-located at the corners of the element. If an alternative volume element node pattern is specified, then GAMBIT creates either 20 or 27 nodes per mesh element.

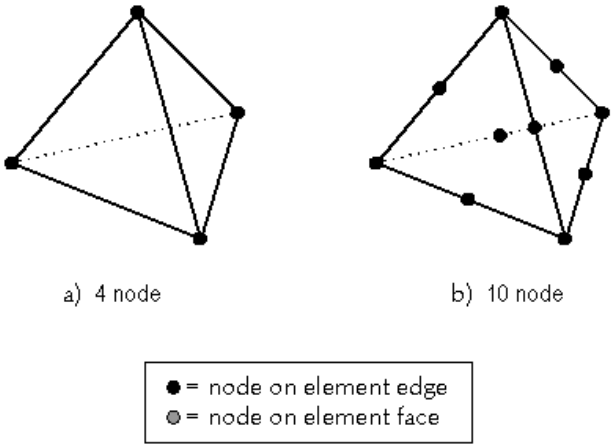

Figure 5-3 Tetrahedron volume element node patterns

5.2.1 General Applicability

The map volume-meshing scheme can only be applied to volumes that can be meshed such that the mesh represents a logical cube. To represent a logical cube, a volume mesh must satisfy the following general requirements.

1. There must be exactly eight mesh nodes that are attached to only three mesh element faces. (These eight mesh nodes comprise the corners of the logical cube.)
2. Each of the eight corner mesh nodes must be connected to three other corner mesh nodes by means of a straight chain of mesh edges-that is, a chain of mesh edges all of which belong to a single logical row of mesh nodes.
3. These include prisms (wedges) or pyramids. (Both conformal and hanging-node meshes are acceptable.)

5.3 Solver Details

FLUENT is a computational technology that enables us to study the dynamics of things that flow. Using this CFD package, we build a computational model that represents a system or device that is to be studied. The fluid flow physics is applied to this virtual prototype, and the

software outputs a prediction of the fluid dynamics. It not only predicts fluid flow behavior, but also the transfer of heat, mass (such as in perspiration or dissolution), phase change (such as in freezing or boiling), chemical reaction (such as combustion), mechanical movement (such as an impeller turning), and stress or deformation of related solid structures (such as a mast bending in the wind).

Table 5-1 Allowable combinations of type options for different CFD solvers

	Type Option					
Solver	Map	Submap	Tet Primitive	Cooper	TGrid	Stairstep
FIDAP	X	X	X	X	X	X
FLUENT/UNS	X	X	X	X	X	X
FLUENT 5/6	X	X	X	X	X	X
FLUENT 4	X	X		X		X
NEKTON	X	X	X	X		X
RAMPANT	X	X	X	X	X	X
POLYFLOW	X	X	X	X	X	X
Generic	X	X	X	X		

Table 5-2 Elements and Type option combinations for volume meshing

	Elements Option		
Type Option	Hex	Hex/Wedge	Tet/Hybrid
Map	X		
Submap	X		
Tet Primitive	X		
Cooper	X	X	
TGrid			X
Stairstep	X		

5.3.1 Modeling capabilities of FLUENT solver

- Flows in 2D or 3D geometries using unstructured solution-adaptive triangular/tetrahedral, quadrilateral/hexahedral, or mixed (hybrid) grids that include prisms (wedges) or pyramids. (Both conformal and hanging-node meshes are acceptable.)
- Incompressible or compressible flows
- Steady-state or transient analysis
- Inviscid, laminar, and turbulent flows
- Newtonian or non-Newtonian flow
- Convective heat transfer, including natural or forced convection

The above are some of the modeling capabilities of Fluent.

5.3.2 Applications of FLUENT

- Process and process equipment applications

- Power generation and oil/gas and environmental applications
- Aerospace and turbo-machinery applications
- Automobile applications
- Heat exchanger applications
- Electronics/HVAC/appliances
- Materials processing applications
- Architectural design and fire research

5.4 Procedure Adopted

Following are the steps involved in the analysis of FSP

Step 1: Generation of the model geometry and grid

The present process of friction stir is modeled using this software. The exact geometry of the pin and shoulder are created. The pin of ϕ 1/8" and the shoulder of ϕ ¾" are modeled and the sheet of dimensions 4"x6"x1/8" are generated. The volumes: the sheet and the pin-shoulder assembly are meshed using mapped hexahedral Figure 5-2 and T-grid tetrahedral Figure 5-3 elements respectively. Figures 5-4 and 5-5 show different views of grid used for the analysis.

Step 2: Defining boundaries and exporting the mesh

- Solver option is selected as Fluent 5/6.
- The sheet is defined as a fluid zone and the pin-shoulder assembly as a solid zone.
- The sheet inlet is defined as velocity inlet and the exit as outflow
- And the remaining surfaces of both the sheet and the pin-shoulder assembly are defined as walls.
- The mesh thus modeled is exported to Fluent5/6.

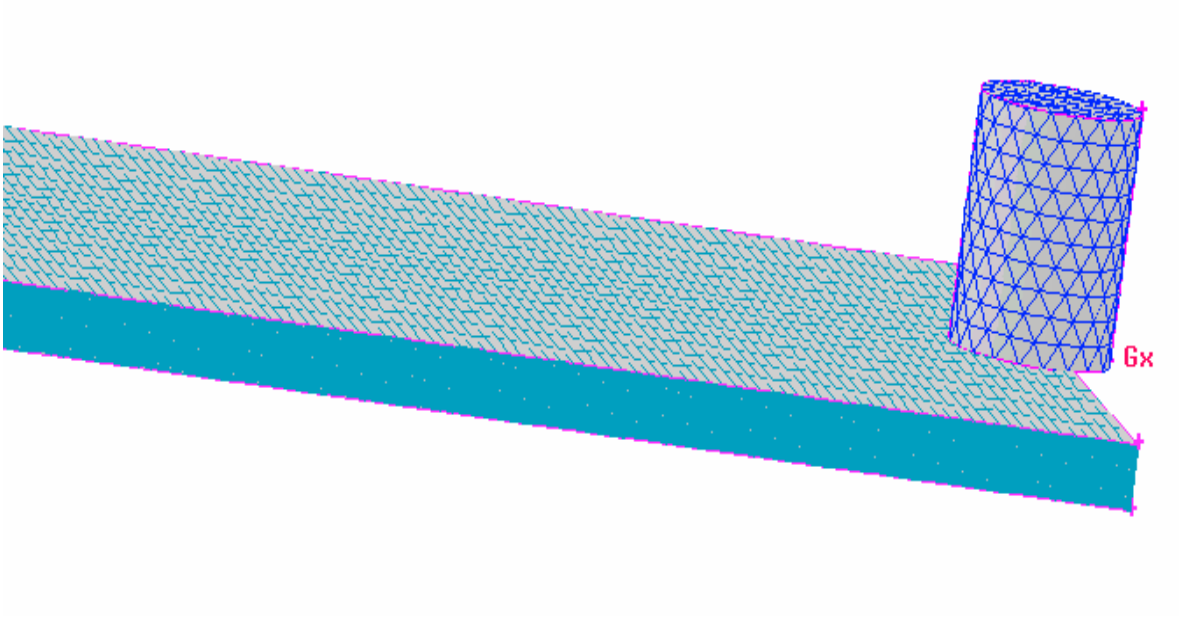

Figure 5-4 Isometric view of the meshed tool and work piece assembly

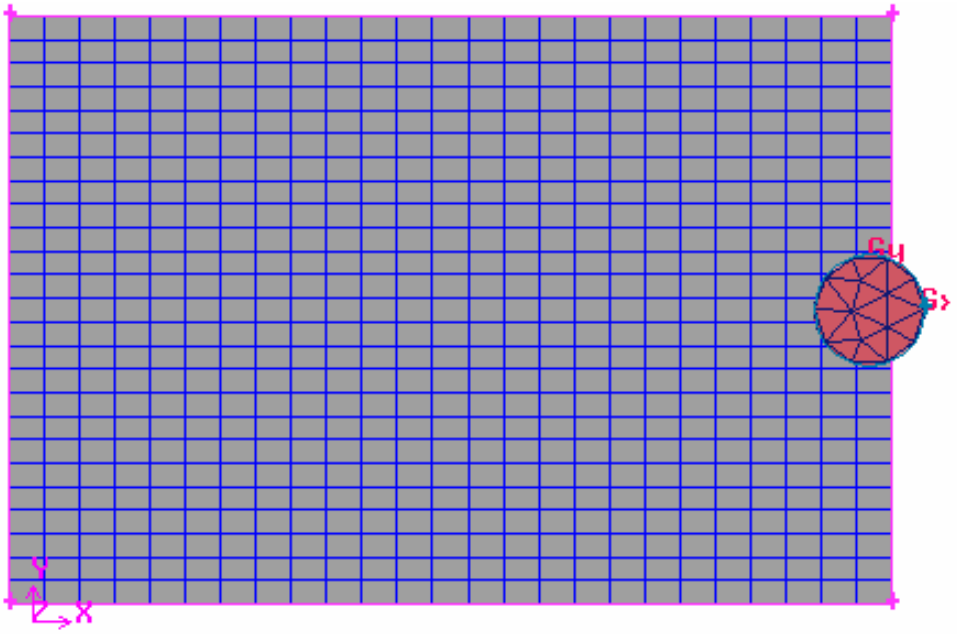

Figure 5-5 Top view of the tool and work piece assembly

Step 3: Solver selection and solving the problem

- Starting the appropriate solver: 3D double precision model

- Importing the grid: The mesh file generated by GAMBIT is imported into FLUENT. The imported mesh is shown in figure 5-6.

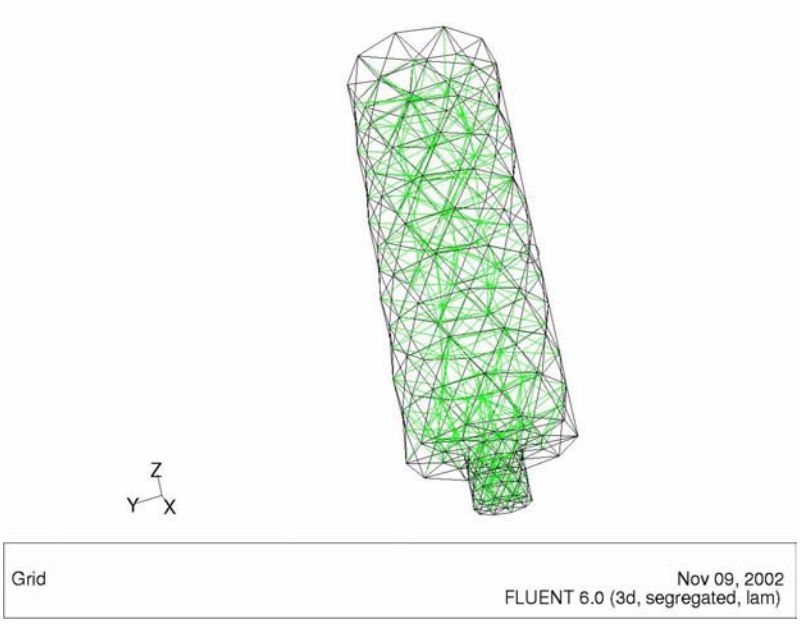

Figure 5-6 Imported mesh in FLUENT6.0

- Checking the grid.
    - The mesh is checked for any irregularities. The mesh imported is a non-confirmal mesh
- Select the solver formulation.
    - Solver : Segregated
    - Formulation : Implicit
    - Time : Steady
    - Space : 3D
    - Velocity Formulation : Absolute
- Chosen basic equations to be solved:
    - Laminar flow
    - Steady state heat transfer models

Discretization of the governing equations can be illustrated most easily by considering the steady-state conservation equation for transport of a scalar quantity ϕ. This is demonstrated by the following equation written in integral form for an arbitrary control volume *V* as follows:

$$\oint \rho\phi\vec{v}.d\vec{A} = \oint \Gamma_\phi \nabla\phi.d\vec{A} + \int_V S_\phi dV$$

where ρ = density, $\vec{v}$ = velocity vector = $u\hat{i} + v\hat{j}$ in 2D,

Γ_ϕ = Diffusion coefficient for ϕ, $\vec{A}$ = surface area vector

∇_ϕ= Gradient of ϕ = $(\partial\phi/\partial x)\hat{i} + (\partial\phi/\partial y)\hat{j}$ in 2D

S_ϕ = source of ϕ per unit volume

- Specifying material properties
  - Pin-shoulder assembly: It is defined as a solid zone with the material properties as in Table 5-3
  - Sheet: It is defined as a fluid zone with the material properties as in Table 5-3.
- Specifying the boundary conditions
  - Pin is defined as a solid zone with constant rotational speed (400-900rpm)
  - Work piece is defined as a fluid zone with a absolute velocity of 1mm/s and with a free stream temperature of 27^0C
  - Pin surface and the shoulder lower surface are defined as walls with constant heat flux of 1000 J/s
  - The sheet inlet is defined as a velocity inlet with flow velocity 1mm/sec
- Adjust the solution control parameters.
- Initialize the flow field on the sheet inlet

- The imported mesh from gambit (Figure 5-6) is solved in Fluent using a simple thermo-mechanical model.

5.5 Results and Discussion

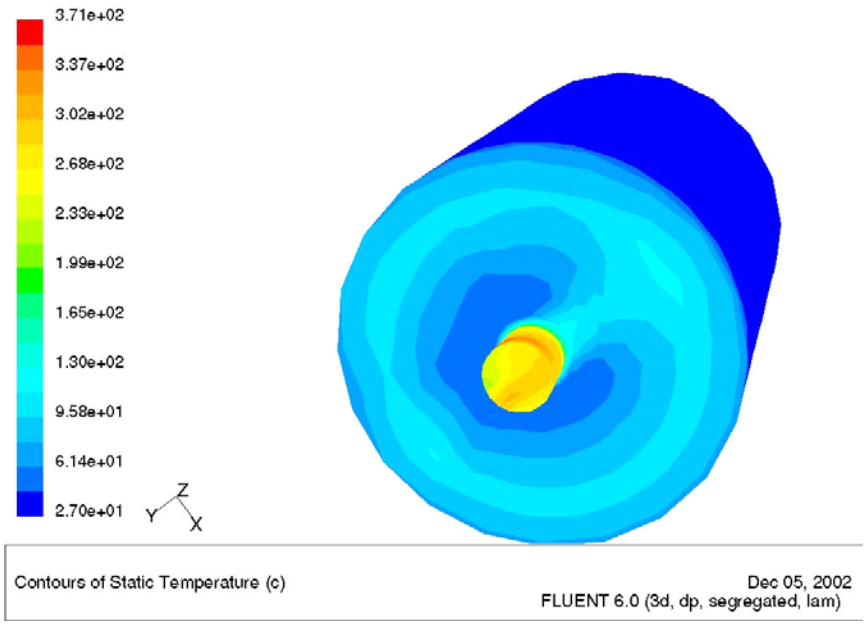

Figure 5-7 Temperature distribution at 400 rpm and transverse speed 1mm/s

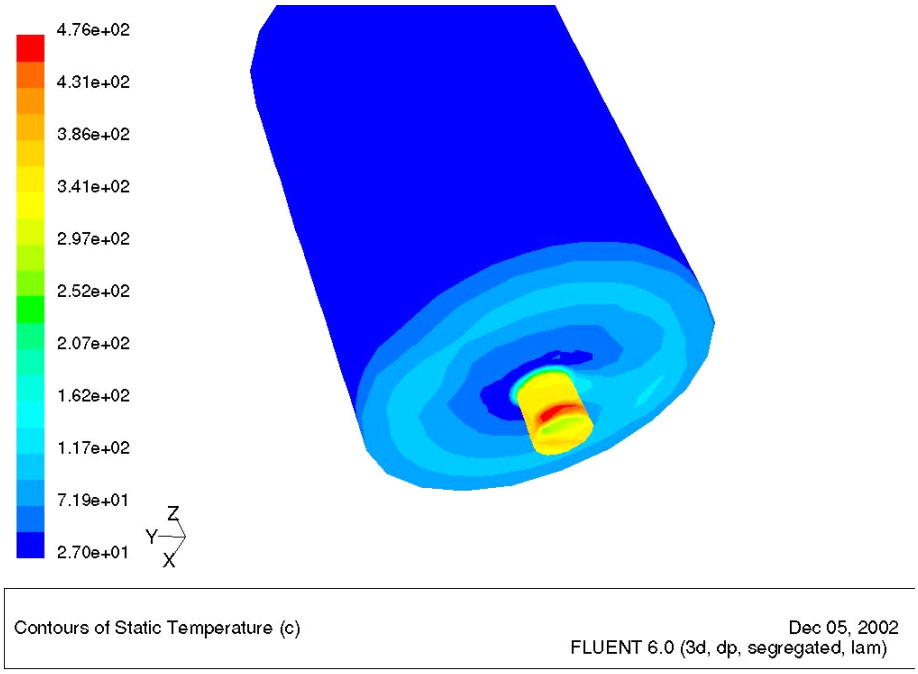

Figure 5-8 Temperature distribution at 600 rpm and transverse speed 1mm/s

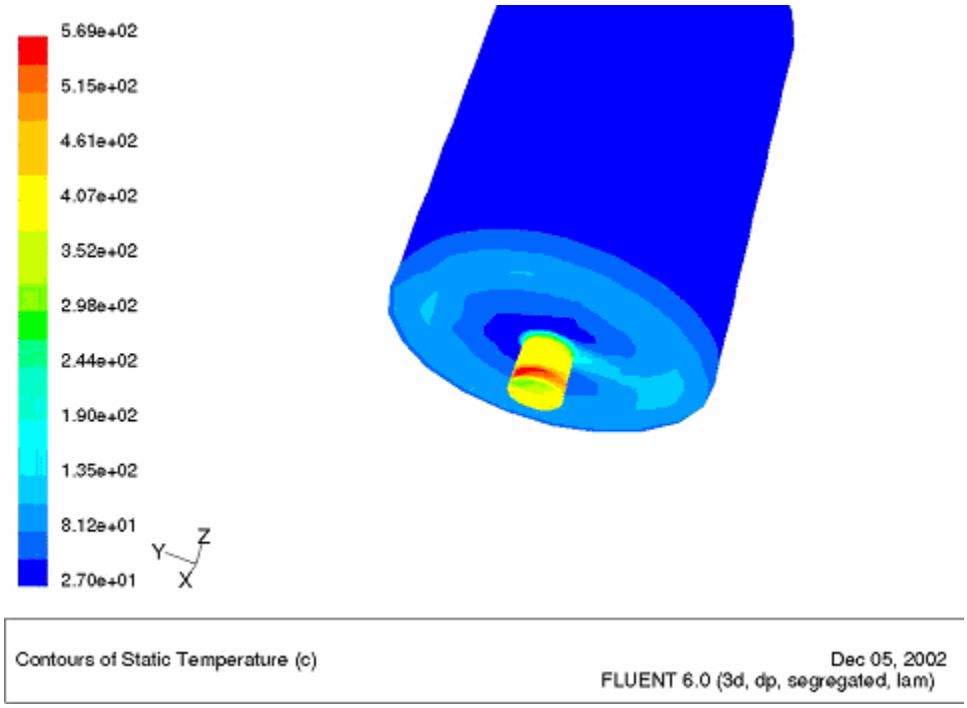

Figure 5-9 Temperature distribution at 750 rpm and transverse speed 1mm/s

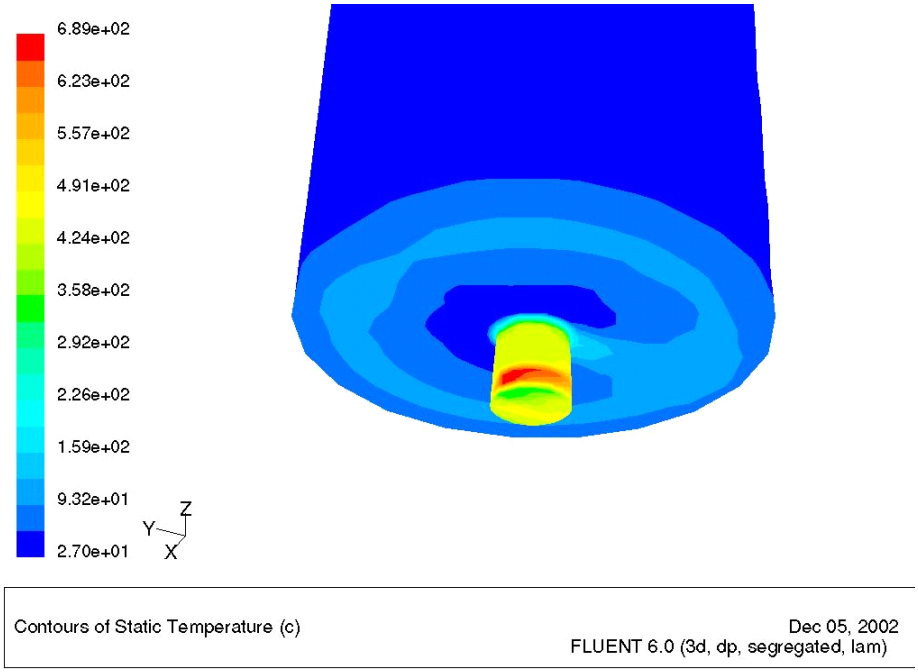

Figure 5-10 Temperature distribution at 900 rpm and transverse speed 1mm/s

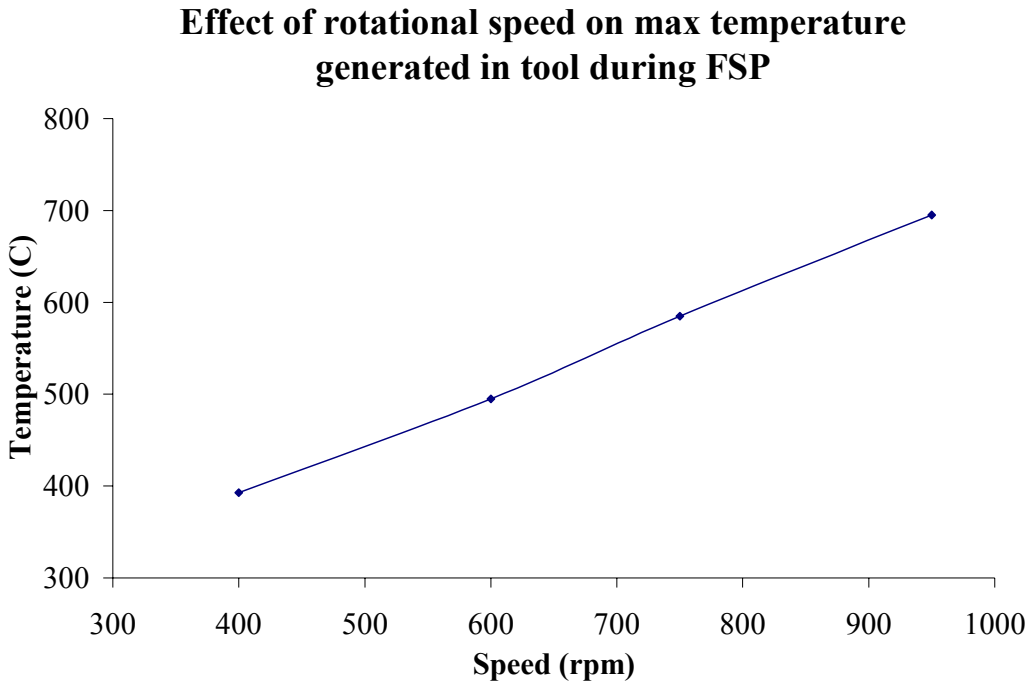

Figure 5-11 Maximum temperature in the tool vs rotational speed at 1.0 mm/s

The temperature distribution over the tool is simulated using a simple thermomechanical model [Figure 5-7 Temperature distribution at 400 rpm and transverse speed 1mm/s). The results indicate that the maximum temperature attained during FSP of AA6061-T6 increase with increasing rotational speeds as shown in Figure 5-11. The maximum temperature attained in the tool follows the same trend as observed by Ulysse [44]. The temperature attained depends on the material that is under processing, material of the tool and also the tool design.

Table 5-3 Material properties [8&9]

Property	**Material**	
	A2-Tool steel (tool assembly)	**Aluminum6061-T6 (work piece)**
Density (kg/m^3)	8120	2719
Thermal conductivity (W/m-^{0}C)	26	150
Specific heat capacity (j/kg-^{0}C)	525	875
Viscosity (kg/m-s)	-	17894

Chapter 6 Conclusion and Future Work

Friction stir processing has immensely high potential in the field of thermo mechanical processing of various alloys especially the aluminum alloys. This thesis presents preliminary investigation of friction stir processing of AA5052. The processing forces and the resultant microstructure for FS processed AA5052 are presented for different combinations of rotational and translational speeds. The correlation of plunge force and microstructure with the process parameters for the optimization of process is a unique approach which has been the main motivation behind this project.

The results presented indicate that there is a significant effect of the process parameters like the rotational and translational speeds on the resulting microstructure and the plunge force during FSP of AA5052. The plunge force increased with increasing rotational speed and also the grain refinement was more at low rotational speeds. Similarly it is seen that the grain refinement is higher at higher translational speeds though it is observed that there is no significant influence of the translation speed on the plunge force. Thus it can be said that monitoring and controlling the forces generated during FSP through the process parameters like rotational and translational speeds is one of the efficient ways of getting a desired grain size refinement and thus optimizing the process and making it more cost effective. The results presented for AA 5052 and AA6061-T6 alloys indicate that the process parameters, forces generated and are different for each alloy and its initial conditions like the heat treatment etc.

Results of the FE analysis of the tool indicate that the maximum temperatures attained in the tool during FSP increase with increasing rotational speeds. Thus it can also be expected that the maximum temperatures generated in the sheet being processed to increase with increasing rotational speed at a constant translational speed.

Thus it can be concluded that understanding of these effects of process parameters on the plunge force and resulting microstructure can be used effectively in not only analyzing the process but also in optimizing it.

Future work

As this preliminary study clearly explains the potential of this new and unique process there are many aspects of the process that can be further investigated in order to establish an empirical relation between these process parameters, the resulting forces and grain size and thereby optimizing the process of FSP and making it more applicable to the industry.

- More experiments are to be performed in order to thoroughly understand the process and its dependence on other process parameters and alloys. As the results of present study indicate, controlling the forces through process parameters and thus obtaining a desired grain size refinement is a unique and effective idea. Hence further investigations on the forces generated during single and multiple passes for different alloys at different conditions and for different process parameters might be very beneficial
- Preheating of the samples be for FSP might reduce the forces significantly and thus produce finer grains and optimize the process
- As the literature suggests that these fine grained FSP alloys might exhibit improved strength as well as ductility. Hence mechanical testing of these FS processed sheets like high temperature tensile testing, microhardness testing, deformation mapping etc. is another area of interest.
- Tool design and material plays a crucial role in FSP hence tool design modifications could be another area for further research.
- FE analysis of FSP using thermomechanical modeling and validating these results by comparing to the temperature profiles obtained by the use of infrared camera during experiment would help in better understanding of the effect of process parameters on the flow of material and temperature fields during the process.

Appendix A

Forces – Time Curves during Friction Stir Processing of AA 5052 for various combinations of rotational and translational speeds

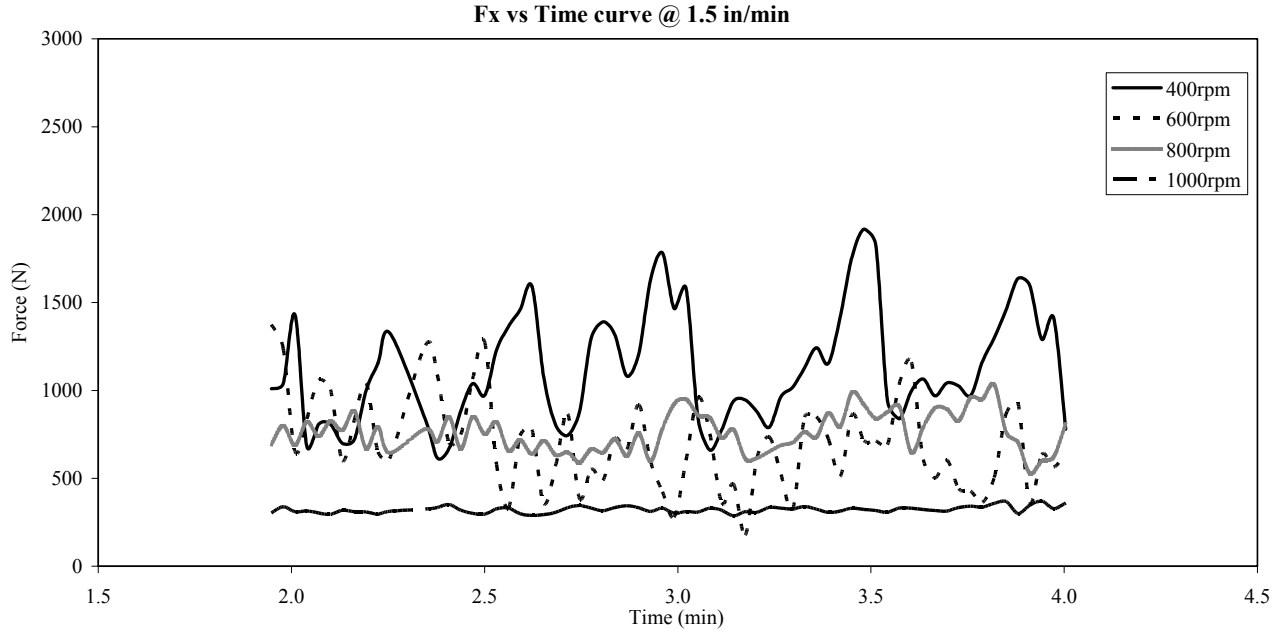

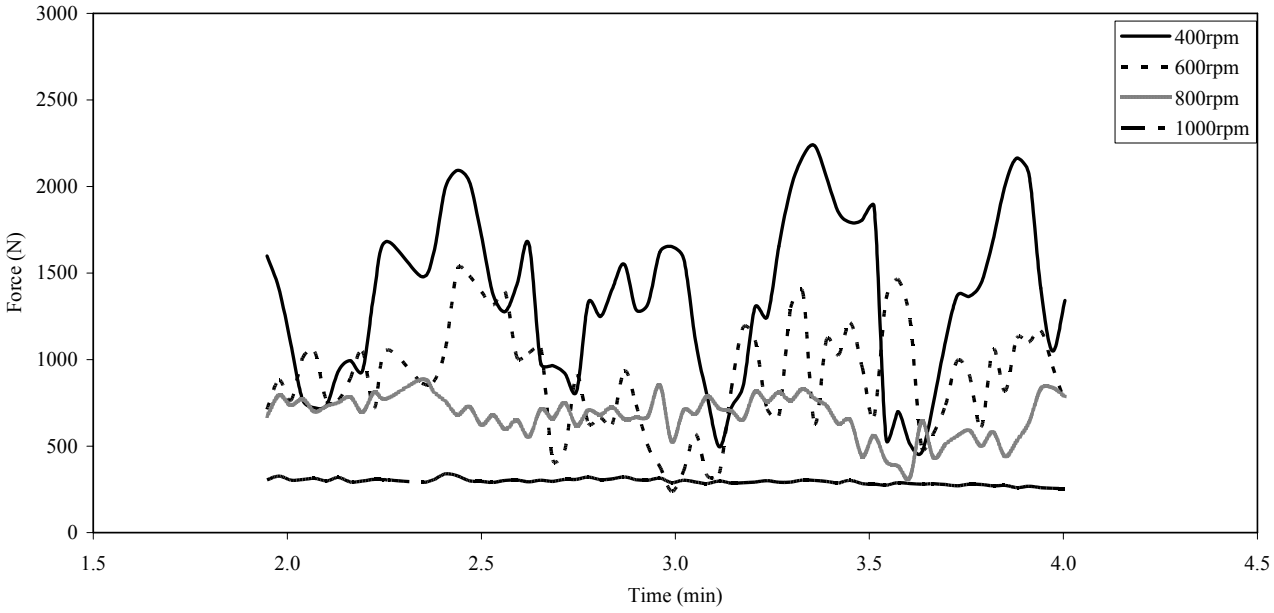

Fz vs Time @ 1.5 in/min

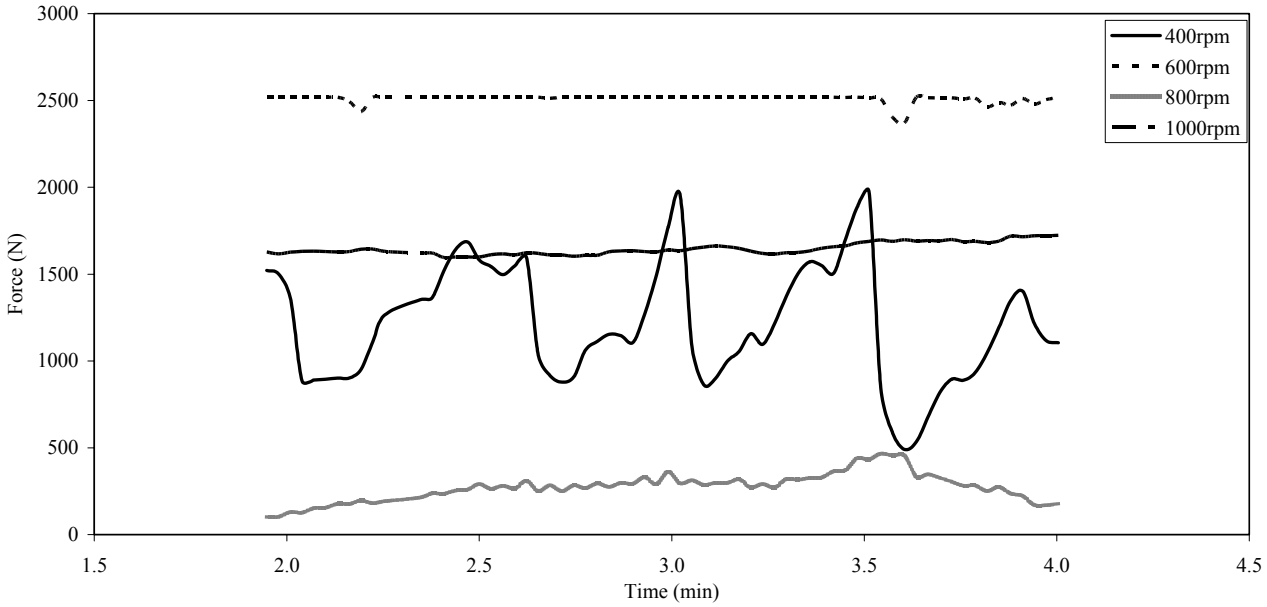

Fx vs Time @ 2 in/min

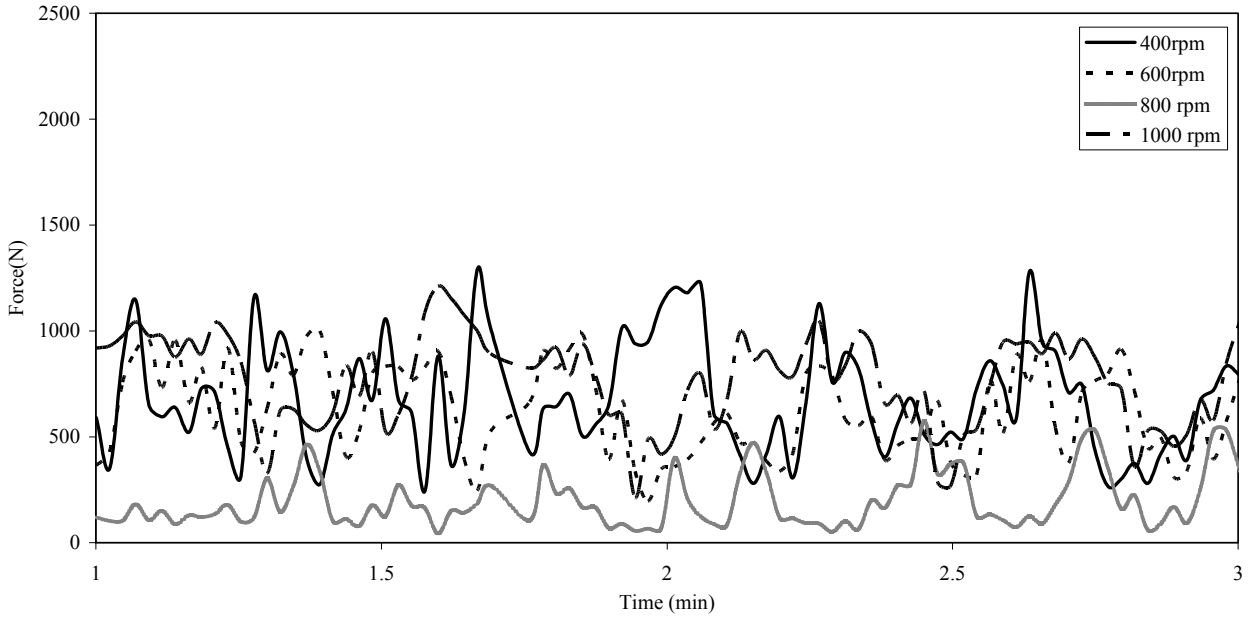

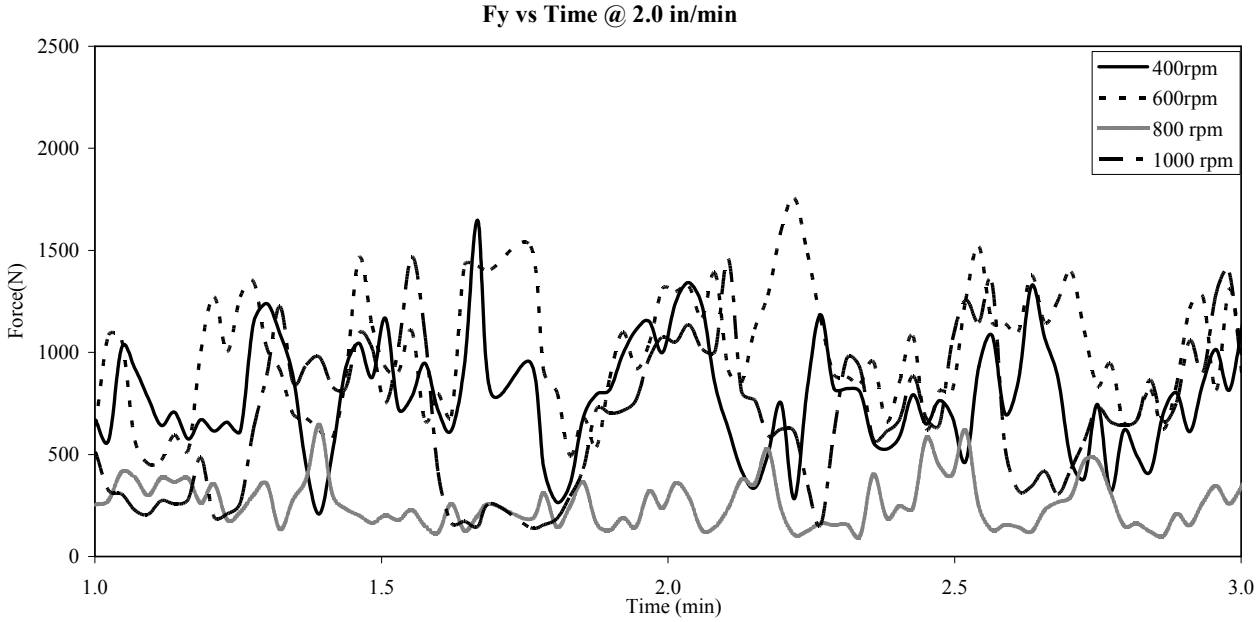
Fy vs Time @ 2.0 in/min
2500
2000
1500
1000
500
0
Force(N)
1.0
1.5
2.0
2.5
3.0
Time (min)
400rpm
600rpm
800 rpm
1000 rpm

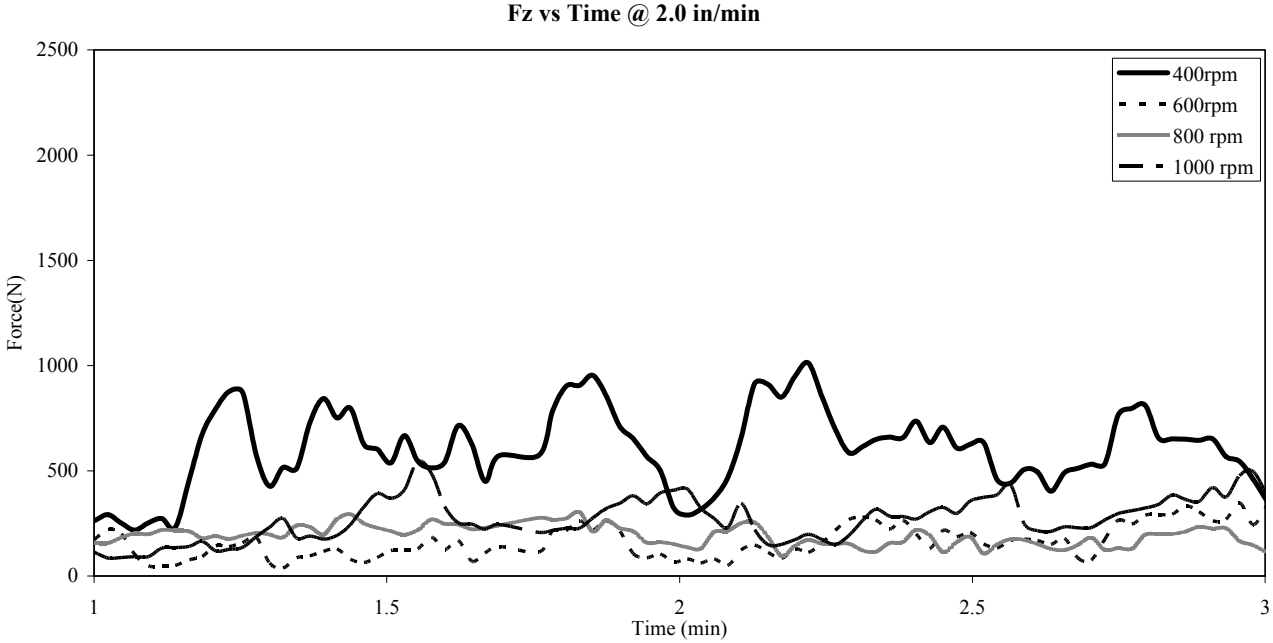
Fz vs Time @ 2.0 in/min
2500
2000
1500
1000
500
0
Force(N)
1
1.5
2
2.5
3
Time (min)
400rpm
600rpm
800 rpm
1000 rpm

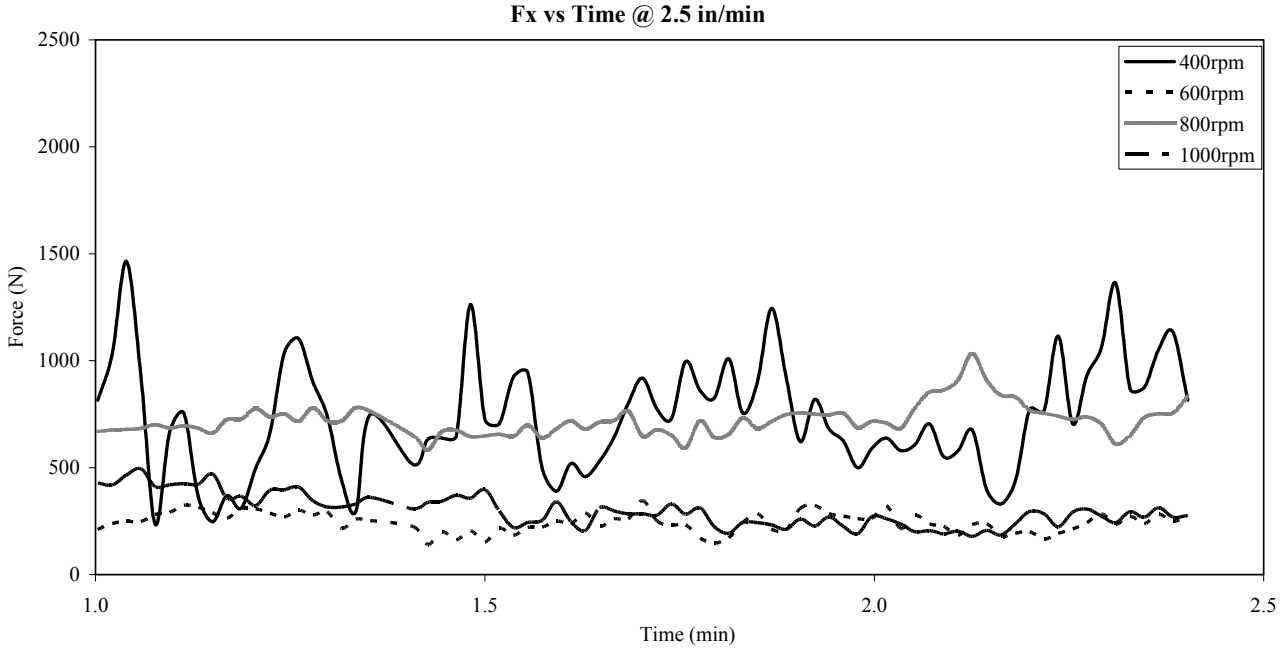
Fx vs Time @ 2.5 in/min
2500
2000
1500
1000
500
0
Force (N)
1.0
1.5
2.0
2.5
Time (min)
400rpm
600rpm
800rpm
1000rpm

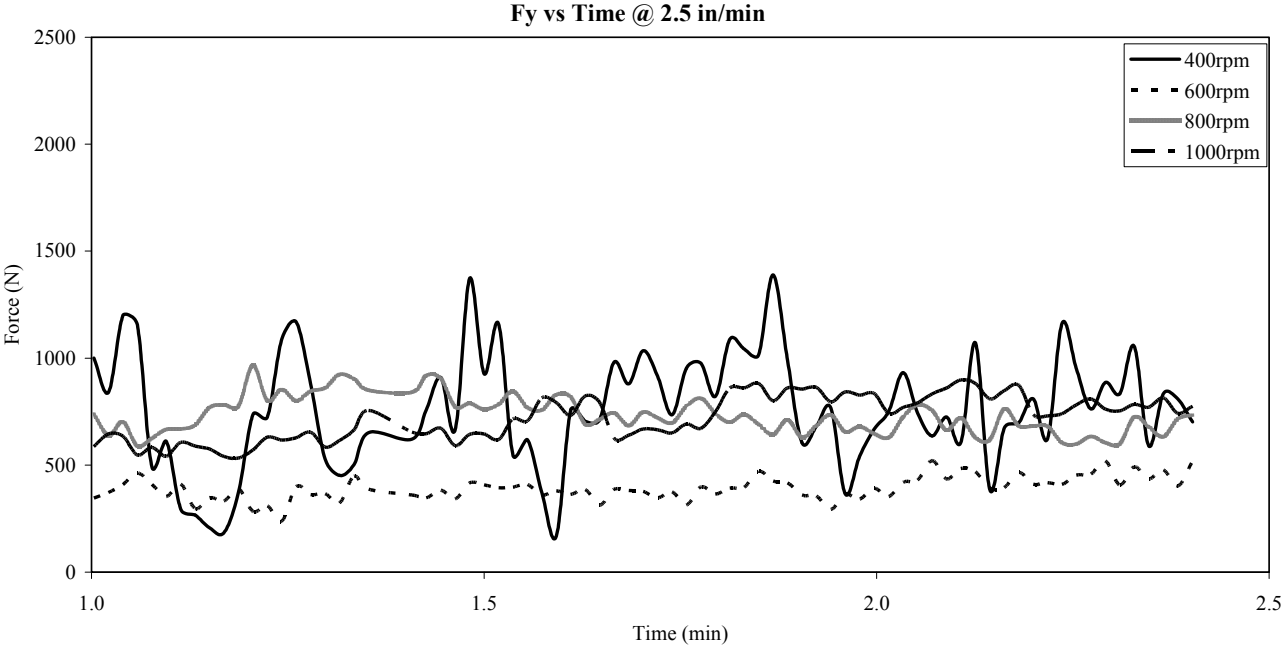
Fy vs Time @ 2.5 in/min
2500
2000
1500
1000
500
0
Force (N)
1.0
1.5
2.0
2.5
Time (min)
400rpm
600rpm
800rpm
1000rpm

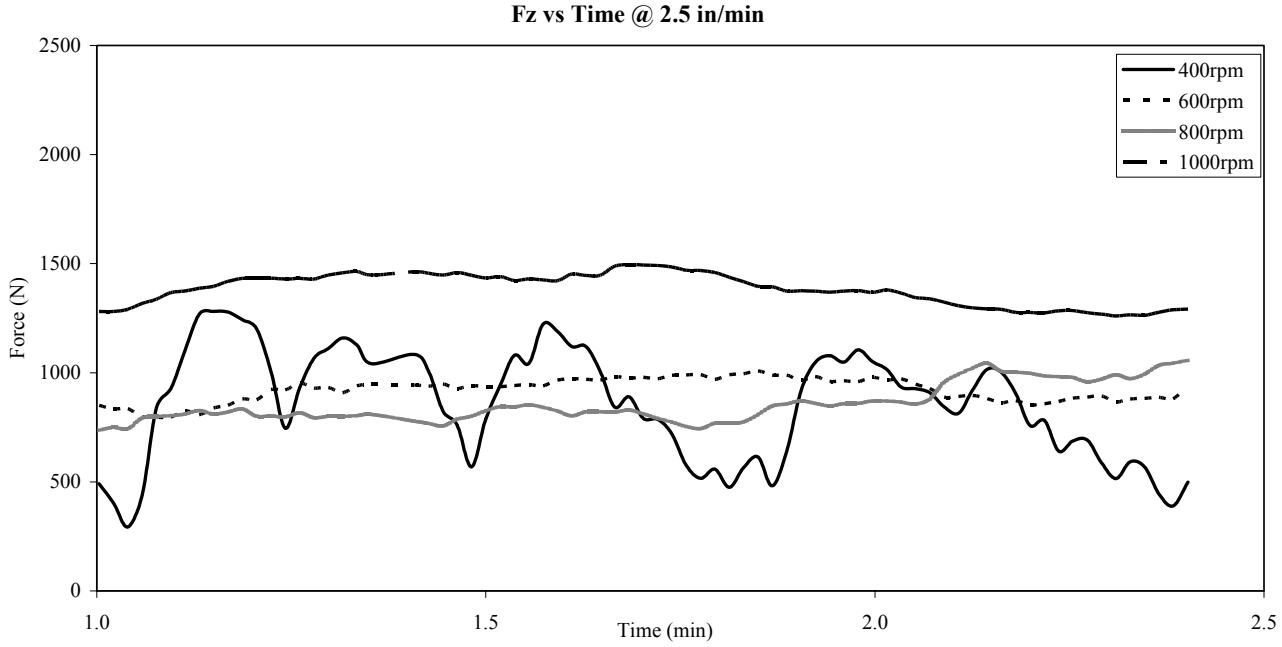
Fz vs Time @ 2.5 in/min
2500
2000
1500
1000
500
0
Force (N)
1.0
1.5
2.0
2.5
Time (min)
400rpm
600rpm
800rpm
1000rpm

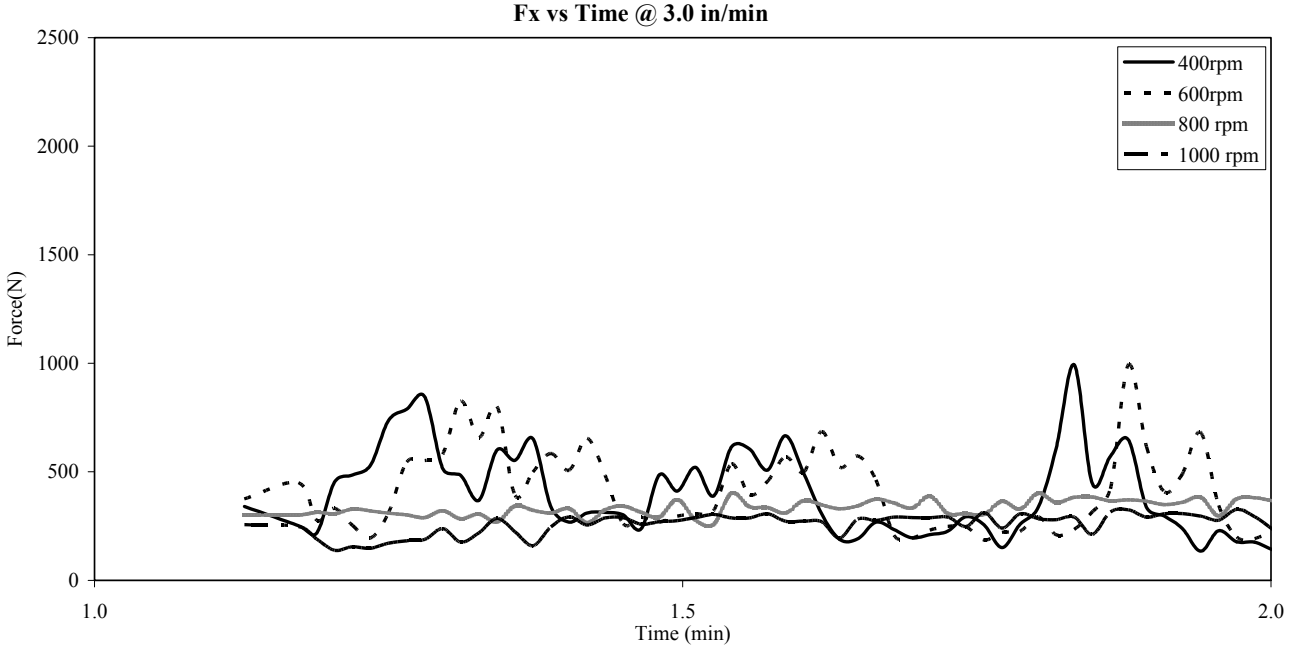
Fx vs Time @ 3.0 in/min
2500
2000
1500
1000
500
0
Force(N)
1.0
1.5
2.0
Time (min)
400rpm
600rpm
800 rpm
1000 rpm

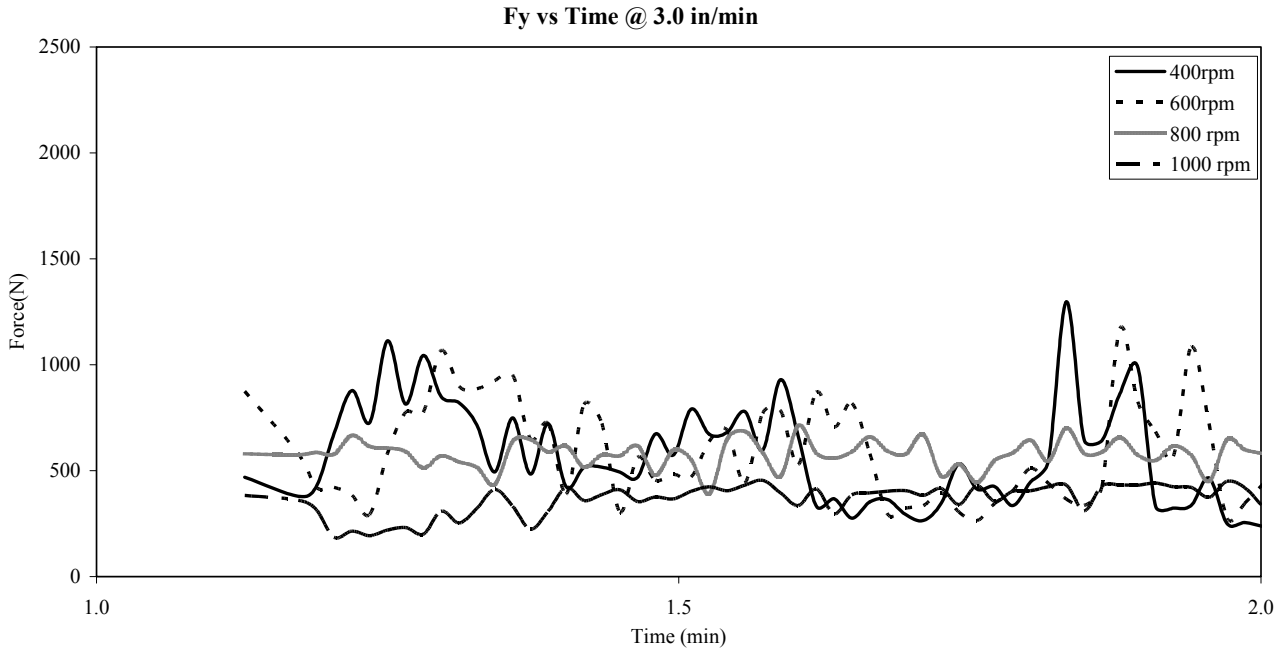
Fy vs Time @ 3.0 in/min
2500
2000
1500
1000
500
0
Force(N)
1.0
1.5
2.0
Time (min)
400rpm
600rpm
800 rpm
1000 rpm

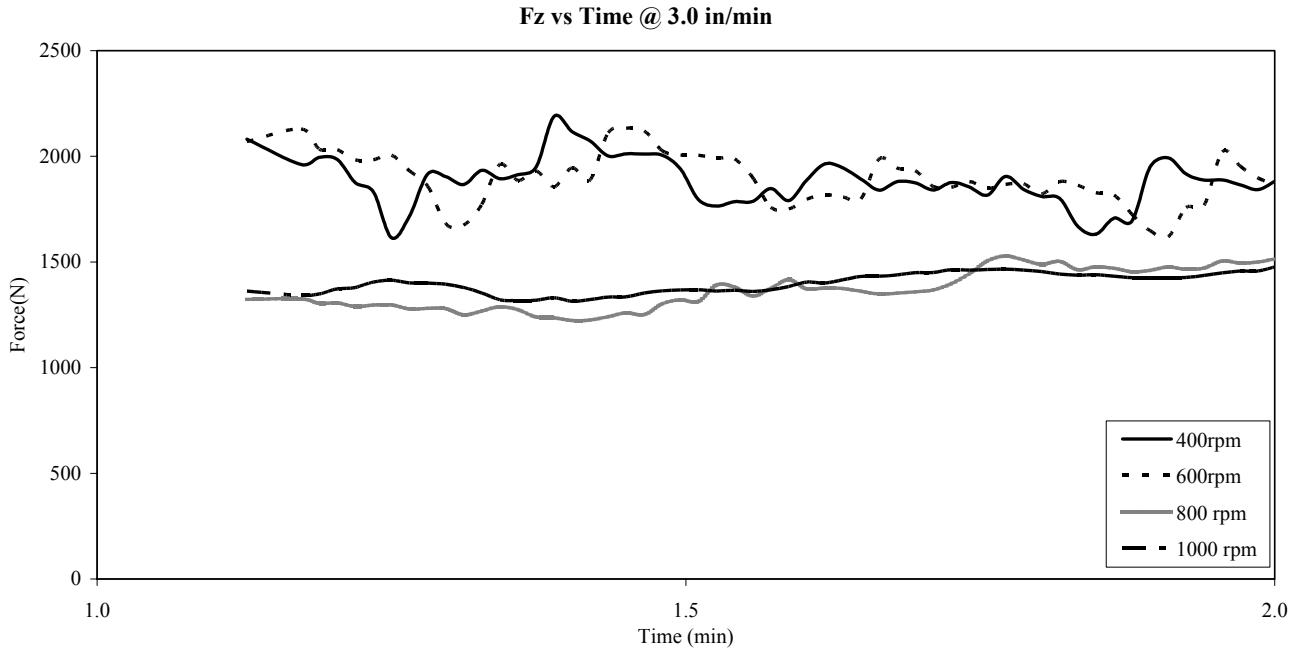
Fz vs Time @ 3.0 in/min
2500
2000
1500
1000
500
0
Force(N)
1.0
1.5
2.0
Time (min)
400rpm
600rpm
800 rpm
1000 rpm

Appendix B

Optical microscopy pictures of Friction Stir processed Al 5052 for various combinations of rotational and translational speeds at 20X magnification

Microstructure @ 1.5 in/min

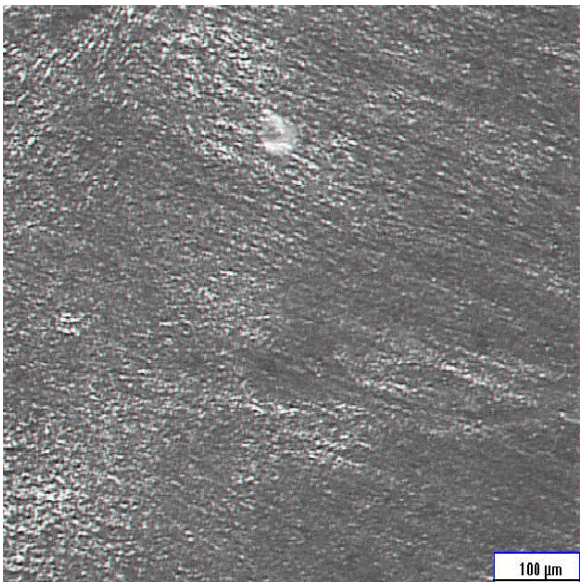

a) At 400 rpm

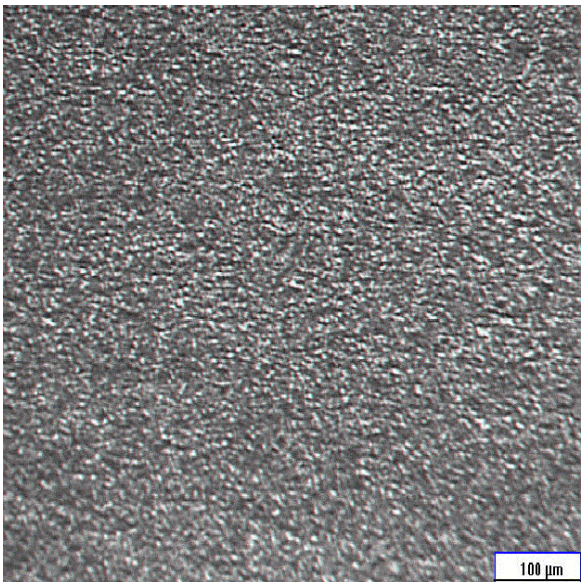

b) At 600 rpm

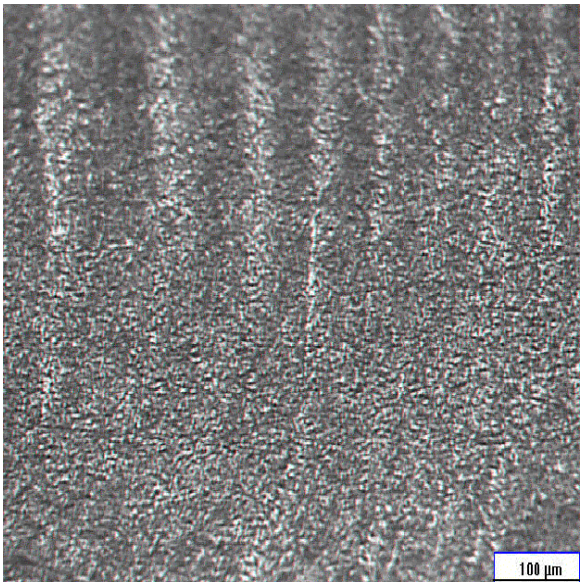

c) At 800 rpm

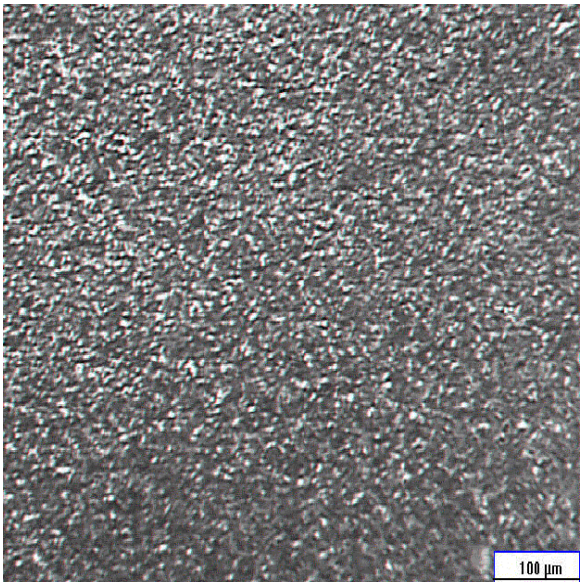

d) At 1000 rpm

Microstructure @ 2.0 in/min

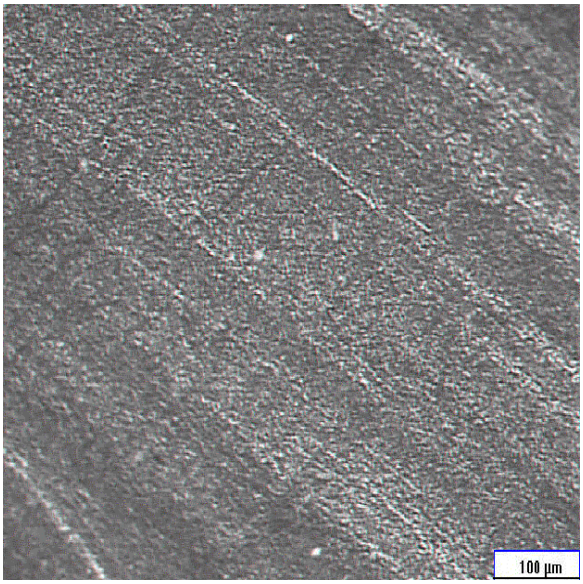

a) At 400 rpm

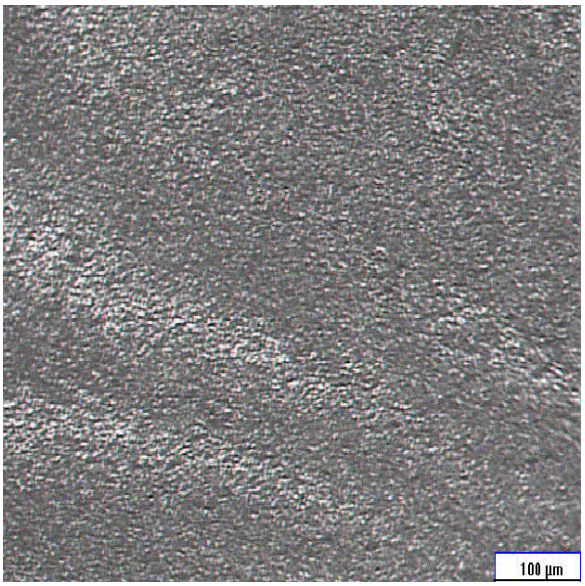

b) At 600 rpm

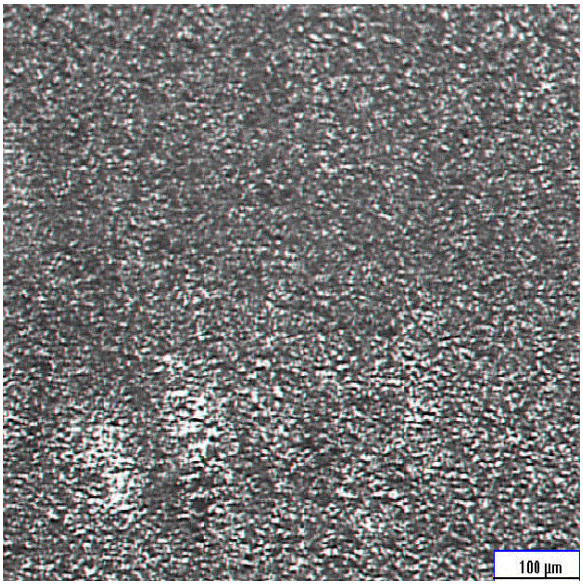

c) At 800 rpm

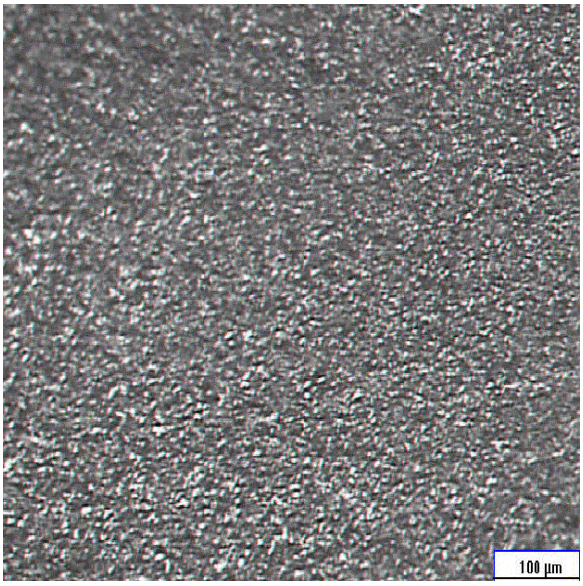

d) At 1000 rpm

Microstructure @ 2.5 in/min

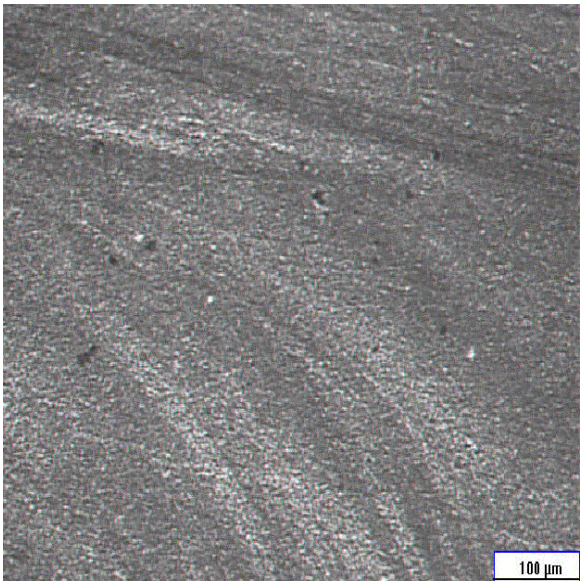

a) At 400 rpm

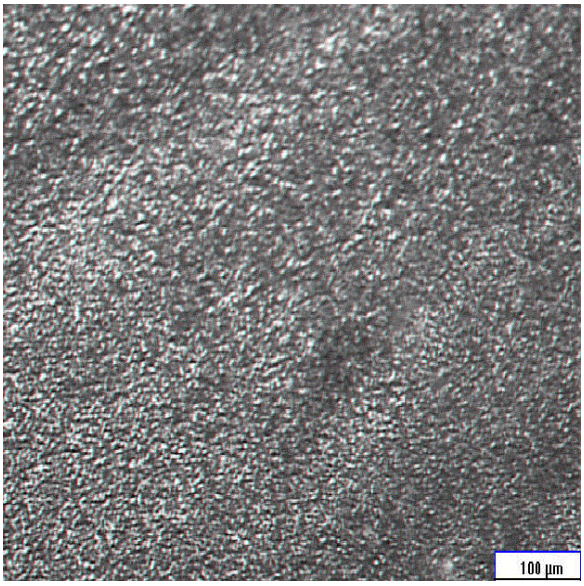

b) At 600 rpm

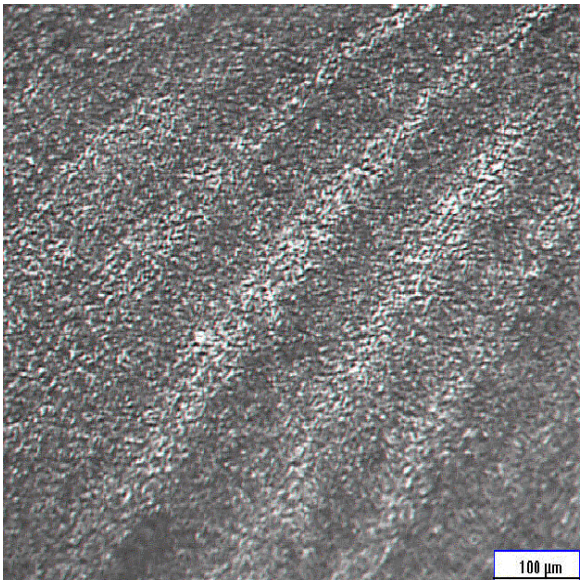

c) At 800 rpm

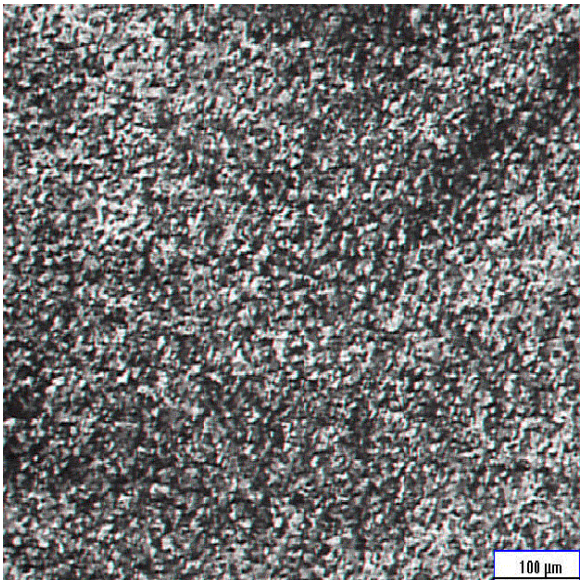

d) At 1000 rpm

Microstructure @ 3.0 in/min

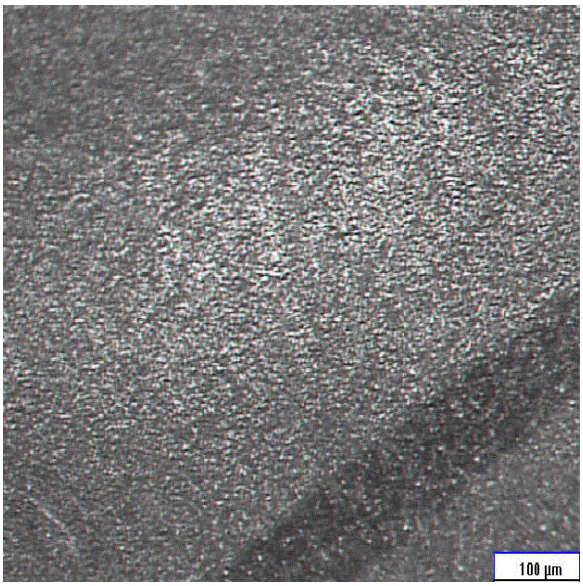

a) At 400 rpm

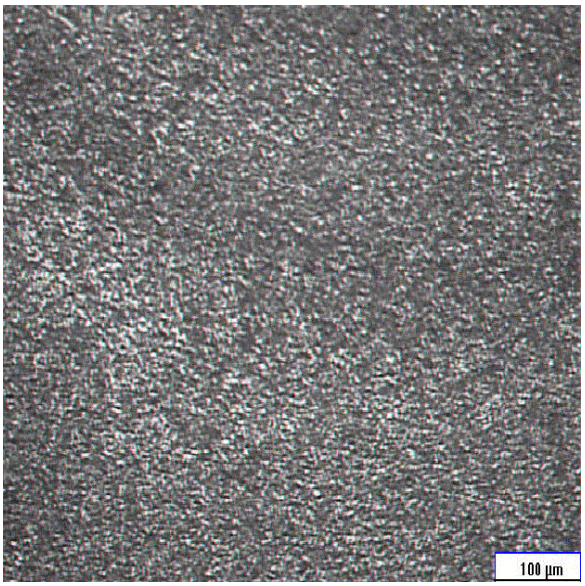

b) At 600 rpm

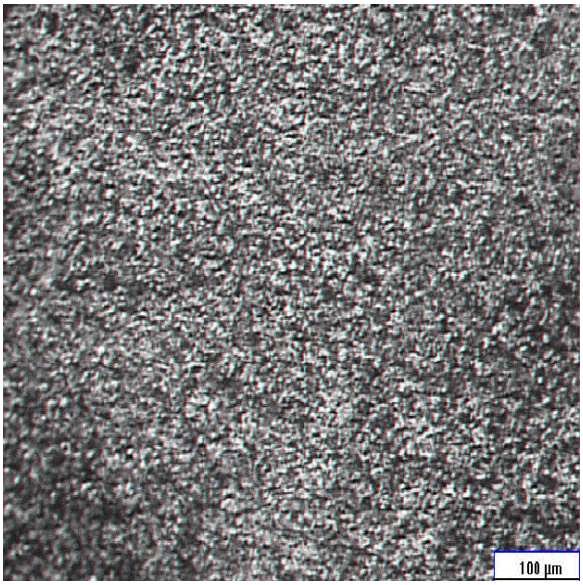

c) At 800 rpm

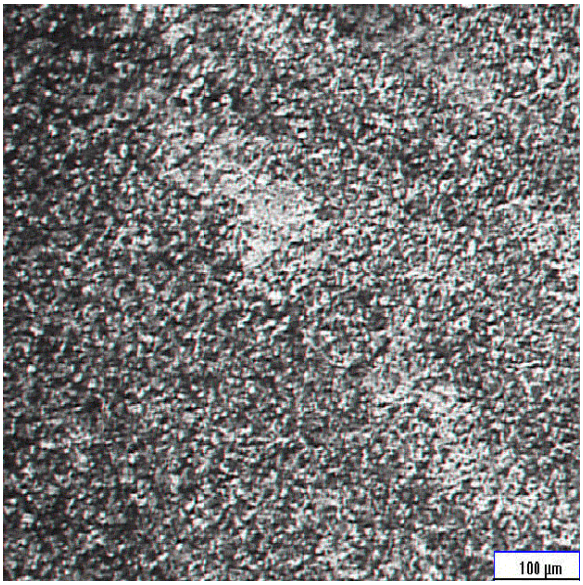

d) At 1000 rpm

References

1 Thomas, W.M., Nicholas, E.D., Kallee, S.W., "Friction based technologies for joining and processing", Friction Stir Welding and Processing, Edited by K.V. Jata, M.W. Mahoney, R.S. Mishra, S.L. Semiatin, and D.P. Field, TMS, 2001, Pages 3-13

2 Powell, H.J. and Wiemer, K., "Joining technology for high volume manufacturing of lightweight vehicle structures", Article ,1996, TWI, Cambridge, UK

3 Thomas, W.M., Nicholas, E.D., "Friction stir welding for the transportation industries. Materials & Design", 1997Volume 18, 269-273

4 Mishra, R.S and Mahoney, M.W, "Friction Stir Processing: A New Grain Refinement Technique in Commercial Alloys", Materials Science Forum, 2001, Volumes357-359, Pages 507-514

5 R. S. Mishra, Z. Y. Ma and I. Charit, "Friction stir processing: a novel technique for fabrication of surface composite", Materials Science and Engineering A, Volume 341, Issues 1-2, 20 January 2003, Pages 307-310

6 Thomas, W.M., Nicholas, E.D., 1996. Emerging friction stir joining technology for stainless steel and aluminium applications, presented at 'Productivity beyond 2000':IIW Asian Pacific Welding Congress, Auckland, New Zealand.

7 M. Peel, A. Steuwer, M. Preuss and P. J. Withers, "Microstructure, mechanical properties and residual stresses as a function of welding speed in aluminium AA5083 friction stir welds", Acta Materialia, Volume 51, Issue 16, 2003, Pages 4791-4801

8 C. G. Rhodes, M. W. Mahoney, W. H. Bingel and M. Calabrese, "Fine-grain evolution in friction-stir processed 7050 aluminum", Scripta Materialia, Volume 48, Issue 10, May 2003, Pages 1451-1455

9 Y. S. Sato, Y. Kurihara, S. H. C. Park, H. Kokawa and N. Tsuji , "Friction stir welding of ultrafine grained Al alloy 1100 produced by accumulative roll-bonding", Scripta Materialia, Volume 50, Issue 1, 2004, Pages 57-60

10 M. Cabibbo, E. Meccia and E. Evangelista , "TEM analysis of a friction stir-welded butt joint of Al–Si–Mg alloys", Materials Chemistry and Physics, Volume 81, Issues 2-3, 28 August 2003, Pages 289-292

11 L. Lityńska, R. Braun, G. Staniek, C. Dalle Donne and J. Dutkiewicz , "TEM study of the microstructure evolution in a friction stir-welded AlCuMgAg alloy", Materials Chemistry and Physics, Volume 81, Issues 2-3, 28 August 2003, Pages 293-295

12 J. Q. Su, T. W. Nelson, R. Mishra and M. Mahoney , "Microstructural investigation of friction stir welded 7050-T651 aluminium", Acta Materialia, Volume 51, Issue 3, 7 February 2003, Pages 713-729

13 Sato, Y.S., Urata, M., Kokawa, H., Ikeda, K., Enomoto, M., "Retention of fine grained microstructure of equal channel angular pressed aluminum alloy 1050 by friction stir welding", Scripta Materialia 45, Is 1, 2001. Pages 109-114

14 Jata, K.V., Semiatin, S. L., 2000. "Continuous dynamic recrystallization during friction stirs welding of high strength aluminum alloys". Scripta Materialia, Volume 43, Iss: 8, 743-749

15 S. Benavides, Y. Li, L. E. Murr, D. Brown and J. C. McClure. 10 September 1999. "Low-temperature friction-stir welding of 2024 aluminum", Scripta Materialia, Vol. 41, Issue 8, Pg. 809-815

16 Rhodes C.G., Mahoney M.W., Bingel W.H., Spurling R.A., Bampton C.C., "Effects of friction stir welding on microstructure of 7075 aluminum", Scripta Materialia, 1997, Volume 36, Iss: 1, Pages 69-75

17 Liu, G., Murr, L.E., Niou, C.S., McClure, J.C., Vega, F.R., "Microstructural aspects of the friction-stir welding of 6061-T6 aluminum", Scripta Materialia, 1997, Volume 37, Iss: 3, 355-361.

18 K. N. Krishnan , "On the formation of onion rings in friction stir welds", Materials Science and Engineering A, Volume 327, Issue 2, 30 April 2002, Pages 246-251

19 Michael A. Sutton, Bangcheng Yang, Anthony P. Reynolds and Junhui Yan, "Banded microstructure in 2024-T351 and 2524-T351 aluminum friction stir welds: Part II". Mechanical characterization, Materials Science and Engineering A, In Press, Corrected Proof, Available online 9 August 2003

20 Reynolds, A.P. and Tang, W., "Alloy, tool geometry, and process parameter effect on friction stir welding energies and resultant FSW joint properties", Friction Stir Welding and Processing, Edited by K.V.Jata, M.W. Mahoney, R.S. Mishra, S.L. Semiatin, abd D.P. Field, TMS, 2001, Pages 3-13

21 Y. J. Kwon, I. Shigematsu and N. Saito, “Mechanical properties of fine-grained aluminum alloy produced by friction stir process”, Scripta Materialia, Volume 49, Issue 8, October 2003, Pages 785-789

22 H. J. Liu, H. Fujii, M. Maeda and K. Nogi , “Tensile properties and fracture locations of friction-stir-welded joints of 2017-T351 aluminum alloy”, Journal of Materials Processing Technology, Volume 142, Issue 3, 2003, Pages 692-696

23 W. B. Lee, Y. M. Yeon and S. B. Jung , “The improvement of mechanical properties of friction-stir-welded A356 Al alloy”, Materials Science and Engineering A, Volume 355, Issues 1-2, 25 August 2003, Pages 154-159

24 Lumsden, J., Pollock, G., and Mahoney, M., “The effect of thermal treatments on the corrosion behavior of friction stir welded 7050 and 7075 aluminum alloys”, Materials Science Forum, 2003, Volumes 426-432, Pages 2867-2872

25 Charit, I., Ma, Z.Y., and Mishra, R.S., “High strain rate superplasticity in friction stir processed aluminum alloys”, 2003 NSF Design, Service and Manufacturing Grantees and Research Conference Proceedings, Edited by R.G.Reddy, The University of Alabama, Pages 2200-2207

26 Berbon, P.B., Bingel, W.H., Mishra, R.S., Bampton, C.C., Mahoney, M.W., 2001. “Friction stir processing: a tool to homogenize nanocomposite aluminum alloys” Scripta Materialia, Volume 44, Iss: 1, Pages 61-66

27 Sato, Y.S., Urata, M., Kokawa, H. “Parameters controlling microstructure and hardness during Friction-stir welding of precipitation hardenable aluminum alloy 6063”, Metallurgical and Materials Transactions A, March 2002, Volume 33A, Pages 625-635.

28 Sato, Y.S., Kokawa, H., Enomoto, M., Jogan, S., Hashimoto, T., “Precipitation sequence in friction stir weld of 6063 aluminum during aging”, Metallurgical and Materials Transactions A, December 1999, Volume 30A, Pg. 3125-3130.

29 Sato, Y.S., Kokawa, H., Enomoto, M., Jogan, S., Hashimoto, T., “Microtexture in friction-stir weld of an aluminum alloy”, Metallurgical and Materials Transactions A, April 2001, Volume 32A, Pg. 941-948.

30 Sato, Yutaka S., Kokawa, Hiroyuki, “Distribution of tensile property and microstructure in friction stir weld of 6063 aluminum”, Metallurgical and Materials Transactions A, 2001, Volume 32A, Pages 3023-3031

31 Lockwood, W.D., Tomaz, B., Reynolds, A.P., “Mechanical response of friction stir welded AA2024: experiment and modeling”, Materials Science and Engineering A, 2002, Volume 323, 348-353.

32 Mahoney, M. W., Rhodes, C.G., Flintoff, J.G., Spurling, R.A., Bingel, W.H. July 1998. “Properties of friction-stir-welded 7075 T651 aluminum”, Metallurgical and Materials Transactions A, Vol. 29A, Pg. 1955-1964.

33 Mitchell, J.E; Cook, G.E and Strauss A.M., “Experimental thermo-mechanics of friction stir welding”, 2002, American welding society 2002 Professional Program & Poster Session, Session 3: Process Modeling

34 Jata K. V., K. K. Sankaran and J. J. Ruschau “Friction-Stir Welding Effects on Microstructure and Fatigue of Aluminum Alloy 7050-T7451”, Metallurgical and Materials Transactions A, September 2000, Volume 31A, Issue 9, Pages 2181-2192

35 Thomas, W.M., Nicholas, E.D., Smith, S.D., “Friction stir welding- tool developments”, Aluminum Joining Symposiums, 2001 TMS Annual Meeting, 11-15.

36 Prado, R. A., Murr, L.E., Shindo, D. J., Soto, K.F., “Tool wear in the friction-stir welding of aluminum alloy 6061+20% Al2O3: a preliminary study” Scripta Materialia, 2001, Volume 45, Iss: 1, 75-80.

37 Li, Y; Murr, L.E; McClure, J.C. “Solid- state flow visualization in the friction stir welding of 2024 Al TO 6061 Al”, Scripta Materialia, 1999, Volume 40, Pages1 041-1046

38 Dong, P; Lu, F; Hong, J.K; and Cao, Z. “Coupled thermo-mechanical analysis of friction stir welding process using simplified models”, Science and Technology of welding and joining, Volume 6, 2001, Pages 281-287.

39 Colligan, K., “Material flow behavior during friction stir welding of aluminum”, Welding Research Supplement, 1999, Pages 229s- 237s

40 Heurtier, P., Desrayaud, C. and Montheillet F., “A thermomechanical analysis of the friction stir welding process”, Materials Science Forum, Volume 396-402, 2002. Pages 1537-1542

41 Frigaard, Ø., Grong, Ø., and Midling O.T., "Modeling of heat flow phenomena in friction stir welding of aluminum alloys", INALCO'98, 7th International Conference Joints in Aluminum, Cambridge, UK, 15th-17th April 1998, Pages 208-218

42 Frigaard, Ø., Grong, Ø., and Midling O.T., "A process model for friction stir welding of age hardening aluminu alloys", Metallurgical and Materials Transactions A, May 2001, Volume 32A, Pages 1189-1200

43 Chao, Y.J. and Qi, X., "Thermal and thermo-mechanical modeling of friction stir welding of aluminum alloy 6061-T6", Journal of Materials Processing & Manufacturing Science, October 1998, Volume 7, Pages 215-233

44 Ulysse, P. " Three-dimensional modeling of the friction stir welding process", International Journal of Machine Tools & Manufacture, 2002, Volume 42, Pages1549-1557

45 Deng, X. and Xu, S., "Solid mechanics simulation of friction stir welding process", Transaction of NAMRI/SME, 2001,Volume XXIX, Pages 631-638

46 Song, M., Kovacevic, R., "Thermal modeling of friction stir welding in a moving coordinate system and its validation", International Journal of Machine Tools & Manufacture, 2003, Volume 43, Pages 605-615

47 Lockwood, W.D., Reynolds, A.P., "Simulation of the global response of a friction stir weld using local constitutive behavior", Materials Science and Engineering A, 2002, Pages 1-8

48 C. M. Chen and R. Kovacevic , "Finite element modeling of friction stir welding—thermal and thermomechanical analysis", International Journal of Machine Tools and Manufacture, Volume 43, Issue 13, October 2003, Pages 1319-1326

49 John Pilling, Norman Ridley., 1989. "Superplasticity in crystalline solids", The Institute of Metals

50 Mishra, R.S., Mahoney, M.W., McFadden, S.X., Mara, N.A., Mukherjee, A.K., 1999. "High strain superplasticity in a friction stir processed 7075 Al alloy" Scripta Materialia 42, Iss: 2, 163-168.

51 Z. Y. Ma, R. S. Mishra and M. W. Mahoney, "Superplastic deformation behavior of friction stir processed 7075Al alloy" Acta Materialia, October 2002,Volume 50, Issue 17, Pages 4419-4430

52 Charit, I., Mishra, R.S. and Mahoney, M.W., "Multi-sheet structures in 7475 aluminum by friction stir welding in concert with post-weld superplastic forming", Scripta Materialia, November 2002, Volume 47, Issue 9, Pages 631-636

53 Charit, I., Mishra, R.S., "High strain rate superplasticity in a commercial 2024 Al alloy via friction stir processing" Materials Science and Engineering A, Volume 359, Issues 1-2, 25 October 2003, Pages 290-296

54 Z. Y. Ma, R. S. Mishra, M. W. Mahoney and R. Grimes, "High strain rate superplasticity in friction stir processed Al–Mg–Zr alloy", Materials Science and Engineering A, Volume 351, Issues 1-2, 25 June 2003, Pages 148-153

55 Mahoney, M; Mishra, R.S; Nelson, T; Flintoff, J; Islamgaliev, R and Hovansky,Y. "High strain rate, Thick section superplasticity created via friction stir processing", Friction Stir welding and Processing, , 2001, Pages 183- 194

56 Hanadi G. Salem, Anthony P. Reynolds and Jed S. Lyons. "Microstructure and retention of superplasticity of friction stir welded superplastic 2095 sheet", Scripta Materialia, March 2002, Vol. 46, Issue 5, Pages 337-342

57 Chow, K.K., Chan, K.C., "The cavitation behavior of a coarse-grained Al5052 alloy under hot uniaxial and equibiaxial tension", Materials Letters, 2001, Volume 49, Pages 189-196

58 Chow, K.K., Chan, K.C., "Effect of stress state on cavitation and hot forming limits of a coarse-grained Al 5052 alloy, Materials Letters, 2002, Volume 52, Pages 62-68

59 Cochran,W.G., "Sampling Techniques" 3rd Edition, John Wiley Publication, New York, 1999

60 Fluent 6.0 Manual

Vita

I was born on December 12th, 1979 in Kurnool, India. I earned my Bachelors degree in Mechanical Engineering from Osmania University in June, 1997. I have presented about 3 technical papers at state and national level technical symposia in different fields of Mechanical engineering during my undergraduation. I was awarded a second prize for my paper titled "Air Ambiator -An innovative technology in the field of air conditioning".

Following my inclination towards research I had joined Department of Mechanical Engineering at University of Kentucky for pursuing my MS in Spring, 2002. I was awarded the Kentucky Graduate Scholarship based on my undergraduate performance, for pursuing my MS. I been working on development and analysis of an innovative material processing technique called the "Friction Stir Processing" under the guidance of Dr. Marwan Khraisheh. My accomplishments from my present work include three papers and a poster presented at prestigious conferences like the TMS Annual meeting 2004. I intend to publish my work in a materials related journal soon.

RAJESWARI R. ITHARAJU